Effects of dimethyl fumarate in two animal models of MS

Doctoral Thesis

In partial fulfillment of the requirements for the degree
"Doctor rerum naturalium (Dr. rer. nat.)"

in the Molecular Medicine Study Program

at the Georg-August University Göttingen

submitted by

Sarah Traffehn

born in Hennigsdorf

Göttingen, March 2017

MEMBERS OF THE THESIS COMMITTEE:

First member of the thesis committee

Prof. Dr. Wolfgang Brück

Department of Neuropathology
University Medical Center, Georg-August-University Göttingen

Second member of the thesis committee

Prof. Dr. Eberhard Fuchs

German Primate Center
Leibniz Institute for Primate Research, Göttingen

Third member of the thesis committee

Prof. Dr. Fred Wouters-Bunt

Department of Neuropathology
University Medical Center, Georg-August-University Göttingen

Supervisor

PD. Dr. Imke Metz

Department of Neuropathology
University Medical Center, Georg-August-University Göttingen

Supervisor

Prof. Dr. Martin S. Weber

Department of Neuropathology and Department of Neurology
University Medical Center, Georg-August-University Göttingen

Date of Disputation: _____

AFFIDAVIT

Here I declare that my doctoral thesis entitled “Effects of dimethyl fumarate in two animal models of MS” has been written independently with no other sources and aids than quoted.

_____

Göttingen, March 2017

Für meine Eltern.

List of Publication

Original article

Licht-Mayer S., Wimmer I., **Traffehn S.,** Metz I., Brück W., Bauer J., Bradl M., Lassmann H. (2015) *Cell type-specific Nrf2 expression in multiple sclerosis lesion.* Acta Neuropathol. 130(2) 263-77

Metz I, **Traffehn S**, Straßburger-Krogias K., Keyvani K., Bergmann M., Nolte K, Weber MS., Bartsch T., Gold R., Brück W. (2015) *Glial cells express nuclear nrf2 after fumarate treatment for multiple sclerosis and psoriasis*. Neurol Neuroimmunol Neuroinflamm. 2(3)

Lehmann-Horn K., Kinzel S., Feldmann L., Radelfahr F., Hemmer B., **Traffehn S.**, Bernard CC., Stadelmann C., Brück W., Weber MS. (2014) *Intrathecal anti-CD20 efficiently depletes meningeal B cells in CNS autoimmunity.*AnnClin Tranl Neurol. 1(7) 490-96

Schmoeckel K., **Traffehn S**., Eger C., Pötschke C., Bröker BM. (2015) *Full activation of CD4$^+$ T cells early during sepsis requires specific antigen.* Shock 43(2) 192-200

Abstract

Traffehn, S., Metz, I., Bernard CC., Brück, W., Weber MS.
In vivo dimethyl fumarate treatment enhances the ability of B cells to present antigen
13th Congress of the International Society of Neuroimmunology, September 26th-29th 2016, Jerusalem, Israel, Poster session

Traffehn, S., Metz, I., Brück, W., Weber MS.
Dimethyl fumarate treatment in a B cell dependent EAE model
12th European Committee for Treatment and Research In Multiple Sclerosis, October 7th-10th 2015, Barcelona, Spain, Poster session

Traffehn, S., Metz, I., Brück, W., Bernard CC. Weber MS.
DMF modulates pathogenic B cell function in chronic CNS autoimmune disease
13th Congress of the International Society of Neuroimmunology, September 26th-29th 2014, Mainz, Germany, Oral presentation

Table of contents

1. Introduction 1

1.1. Multiple Sclerosis 1

1.1.1. Symptoms, clinical course and diagnosis 1

1.1.2. Pathogenesis and Pathology 3

1.1.3. B cells in MS 5

1.1.4. Therapy of MS 7

1.2. Animal models of MS 9

1.2.1. The cuprizone model 9

1.2.2. Experimental autoimmune encephalomyelitis 10

1.3. The oral agent dimethyl fumarate (DMF) 12

1.3.1. Clinical MS trials of DMF 12

1.3.2. Experimental DMF studies *in vivo* 13

1.3.3. DMF effects on CNS resident cells *in vitro* 14

1.3.4. DMF effects on immune cells *in vitro* and *in vivo* 15

1.4. Aim of the study 16

2. Material and Methods 17

2.1. Material 17

2.1.1. Reagents 17

2.1.2. Solutions, buffers and cell culture media 19

2.1.3. Antibodies, enzymes and proteins 22

2.1.4. Oligonucleotide primers 25

2.1.5. Consumables 26

2.1.6. Technical devices 27

2.1.7. Software 27
2.2. Patients 28
2.3. Animals 29
2.4. Methods 29
2.4.1. Genotyping 29
2.4.2. Cuprizone treatment 30
2.4.3. EAE induction 31
2.4.4. DMF treatment 31
2.4.5. Extraction of mouse plasma 31
2.4.6. Analysis of monomethyl fumarate (MMF) in plasma and brain 32
2.4.7. Detection of anti-MOG antibodies 32
2.4.8. Analysis of immune cells ex vivo 32
2.4.9. Flow cytometry 34
2.4.10. Co-culture experiments 36
2.4.11. In vitro stimulation of cytokine secretion 37
2.4.12. Detection of cytokines using ELISA 37
2.4.13. Histology 38
2.4.14. Histochemical staining 39
2.4.15. Immunohistochemical staining 40
2.5. Morphometry 42
2.6. Data analysis and statistics 42
3. Results 43
3.1. DMF treatment in the cuprizone model 43
3.1.1. DMF effects after short-term cuprizone intoxication 43

3.1.2. Long-term effects of DMF in the cuprizone mouse model 49
3.1.3. DMF effects after cuprizone withdrawal 53
3.1.4. MMF was detectable in the brain of DMF-treated mice 55
3.1.5. DMF did not reduce apoptosis of oligodendrocytes in Nrf2 k.o. mice 56
3.2. DMF effects in a B cell-mediated EAE model 58
3.2.1. DMF treatment decreased EAE severity and demyelination of the spinal cord 59
3.2.2. DMF had opposing effects on B cells and T cells during the early phase of EAE63
3.2.3. DMF effects on human B cells 87
4. Discussion 90
4.1. DMF shows neuroprotective and potentially regenerative effects in the cuprizone mouse model 90
4.1.1. DMF exerts neuroprotective effects during short-term cuprizone treatment . 91
4.1.2. DMF treatment increases differentiation and regeneration of oligodendrocytes after long-term cuprizone treatment 95
4.1.3. Therapeutic DMF treatment shows neuroprotective effects on axons 96
4.2. DMF treatment shows opposing effects on lymphocytes in B cell-mediated EAE ... 98
4.2.1. DMF treatment improves clinic and pathology of EAE mice 99
4.2.2. DMF treatment has immunomodulatory effects on peripheral B cells and T cells 101
4.2.3. DMF-treated B cells are more potent antigen-presenting cells 105
4.3. DMF altered B cell properties in MS patients 110
5. Outlook 111
6. Bibliography 112

Danksagung

Ein besonderer Dank gilt **PD Dr. Imke Metz**, welcher ich als allererstes dafür danke dass sie mich mit diesem Projekt betraut hat. Die Arbeit mit dir hat mich sowohl in professioneller als auch in persönlicher Hinsicht sehr vorangebracht.

Ein großer Dank geht auch an **Prof. Dr. Martin S. Weber**, dem ich auch dafür danke dass er mich mit diesem Projekt betraut hat. Ich fand unsere Unterhaltungen stets sehr angenehm und aufschlussreich. Ich hatte eine sehr schöne Zeit in deiner Arbeitsgruppe.

Ich bedanke mich sehr bei **Prof. Dr. Wolfgang Brück** für die Gelegenheit meine Doktorarbeit in dem Institut für Neuropathologie anzufertigen sowie für die Betreuung meines Projektes als Thesis committee Mitglied.

Des Weiteren bedanke ich mich auch bei Prof. **Dr. Eberhard Fuchs** und **Prof. Dr. Fred Wouters-Bunt** für Ihr Interesse, Ihr kritisches Hinterfragen und Ihre Unterstützung während der jährlichen Thesis committee Treffen.

Ich bedanke mich auch sehr bei **Cynthia** und **Heidi** für ihre Hilfe sowie den Mitarbeitern des Promotionsprogrammes Molekulare Medizin, vor allem **Dr. Erik Meskauskas**.

Ich möchte mich auch sehr bei **Mareike Gloth** bedanken, die sämtliche Schnitte und histologischen Färbungen übernommen hat. Ich hatte sehr viel Spaß mit dir bei der Arbeit und auch bei unseren Treffen außerhalb des Klinikums.

Ein riesiger Dank geht an **Caroline Jaß, Jan Einar Albin, Julian Koch** und **Katja Grondey**, die mir bei allen Experimenten tatkräftig zu Seite standen. Ihr habt dafür gesorgt, dass jedes große Experiment nicht in den größten Stress ausgeartet ist, wir stets sehr viel Spaß und Grund zum Lachen hatten.

Ein großer Dank geht an **Darius**, an den ich mich mit jeder Frage oder Problemstellung wenden konnte. Vielen Dank für die viele Hilfe und auch für die angenehme und oft lustige Stimmung im Labor.

Ich bedanke mich sehr bei meinen Kolleginnen **Verena, Insa, Ulla, Christin** und **Nasrin** die von Anfang an dafür sorgten, dass ich mich herzlich aufgenommen gefühlt habe. Vielen Dank für die schöne und lustige Zeit die wir miteinander verbracht haben.

Außerdem möchte ich mich wirklich sehr bei Kim und Linda bedanken.

Kim, deine stets positive und liebevolle Art haben immer dafür gesorgt, dass ich mich in deiner Gegenwart sehr wohl fühle und ich bin sehr froh dass du ein Teil unserer lustigen Büroclique geworden bist. Ich bin dir sehr dankbar für deine Freundschaft und deine Unterstützung während der letzten 1,5 Jahre.

Linda, du hast es immer geschafft mir auch an stressigen und tristen Tagen ein Lächeln zu entlocken und hast mich aufgebaut wenn mich mein Projekt mal wieder absolut in den Wahnsinn getrieben hat. Du bist meine Nummer 1!

Ich möchte mich auch sehr bei meiner Mitbewohnerin **Lisa** bedanken, die dafür sorgte dass ich mich in Göttingen sofort wohl gefühlt habe. Ich finde es toll mir dir zusammen zu wohnen und habe unsere gemeinsamen Abende immer genossen.

Ich bedanke mich bei meinen Freunden **Carmen, Tom, Jule, Steffi** und **Tony** für eure Besuche in Göttingen und die tolle Zeit die wir immer wieder miteinander verbracht haben.

Der allergrößte Dank geht an meine Familie.

Ich bedanke mich bei meinen Großeltern, die immer für mich da sind, mir Trost spenden, sich mit mir freuen und immer an mich glauben. Ich bin sehr stolz darauf eure Enkelin zu sein.

Der mit Abstand größte Dank geht an meine Eltern. Ohne euch hätte ich es nicht geschafft die gesamte Zeit hier in Göttingen durchzuhalten. Ich bin sehr glücklich eure Tochter zu sein und liebe euch aus tiefstem Herzen!

Am Schluss möchte ich mich bei Sebastian bedanken, der es jeden Tag aufs Neue schafft dass ich mich glücklich fühle.

Abstract

MS is a heterogeneous disease characterized by transient and later permanent disability caused by inflammatory CNS lesions with profound axonal loss and demyelination. Although the exact pathogenesis of the disease is still unknown, it is assumed that MS is an autoimmune disease. While earlier concepts focused on the role of T cells, B cells are increasingly recognized to play an important role. The fumaric acid ester DMF is an immunomodulatory agent which is approved for the therapy of relapsing-remitting MS. In MS patients, DMF effectively reduces the relapse rate as well as the number and extent of MRI lesions. DMF shows anti-inflammatory properties by modulating immune cell functions leading to a decrease in pro-inflammatory cytokine production. Furthermore, DMF may exert neuroprotective effects in part mediated by the induction of Nrf2 resulting in the activation of antioxidant response pathways. In our study, we investigated whether DMF has neuroprotective and/or neuroregenerative function independent of its effect on the peripheral immune system. For this purpose, DMF effects were studied in a setting of toxic demyelination, namely the cuprizone model. In the second part of our study, it was also analyzed to what extent DMF influences pathogenic B cell and T cell properties in in an EAE model, in which B cells are involved in a pathogenic manner.

Regarding the first part of the project, we found that DMF significantly diminished the cuprizone-induced apoptosis of oligodendrocytes and increased the number of oligodendrocytes over time during cuprizone intoxication. Upon short-term cuprizone exposure, DMF increased the number of oligodendrocyte progenitor cells (OPCs) whereas after long-term cuprizone diet higher numbers of mature oligodendrocytes could be observed. Although DMF treatment did not influence demyelination and remyelination of the corpus callosum, acute axonal damage was significantly decreased in DMF treated mice. In conclusion, DMF was found to exert moderate neuroprotective and neuroregenerative effects independent of the peripheral immune system. The observation of higher OPC numbers in conjunction with a higher number of mature oligodendrocytes after long-term cuprizone diet may suggest that DMF treatment potentially promotes the differentiation of oligodendrocytes.

In the second part, preventive as well as therapeutic DMF treatment was effective in a B cell-mediated EAE model. Clinical benefit of DMF treatment in mice with established EAE was associated with decreased demyelination and inflammation of the spinal cord. The infiltration of macrophages/microglia and partially also of T cells was reduced by DMF treatment, whereas DMF had no detectable effect on the number of infiltrating B cells. In peripheral compartments, DMF led to a lower T cell frequency in the blood, while a complementary accumulation of T cells could be observed in lymph node and spleen of DMF-treated mice with EAE. Besides its effect on T cell frequencies, DMF treatment significantly reduced activation, differentiation and proliferation of peripheral T cells. In contrast, DMF-treatment exerted no inhibitory effect on peripheral B cells and caused an enhanced activation and differentiation of B cells. Most persistently, we observed an upregulation of MHC II on B cells. Functionally, these alterations were associated with an enhanced capacity of B cells to act as antigen presenting cells for activation of T cells. In conclusion, the observed clinical and pathological benefit in EAE with pathogenic B cell function thus appears to be mediated by an immunomodulatory effect of DMF directly on T cells. Contrary, we found that DMF treatment promoted antigen-presenting properties of B cells, while this study could not conclusively reveal which T cell phenotype is induced by these more potent B cells. Nevertheless, the primary observation of an enhanced B cell activation and antigen presenting function upon DMF treatment might be of significant relevance in specific therapeutic decisions, such as choosing the appropriate MS medication subsequent to therapeutic B cell depletion.

List of Figures

Figure 1: Effect of DMF treatment on cuprizone induced weight loss. 44

Figure 2: DMF treatment reduces cuprizone-induced apoptosis of oligodendrocytes in the CC. 45

Figure 3: DMF treatment increases number of oligodendrocytes after 7 days of cuprizone exposure. 46

Figure 4: DMF treatment reduces the acute axonal damage induced by cuprizone diet. 47

Figure 5: DMF treatment does not prevent apoptosis of oligodendrocytes in the CC after 2 weeks of cuprizone diet. 48

Figure 6: DMF application does not reduce demyelination in the CC. 50

Figure 7: No significant effect of DMF on acute axonal damage, astrogliosis and macrophage/microglial numbers after long-term cuprizone treatment. 51

Figure 8: DMF treatment shows no significant effect the axonal density. 52

Figure 9: Higher numbers of mature oligodendrocytes after 6 weeks of cuprizone exposure with DMF treatment. 53

Figure 10: DMF has no effect on the remyelination of the CC. 54

Figure 11: DMF treatment decreases acute axonal damage after cuprizone withdrawal. 55

Figure 12: MMF, the active metabolite of DMF, is present in the brain of DMF-treated mice. 56

Figure 13: DMF treatment does not decrease apoptosis of oligodendrocytes in the CC of Nrf2 k.o. mice. 57

Figure 14: Schematic representation of the experimental setup. 58

Figure 15: Clinical course of EAE is ameliorated by preventive and therapeutic DMF treatment. 59

Figure 16: Anti-MOG Ab serum levels remain constant under preventive and therapeutic DMF treatment. 60

Figure 17: Spinal cord demyelination and infiltration is reduced after DMF treatment..... 62

Figure 18: T cell frequencies in blood, lymph node and spleen are altered under DMF treatment at day 12 p.i. 64

Figure 19: DMF decreases the expression of activation markers on T cells. 65

Figure 20: DMF decreases the frequency of $CD44^{high}$ $CD4^{+}$ T cells. 68

Figure 21: The frequency of $CD44^{high}$ $CD8^{+}$ T cells is reduced by DMF. 70

Figure 22: DMF treatment reduces the differentiation of $IFN\gamma^{+}$ T cells and $IL17^{+}$ T cells 72

Figure 23: DMF treatment does not alter regulatory T cell frequencies. 74

Figure 24: Proliferation of *in vivo* DMF-treated T cells is decreased after antigen-independent stimulation. 77

Figure 25: MHC-II expression on B cells is increased after DMF treatment. 78

Figure 26: Expression levels of activation markers on B cells remain constant after DMF treatment. 80

Figure 27: DMF induces a shift in B cell subpopulations. 82

Figure 28: B cell phenotypes are not significantly affected by DMF treatment. 83

Figure 29: DMF has no effect on the $rMOG_{1-117}$-binding capacity B cells. 84

Figure 30: In vivo DMF treatment enhances the antigen-presenting function of B cells. 86

Figure 31: In vivo DMF-treated B cells do not alter T cell differentiation in vitro. 87

Figure 32: DMF effects on B cells of MS patients. 88

List of Tables

Table 1: The new 2016 MAGNIMS MRI criteria 3

Table 2: Reagents 17

Table 3: Solutions, buffers and cell culture media 19

Table 4: Proteins, enzymes and inhibitors 22

Table 5: Monoclonal antibodies for flow cytometry 22

Table 6: Monoclonal antibodies for antigen-independent activation of T cells in vitro 24

Table 7: Primary antibodies for immunhistochemical staining 24

Table 8: Secondary antibodies for immunohistochemical staining 25

Table 9: Applied Kits 25

Table 10: Primers 25

Table 11: Consumables 26

Table 12: Technical devices 27

Table 13: Software 27

Table 14: Clinical characteristics of MS patients 28

Abbreviations

APC	Allophycocyanin
APC	Antigen-presenting cell
APP	Amyloid precursor protein
Ag	Antigen
BAFF	B cell activation factor
BBB	Blood brain barrier
BCR	B cell receptor
BDNF	Brain-derived neurotrophic factor
BV	Brilliant violet
Casp3	Caspase 3
CC	Corpus callosum
CD	Cluster of differentiation
CFSE	Carboxyfluorescein succinimidyl ester
CIS	Clinical isolated syndrome
CNS	Central nervous system
CSF	Cerebrospinal fluid
ctrl	control
DAPI	4’,6-diamidino-2-phenylindole
dH_2O	Distilled water
ddH_2O	Bidistilled water
DMD	Disease-modifying drug
DMF	Dimethyl fumarate
DMSO	Dimethyl sulfoxide
DNA	Deoxyribonucleic acid
EAE	Experimental autoimmune encephalomyelitis

EC	Endothelial cell
EDSS	Expanded disability status scale
e.g.	*Exempli gratia*
FACS	Fluorescence activated cell sorting
FCS	Fetal calf serum
FITC	Fluorescein isothiocyanate
GA	Glatiramer acetate
GFAP	Glial fibrillary acidic protein
h	Hour(s)
H&E	Haematoxilin and eosin
H_2O_2	Hydrogen peroxide
HCl	Hydrochloric acid
IFN	Interferon
Ig	Immunglobulin
i.p.	intrapertoneal
JCV	JC Virus
mAb	Monoclonal antibody
MBP	Myelin basic protein
mg	Milligram
MHC	Major histocompatibility complex
min	Minute(s)
µl	Microliter
ml	Milliliter
µm	Micrometer
µM	Micromolar
MOG	Myelin oligodendrocyte glycoprotein

MRI	Magnetic resonance imaging
MS	Multiple Sclerosis
OPC	Oligoclonal Band
PBMC	Peripheral blood mononuclear cell
PBS	Phosphate buffered saline
PE	Phycoerithrin
PFA	Paraformaldehyde
p.i.	Post immunization
PPMS	Primary progressive multiple sclerosis
PML	Progressive multifocal leukoencephalopathy
PLP	Proteolipid protein
PTX	Pertussis Toxin
RIS	Radiologically isolated syndrome
rMOG	Recombinant Myelin oligodendrocyte glycoprotein
RRMS	Relapsing-remitting multiple sclerosis
RT	Room temperature
s	Second(s)
s.c.	Subcutaneous
SPMS	Secondary progressive multiple sclerosis
Th1	T helper cells 1
Th17	T helper cells 17
TNF	Tumor necrosis factor

1. Introduction

1.1. Multiple Sclerosis

Multiple sclerosis (MS) is the most common autoimmune disease of the central nervous system (CNS) with approximately 2.5 million affected people worldwide (healthline.com/health/multiple-sclerosis/facts-statistics-infographic). MS is most commonly diagnosed in adults in their late twenties or early thirties. The clinical characteristics and pathology of MS were first described by Robert Carswell in 1838, who described and illustrated lesions of the spinal cord. The pathological hallmarks of MS lesions are inflammation, demyelination, gliosis and axonal loss (Brück and Stadelmann, 2003). The inflammation is caused by microglia and infiltrating macrophages, T cells and B cells. Despite that MS was mainly described as a T cell-driven disease, growing evidence suggests that B cells play an important role in the pathogenesis of the disease (Weber et al., 2010; Franciotta et al., 2008).

1.1.1. Symptoms, clinical course and diagnosis

MS is associated with a large variety of symptoms, like vision loss (partly or complete), changed sensation in arms or legs as well as fatigue and impairment of balance (Smith and McDonald, 1999). The symptoms can be transient but may also persist.

In 1996 the US National Multiple Sclerosis Society (NMSS) Advisory Committee on Clinical Trials in Multiple Sclerosis described 4 phenotypes of MS: *relapsing-remitting* (RRMS), *secondary progressive* (SPMS), *primary progressive* (PPMS), and *progressive relapsing* (PRMS) (Lublin and Reingold, 1996). The definition of these subtypes was revised in 2013 and the *clinical isolated syndrome* (CIS) and the *radiologically isolated syndrome* (RIS) were added as new subtypes (Lublin et al., 2014). The progressive relapsing phenotype was removed since those patients would now be categorized as PPMS patients with superimposed relapses and/or MRI activity.

RRMS occurs in about 85% of patients and is therefore the most common subtype of MS (Weinshenker, 1998). The characteristics of RRMS are disease relapses with full recovery or remaining deficits after partial recovery. Relapses are defined by an acute worsening of disease over a short period of time, which is often followed by a varying degree of remission. The clinical course remains stable between relapses. Typical symptoms of RRMS are sensory dysfunctions, optic neuritis and bladder as well as bowel difficulties (Noseworthy et al., 2000). When the disease

progresses continuously between relapses, the RRMS patient has converted to a secondary progressive phenotype. Approximately 70% of RRMS patients develop a SPMS after about 20 years (Weinshenker, 1998).

SPMS is defined by a steady progression of disease after an initial relapsing-remitting disease course and rarely by additional occasional relapses with minor recovery (Lublin and Reingold, 1996).

The small proportion of MS patients who do not display the characteristics of RRMS or SPMS show the phenotype of **PPMS.** PPMS is characterized by a continuous disease progression from onset. Disease plateaus or minor improvements can occur over time. PPMS affects approximately 10-15% of MS patients and the disease onset is about 10 years later compared to RRMS (Miller and Leary, 2007; Ontaneda and Fox, 2015; Thompson et al., 1997). The most important difference between RRMS and PPMS is how fast symptoms develop. In RRMS, new neurological deficits occur within days, but symptoms can resolve quickly. PPMS, in contrast, is characterized by accumulating disability over months and years and symptoms do not regress. Patients with PPMS often suffer from a progressive myelopathy which can emerge as a spastic, atactic paresis with dysfunction of the annular muscle (Ontaneda and Fox, 2015).

Nowadays, MS is diagnosed by application of the McDonald criteria (McDonald et al., 2001), which were first described in 2001 and revised in 2005 and 2010 (Polman et al., 2005, 2011). Following these criteria, MS is diagnosed after consideration of the clinical symptoms, MRI data and cerebrospinal fluid parameters (e.g. oligoclonal IgG bands). MRI criteria support an accurate diagnosis by depicting dissemination of lesions in time and space and thereby assist to exclude disorders which can mimic clinical and laboratory aspects of MS (Filippi et al., 2016). The European collaborative research network that studies MRI in MS (MAGNIMS) recommended in 2016 modifications to 2010 McDonald criteria which are depicted in Table 1 (Filippi et al., 2016).

Table 1: The new 2016 MAGNIMS MRI criteria (modified from Radiopedia.org)

Dissemination in space (established by two of five following areas)	Dissemination in time (established by one of two ways)
• cortical-juxtacortical: ≥1 lesions • infratentorial: ≥1 lesions • optic nerve: ≥1 lesions • periventricular: ≥3 lesions • spinal cord: ≥1 lesions	• a new lesion when compared to a previous scan (irrespective of timing) → T2 bright lesion and/or gadolinium-enhancing • presence of enhancing lesion and a non-enhancing T2 bright lesion on any one scan

1.1.2. Pathogenesis and Pathology

1.1.2.1. MS Pathogenesis

Based on results which were found in experimental autoimmune encephalomyelitis (EAE), an animal model of MS, it is assumed that peripheral immune cells cause an pro-inflammatory response in the CNS (Hemmer et al., 2015). T cells are assumed to be the cells activated first, which infiltrate the prior unaffected CNS tissue. The infiltrating auto-reactive T cells release pro-inflammatory cytokines like TNF-α and IFNγ which trigger an increased release of other cytokines and chemokines (e.g..: CCL3, CCL5, CXCL8, CXC3L1) (Larochelle et al., 2011). As a result of this inflammatory condition, endothelial cells (ECs) of the blood brain barrier (BBB) become activated and their expression of cell adhesion molecules (CAMs) increases (Bartholomäus et al., 2009). This process leads to the attraction of additional immune cells, including monocytes, B and T cells, plasma cells and dendritic cells which numerously invade the CNS tissue. The resulting inflammation interferes with the astroglial and oligodendroglial homeostasis. The infiltrating plasma cells produce antibodies which might lead to the damage of glial cells and the myelin sheath (Hemmer et al., 2015). Microglia and macrophages can cause axonal damage and injure the myelin by release of reactive oxygen and nitrogen species (ROS) (Fischer et al., 2012). The interaction of those macrophages/microglial cells and lymphocytes leads to the formation of an inflammatory phagocytic lesion. The initiation of the disease by T cells, however, is just one of the hypothesized mechanisms.

As newly forming MS lesions are associated with large numbers of activated microglia and only few infiltrating lymphocytes, an alternative hypothesis suggests that local CNS inflammation causes lesion formation (Barnett and Prineas, 2004; Henderson et al., 2009).

1.1.2.2. Pathology

Demyelination, inflammation, gliosis and axonal damage are the pathological hallmarks of MS (Kuhlmann et al., 2002). MS plaques (focal white matter lesions) can be present all over the CNS with predominant occurrence in the spinal cord, optic nerve, periventricular areas and brain stem (Stadelmann et al., 2011). Active plaques, defined by minor and major myelin protein degradation products within macrophages, most frequently arise in early disease stages, whereas smoldering (slowly expanding), inactive or shadow plaques are more prominent in chronic disease stages (Frischer et al., 2015). Inactive lesions show a sharp border and no or few macrophages and activated microglia. White matter lesions which are completely remyelinated are the so-called shadow plaques (Barkhof et al., 2003; Patrikios et al., 2006). Active lesions are more pronounced in RRMS patients but also occur in lower numbers in progressive MS. Smoldering plaques are characterized by an inactive center containing few macrophages but activated microglia are still present. These lesions seem to be characteristic of progressive MS, as they are exclusively found in progressive disease courses. Furthermore, patients with PPMS or SPMS show a higher frequency of cortical lesions and the injury of the normal-appearing white matter (NAWM) is more pronounced compared to RRMS patients (Kutzelnigg et al., 2005). It is characterized by a diffuse inflammation and axonal injury in non-demyelinated areas.

Early and chronic MS lesions differ in the extent of inflammatory cell infiltrates, demyelination and axonal damage (Brück et al., 1995; Kuhlmann et al., 2002, 2008a). Early lesions are characterized by a dominant accumulation of macrophages filled with myelin degradation products, a variable density of T cells in perivascular and parenchymal tissue, varying numbers of B cells and plasma cells, sometimes incomplete demyelination and a pronounced acute axonal damage. In chronic MS lesions only few lymphocytes and phagocytic cells are present, mature oligodendrocytes are often reduced, whereas oligodendrocyte precursor cells (OPC) may still be present. A pronounced reduction in the axonal density is especially found in lesions of MS patients, but also occurs in the NAWM (Evangelou et al., 2000; Tallantyre et al., 2009). The extent of remyelination is more pronounced in early than in chronic lesions (Goldschmidt et al., 2009).

Early active MS lesions represent early stages of lesion formation. In those lesions, four different patterns of demyelination can be differentiated that are defined by the loss of myelin proteins, extent of oligodendrocyte destruction, extension and localization of plaques and evidence of immunoglobulin and complement deposition (Lucchinetti et al., 2000).

Pattern I lesions are characterized by active demyelination accompanied by a prominent T cell- and macrophage-associated inflammation. The myelin protein loss in pattern I is evenly distributed and the lesions show sharply demarcated edges.

MS pattern II is similar to pattern I, but additionally shows deposits of immunoglobulins (Ig) and complement C9neo antigens. As these hallmarks are most prominent at sites of active demyelination and within phagocytic cells, it has been suggested that the myelin injury in this pattern could be mediated by the humoral immune system.

MS pattern III and pattern IV lesions also show inflammatory infiltrates consisting of macrophages/microglia and T lymphocytes. Deposition of immunoglobulin and complement is not present in these lesions.

In contrast to pattern I and II lesions, pattern III lesions show a diffuse spread into the normal-appearing white matter and the myelin around the vessels is mostly intact. The characteristic features of this pattern are a preferential loss of the myelin-associated glycoprotein (MAG) compared to other myelin proteins (e.g. myelin oligodendrocyte glycoprotein (MOG) and the apoptosis of oligodendrocytes.

The hallmark of pattern IV lesions is DNA fragmentation in oligodendrocytes in the absence of morphological features of apoptotic cell death. This pattern was only described in single autopsy cases and can thus be neglected.

1.1.3. B cells in MS

In the past years, the hypothesis of MS as a mainly T cell-mediated disease has been questioned and the role of B cells in the pathogenesis has been reevaluated (Franciotta et al., 2008). Activation of naïve B cells is triggered by antigen which they present in the context of the major histocompatibility complex-II (MHC-II) to $CD4^+$ T cells.

Full activation of B cells usually requires T cell help, namely the interaction of co-stimulatory molecules and the secretion of cytokines (Chen and Flies, 2013). Once B cells are activated, they

can differentiate into antibody-secreting plasma cells and memory B cells. These responses are crucial for a proper humoral and cellular immune response to effectively eliminate pathogens. Furthermore, activated B cells produce various pro-inflammatory cytokines (e.g. IL-6, TNFα, IFNγ) that on one side are important for an inflammatory response against pathogens but on the other side could promote inflammation in autoimmune diseases leading to the exacerbation of the disease course (Krumbholz and Meinl, 2014). Besides pro-inflammatory cytokines, B cells also secrete regulatory cytokines (e.g. IL-10, IL-35) which can control the extent of inflammation and could therefore exert beneficial effects in autoimmune diseases like MS (Fillatreau et al., 2002). In conclusion, B cells can exert beneficial and detrimental effects by antigen presentation, (auto-) antibody production and cytokine secretion.

The presence of oligoclonal bands (OCBs) in the CSF of MS patients was a first indication that B cells could contribute to the pathogenesis of the disease (Karcher et al., 1959; Lowenthal et al., 1960). OCBs occur in more than 95% of patients with MS and originate from the intrathecal production of IgG by clonally expanded plasma cells which are observed in the CNS parenchyma (Obermeier et al., 2011; Owens et al., 2003). Plasma cells are found in the perivascular spaces within lesions of subacute and chronic MS patients and it is assumed that antibodies (e.g. IgG) are synthesized at these sites (Henderson et al., 2009; Prineas, 1979). Additionally to the CNS parenchyma, B cell infiltrates are also found in the meninges of MS patients. Although only minor numbers of B cells and plasma cells are observed in MS lesions compared to T cells and myeloid cells, Type II lesions (that display deposits of Igs and complement and thus suggest a role of the humoral immune system in lesion development) are the most common lesion type in MS (Barnett et al., 2009; Lassmann et al., 2007; Lucchinetti et al., 2000).

While these first observations focused mainly on the pathogenic contribution of antibodies, emerging evidence suggests that the cellular function of B cells as highly effective and selective antigen-presenting cells (APC) may be equally important. An evidence for a pathogenic cellular function of B cells was the observation that memory B cells of RRMS patients are capable of inducing $CD4^+$ T cell proliferation and secretion of IFNγ in the presence of myelin proteins (Harp et al., 2010). B cells bind antigen via their B cell receptor (BCR), afterwards the antigen is internalized, processed and finally presented on the surface in the context of the major histocompatibility complex-II (MHC-II). B cells simultaneously increase the expression of co-stimulatory molecules

like CD80, CD86 and CD40 for an optimal capability to activate T cells. The co-stimulatory molecules CD80 and CD86 are upregulated on peripheral B cells from MS patients when compared to healthy controls (Fraussen et al., 2014). These B cells are capable of inducing a myelin-specific, pro-inflammatory T cell response, emphasizing the important role of B cell-dependent antigen presentation and co-stimulation in MS pathogenesis. Additionally, B cells can contribute to a pro-inflammatory response through the production of cytokines like Interleukin (IL)-6 and tumor necrosis factor alpha (TNF-α) (Meinl et al., 2006). It was demonstrated that B cells isolated from MS patients and afterwards stimulated *in vitro* showed a significant higher production of IL-6 when compared to healthy controls (Barr et al., 2012). Furthermore, MS plaques show an up-regulation of the B cell activation factor (BAFF) with an expression level comparable to lymphoid tissue (Krumbholz et al., 2005). BAFF serves as a crucial survival factor for B cells, especially for autoantigen binding B cells (Lesley et al., 2004). Therefore, an increased BAFF expression could promote the long-term-survival of plasma cells in the CNS. In contrast to these findings, it was shown that the frequency of regulatory B cells is decreased in the peripheral blood of MS patients compared to healthy controls (Knippenberg et al., 2011). B cells themselves can regulate immune responses through the production of IL-10 and IL-35 (Fillatreau et al., 2002; Shen et al., 2014). Besides, human regulatory B cells can control dendritic and macrophage cell functions, suppress proliferation of T cells and induce the generation of regulatory T cells (Krumbholz and Meinl, 2014). Balancing the pro-inflammatory and regulatory functions of B cells, for example through influencing the BAFF expression level, could be an important therapeutic target for MS.

The most conclusive evidence for a pathogenic contribution of B cells in MS pathogenesis were the beneficial effects of the B cell-depleting antibody rituximab and ocrelizumab (and other B cell-depleting therapeutics in clinical development) in RRMS patients (Hauser et al., 2008a, 2017).

1.1.4. Therapy of MS

The treatment approaches in MS can be divided into disease-modifying therapies and the treatment of acute relapses. The choice for the initial disease-modifying MS medication depends on the disease activity and is also based on a benefit-risk evaluation. Today, more than ten different disease-modifying drugs (DMDs) are approved for the long term treatment of MS in Europe.

The DMDs for patients with mild/moderate disease activity are the injectable drugs interferon-beta (IFNβ) and glatiramer acetate (GA) as well as the recently developed orally active drugs dimethyl fumarate (DMF) and teriflunomide. These drugs are characterized by moderate immunomodulatory functions and a generally high safety profile. Teriflunomide should not be used for women who are pregnant or are planning a pregnancy within the next 2 years. Several clinical trials could show that IFNβ, GA, teriflunomide and DMF efficiently reduce the relapse rate, decrease the development of new MRI lesions and counteract Expanded Disability Status Scale (EDSS) worsening (Claussen and Korn, 2012; Fox et al., 2012; Gold et al., 2012; Kappos et al., 2007; McCormack and Scott, 2004; Mikol et al., 2008; Paty and Li, 1993). The effects of DMF are described in detail in section 12.

For MS patients with a (highly) active disease course, monoclonal antibodies (mAbs) such as natalizumab and alemtuzumab or the oral agent fingolimod can be used as first choice of treatment. All three medications are characterized by a higher therapeutic efficacy than for example IFNβ. These drugs are highly effective in reducing the relapse rate as well as decreasing the accumulation of disability and MRI activity (Cohen et al., 2010; Coles et al., 2012; Polman et al., 2006). Although natalizumab was proven to be very effective, the development of progressive multifocal leukoencephalopathy (PML) in natalizumab-treated patients became a major safety issue (Langer-Gould and Steinman, 2006). Since the risk to develop PML is associated with the presence of antibodies against the JCV, patients should be tested for those antibodies before starting natalizumab treatment and while on therapy (Plavina et al., 2014). If these first line drugs fail to effectively control disease activity, daclizumab, mitoxantrone and ocrelizumab (expected to be approved in 2017) are considered as alternative treatment option. Daclizumab and ocrelizumab are mAbs which significantly lower the relapse rate of MS patients (Gold et al., 2013; Kappos et al., 2011). Mitoxantrone is an immunosuppressive drug which was approved in 2000 for the therapy of worsening RRMS and is known to significantly reduce the relapse rate and worsening of symptoms (Vollmer et al., 2010).

The standard medication for an acute relapse is the daily intravenous administration of high dose corticosteroids (e.g. 1g/day methylprednisolone) for 3-5 days (Sellebjerg et al., 2005). Should the symptoms persist, a second application of 2g/day is given after a timeframe of 10-14 days. As a

second therapy option, immunoadsorption or plasma exchange are utilized for patients with no or incomplete recovery after steroid treatment (Heigl et al., 2013; Trebst et al., 2009).

Besides the primary treatment objective to reduce relapse rate and to retard disease progression, the symptomatic MS therapy targets known signs and comorbidities of MS. Therapeutic approaches such as physical therapy, application of muscle relaxants and medications against fatigue, depression, bowel/bladder control problems or visual dysfunctions are important to improve the quality of life for patients (de Sa et al., 2011).

Most of the disease modifying drugs described above have also been tested for the therapy of progressive MS (PMS) with largely disappointing results (Ontaneda et al., 2016). It was shown that mitoxantrone was effective in patients with SPMS, but it rather reduced the relapse rate and did not affect the continuous disease progression (Ontaneda and Fox, 2015; Stüve et al., 2004). The limited success of these immunomodulatory and immunosuppressive drugs suggested that neuroprotective and repair-promoting approaches might be more effective for the therapy of PMS. However, the incomplete understanding of pathological processes contributing to the progression of disease complicates the development of such approaches. Hence, a broad range of treatments are currently under investigation. One example is the clinical trial MS-SMART, which currently investigates three neuroprotective agents (amiloride, riluzole, fluoxetine) for the therapy of SPMS patients.

1.2. Animal models of MS

Based on the restricted access to *ex vivo* specimens and the heterogeneity of MS, animal models are essential for a better understanding of the disease pathogenesis and for developing new therapeutic approaches. Several animal models of MS, like the cuprizone and EAE model, have been established, reproducing specific features of the disease.

1.2.1. The cuprizone model

The cuprizone model is a toxic demyelination model, which was developed to investigate demyelination and remyelination. The hallmark of this model is that the blood-brain-barrier (BBB) remains intact, which allows the analysis of de- and remyelination without major influences of the peripheral immune system (Bakker and Ludwin, 1987; McMahon et al., 2002). Cuprizone (bis-cyclohexanone-oxaldihydrazone) is a copper chelating agent and feeding cuprizone to young adult

mice leads to apoptosis of oligodendrocytes and the spontaneous demyelination of the corpus callosum (CC) (Bénardais et al., 2013; Matsushima and Morell, 2001a). The most common mouse strain used for the cuprizone model is the C57BL/6 strain. C57BL/6 mice fed with 0.2 – 0.25 % cuprizone for six weeks suffer from an almost complete demyelination of the CC (Hiremath et al., 1998). Besides weight loss and a slightly decreased activity, no major clinical signs (e.g. paralysis) can be observed under 0.2 – 0.25% cuprizone exposure (Praet et al., 2014). Several studies showed that cuprizone also leads to demyelination in several other brain regions such as the cerebellum, the hippocampus, the caudate-putamen and cortex (Groebe et al., 2009; Gudi et al., 2009; Hoffmann et al., 2008; Koutsoudaki et al., 2009; Norkute et al., 2009; Skripuletz et al., 2010). The exact mechanism of cuprizone-induced demyelination and apoptosis of oligodendrocytes is not completely understood. It is assumed that the cuprizone-mediated inhibition of mitochondrial enzymes leads to oligodendrocyte apoptosis and initiation of demyelination (Bénardais et al., 2013; Matsushima and Morell, 2001a; Ransohoff, 2012; Venturini, 1973). Oligodendroglial cell death starts early after initiation of cuprizone diet, weeks before demyelination is detectable (Hesse et al., 2010a). In the early phase, dying oligodendrocytes express activated caspase 3, which decreases in later stages suggesting a switch to a caspase 3-independent cell death mechanism. The early loss of oligodendrocytes leads to an enhanced recruitment of microglia/macrophages which is followed by an extensive astrogliosis (Hiremath et al., 1998). Microglia accumulation reaches its maximum with the peak of demyelination after 4-5 weeks of cuprizone exposure (Mason et al., 2001). Spontaneous remyelination occurs either upon cuprizone withdrawal or after 5-6 weeks of ongoing cuprizone diet. After cuprizone removal, the majority of axons is remyelinated within 2 weeks (Lindner et al., 2008a).

1.2.2. Experimental autoimmune encephalomyelitis

EAE is the most common model of MS and was first described in 1933 (Rivers et al., 1933). The model is mainly used to study the immune cell-mediated inflammation and demyelination of the CNS. EAE can be induced by active immunization with distinct myelin components emulsified in complete Freund's adjuvant (CFA) or by adoptive transfer of myelin-specific T cells (Stromnes and Goverman, 2006a, 2006b).

Several murine EAE models were established in the past years including $PLP_{139-151}$ peptide-induced relapsing EAE in SJL mice, MBP-induced EAE in PL/J mice, MOG_{35-55} peptide-induced disease in

C57/BL6 mice and active immunization with CNS tissue homogenates or MOG that induces a relapsing-remitting disease in Biozzi ABH mice (Amor et al., 1994; Ando et al., 1989; Mendel et al., 1995; Tuohy et al., 1992). First clinical signs of EAE can be observed 9-12 days after immunization, depending on the species and the specific disease-inducing agents (Gold et al., 2006). The main clinical characteristic of EAE is an ascending paralysis, gradually affecting the hind limbs, abdominal muscles and fore limbs.

EAE is mediated by complex interactions of the adaptive and the innate immune system. The most common active immunization model is the MOG_{35-55} peptide EAE model that leads to a relapsing-remitting (SJL, Biozzi) or a chronic-progressive (C57BL/6) disease course. The immunization together with CFA leads to a primarily $CD4^+$ T cell-mediated disease (Fletcher et al., 2010; Kurschus, 2015). The MOG_{35-55} peptide-containing CFA is recognized by antigen-presenting cells (APCs), such as dendritic cells, macrophages and B cells, which present the antigen in a complex with MHC-II molecules on their surface leading to an activation of peripheral encephalitogenic T cells (Slavin et al., 2001). These autoreactive T cells migrate into the CNS mediating a subsequent breakdown of the BBB (Furtado et al., 2008; O'Connor et al., 2008). Inside the CNS, T cells become reactivated by local and infiltrating APCs which present myelin fragments in association with MHC-II leading to further inflammatory processes and subsequently to demyelination and axonal injury (Fletcher et al., 2010; Steinman and Zamvil, 2005). The disease worsening caused by depletion of B cells led to the assumption that this model can be considered as a rather "B cell-independent" EAE (Weber et al., 2010). An EAE model which generates antigen-activated B cells is achieved by immunization with recombinant MOG protein (recombinant (r) MOG_{1-117}). After mice are immunized with MOG_{35-55} peptide, autoreactive $CD4^+$ T cells become directly activated because the peptide is bound by MHC-II on APCs without processing (Constant et al., 1995; Slavin et al., 2001). In contrast, after immunization with $rMOG_{1-117}$ the native MOG needs to be internalized and processed by APCs to present the encephalitogenic peptide to autoreactive $CD4^+$ T cells (Slavin et al., 2001). This leads to the generation of pathogenic B cells, which recognize the MOG-protein via their B cell receptor (BCR). These B cells can, subsequently, efficiently activate $CD4^+$ T cells and develop into antibody-secreting plasma cells (Marta et al., 2005).

Although these EAE models represent several histopathological and immunological features of MS, their mode of induction does not model the triggers of CNS autoimmunity completely. Models

more suitable to investigate the initiation of the disease are spontaneous EAE models. Opticospinal encephalomyelitis (OSE) mice spontaneously develop lesions restricted to the optic nerve and spinal cord (Krishnamoorthy et al., 2006). These mice are double-transgenic animals on a C57BL/6 background, which have transgenic T cells specific for myelin oligodendrocyte glycoprotein peptide 35-55 (MOG 35-55) and transgenic B cells recognizing MOG antigen (Litzenburger et al., 1998). Approximately 50% of OSE mice develop spontaneous EAE. Another spontaneous EAE model is the RR mouse model (SJL/J background) which represents the first spontaneous animal model for the relapsing-remitting form of MS (Pöllinger et al., 2009). These single-transgenic mice carry T cells with a T cell receptor (TCR) specific for the MOG_{91-106} peptide presented by MHC-II. Within one year 90% of the animals develop a relapsing-remitting course of EAE with lesions distributed throughout the CNS.

1.3. The oral agent dimethyl fumarate (DMF)

The fumaric acid ester DMF (Tecfidera®) is approved for the therapy of RRMS in Germany since February 2014. Previously DMF had been approved as a compound of the anti-psoriatic drug Fumaderm® since 1994, based on successful clinical studies (Altmeyer et al., 1994; Mrowietz et al., 1998; Nieboer et al., 1990). DMF has several immunomodulatory functions, but the mechanism of action is not completely understood. In the circulation, DMF is rapidly hydrolyzed to its metabolite monomethyl fumarate (MMF), which is supposed to be the active form in the body (Nibbering et al., 1993). However, *in vitro* and *in vivo* studies could show that both DMF and MMF have immunomodulatory effects (de Jong et al., 1996; Ockenfels et al., 1998; Treumer et al., 2003).

1.3.1. Clinical MS trials of DMF

Several clinical studies assessed the therapeutic effects, safety and tolerability of DMF in RRMS patients. The initial study was performed with Fumaderm® which is composed of ethylhydrogen fumarate-Ca salt, ethylhydrogen fumarate-Mg salt, ethylhydrogen fumarate-Zn salt and dimethyl fumarate. This pilot study showed that treatment of RRMS patients with fumaric acid esters (FAE) could significantly reduce the number and volume of gadolinium-enhanced (Gd+) lesions and modulate T cell-mediated cytokine production (Schimrigk et al., 2006). Based on these preliminary findings, an oral formulation of dimethyl fumarate, named BG-12, was tested in a phase II study in patients with RRMS (Kappos et al., 2008). Treatment with 240 mg DMF three times daily decreased the number of new Gd+ lesions by 69% and the annualized relapse rate by 32%

compared with placebo treated patients. Furthermore, the number of new or enlarging T2-hyperintense and new T1-hypointense lesions was reduced by DMF. Two randomized, double-blind phase III studies, the DEFINE (Gold et al., 2012) and the CONFIRM study (Fox et al., 2012), were performed.

The DEFINE study demonstrated that DMF significantly reduces the number of relapses in MS patients (relapse rate: 27% with DMF twice daily and 26% with DMF thrice daily vs. 46% placebo) as well as the number of Gd+ and new or enlarging T2-hyperintense lesions. The risk of disability progression was reduced by 38% and 34% with DMF treatment twice or thrice per day, respectively. In the CONFIRM study, the active agent GA was included as a reference comparator. The results regarding the efficacy and safety of DMF compared to placebo were fairly similar to the results of the DEFINE study. The comparison of DMF versus GA showed significant differences in favour of DMF in the annualized relapse rate (thrice-daily DMF), new or enlarging T2-hyperintense lesions (both DMF doses), and new T1-hypointense lesions (thrice-daily DMF).

Adverse effects include gastrointestinal symptoms like abdominal pain and diarrhea, flushing and decreased lymphocyte counts. To minimize the risk of severe lymphopenia it is recommended to monitor complete blood count and absolute lymphocyte counts before the initiation and during DMF treatment. To date, 5 cases of PML have been reported with the use of fumaric acid esters in patients with psoriasis and 4 cases of PML in patients with MS treated with DMF (Rosenkranz et al., 2015; Williamson and Berger, 2015).

The FDA approved DMF (Tecfidera®) in 2013 and the European Commission in 2014 as first-line oral treatment for patients with RRMS. The starting dose of Tecfidera® is 120 mg twice a day orally, after seven days the dose should be increased to 240 mg twice daily.

1.3.2. Experimental DMF studies *in vivo*

The effects of DMF were investigated in different animal models. In MOG_{35-55} peptide induced EAE, preventive DMF treatment of mice with 15 mg/kg twice daily could significantly ameliorate the clinical course compared to controls (Chen et al., 2014; Schilling et al., 2006; Schulze-Topphoff et al., 2016). The infiltration of macrophages into the spinal cord was significantly reduced in the early phase of EAE. Therapeutic application of DMF, started after EAE onset, could also attenuate EAE severity and first effects became apparent 10 days after treatment start (Linker et al., 2011).

Histological analysis revealed that DMF leads to a significantly better preservation of myelin and axons in inflamed lesions as well as to a reduced astrogliosis.

A quantification of neuronal cells in spinal cord and cerebellum showed significantly higher numbers of neurons in DMF-treated mice compared to controls. It was shown that DMF can induce the nuclear factor erythroid 2-related factor (Nrf2) which leads to an increased activation of antioxidant response pathways (Thiessen et al., 2010). *In vivo* application of DMF led to an increased induction of Nrf2 target genes such as NADP(H) quinolone oxidoreductase-1 (NQO-1) in liver and cerebellum of MOG-peptide immunized rats (Linker et al., 2011). Furthermore, histological evaluation of DMF-treated EAE animals revealed an increased expression of Nrf2 in neurons and glial cells in the brain and spinal cord, suggesting that the observed neuroprotective effects of DMF are Nrf2-dependent. The study of Linker et al. demonstrated that DMF treatment could not ameliorate the EAE course of Nrf2 k.o. mice and thereby supported the hypothesis that DMF effects are mostly Nrf2-dependent. Nevertheless, a recent study showed that DMF treatment also ameliorated EAE of Nrf2 k.o. mice to the same extent as in WT mice, indicating that DMF may as well act via alternative pathways (Schulze-Topphoff et al., 2016). A further study suggested that the hydroxycarboxylic acid receptor 2 (HCA_2) could contribute to the protective effects of DMF in EAE, since DMF could not ameliorate the EAE course in HCA_2k.o. mice (Chen et al., 2014). MMF was shown to be a potent agonist of the HCA_2 receptor, which is expressed on immune cells, especially neutrophils (Lukasova et al., 2011). Chen et al. assumed that DMF treatment could exert secondary immunomodulatory functions by impairing the recruitment of neutrophils.

DMF and MMF were also analyzed in the toxic cuprizone model, a model to investigate direct CNS effects of treatments independent of the peripheral immune system. MMF and DMF treatment revealed only minor effects on the demyelination of the CC (Moharregh-Khiabani et al., 2010). Furthermore, neither MMF nor DMF induced significant changes concerning the number of mature oligodendrocytes or OPCs. The cuprizone-induced microgliosis, astrogliosis and acute axonal damage were also not majorly changed by MMF or DMF treatment. MMF and DMF could slightly accelerate the remyelination in the CC.

1.3.3. DMF effects on CNS resident cells *in vitro*

DMF treatment in EAE showed that it exerts beneficial effects on different CNS cell populations. DMF increased the preservation of axons and neurons and reduced the number of activated

astrocytes (Linker et al., 2011; Reick et al., 2014). The effects of DMF were also investigated on microglia, endothelial cells, astrocytes, neurons and oligodendrocytes *in vitro*. Both, MMF and DMF application leads to an increased activation of antioxidant response pathways via induction of Nrf2 (Linker et al., 2011; Thiessen et al., 2010). DMF treatment of neurons and astrocytes *in vitro* resulted in an upregulation of a Nrf2-dependent antioxidant response and could significantly increase the cell viability after toxic oxidative challenge (Scannevin et al., 2012a). Low concentrations of DMF (10 µM) increase the synthesis and recycling of glutathione, an important intracellular antioxidant, in neuronal cells (Albrecht et al., 2012). Enhanced levels of antioxidant molecules (e.g. glutathione) are produced by oligodendrocytes when these were treated *in vitro* with DMF leading to an increased protection against oxidative stress (Albrecht et al., 2012). Furthermore, DMF decreases the synthesis of pro-inflammatory cytokines like TNF-α, IL-1β and IL-6 in activated astrocytes and microglia *in vitro* (Wilms et al., 2010). DMF also profoundly decreases the TNFα-induced expression of adhesion molecules E-selectin, ICAM-1 and VCAM-1 on endothelial cells and reduces lymphocyte rolling, firm adhesion and diapedesis *in vitro* (Wallbrecht et al., 2011).

1.3.4. DMF effects on immune cells *in vitro* and *in vivo*

Besides the induction of the Nrf2-dependent antioxidant response element (ARE) pathway, DMF and MMF were able to inhibit the translocation and DNA-binding of nuclear factor κB (NF-κB), resulting downstream in altered cell maturation, reduced inflammatory cytokine production and function of antigen-presenting cells (Ghoreschi et al., 2011; Gillard et al., 2015; Litjens et al., 2006; Loewe et al., 2001). Several studies could reveal that ARE induction can inhibit the NF-κB signaling pathway and indirectly regulate inflammatory chemokine and cytokine production (Wakabayashi et al., 2010).

Application of DMF or MMF *in vitro* reduces the CCL-2 induced chemotaxis of human monocytes that is needed for CNS infiltration (Cross et al., 2011). In addition, *in vitro* experiments with cultured mononuclear blood cells revealed that DMF has anti-inflammatory functions by inducing T-helper cell type 2 (Th2) immune responses (de Jong et al., 1996). The DMF metabolite MMF increases the production of IL-5 and IL-4, which are driving Th2 cell development. It was later shown, that this effect could be linked to a direct effect of MMF on dendritic cells (DCs) (Litjens et al., 2004a). MMF treatment of monocyte-derived DCs leads to a down-regulation of Th1 cell

responses, such as IFNγ secretion, by modulating the polarization of DCs. In humans and mice, DMF treatment stimulates the development of type II DCs that produce IL-10 and induce IL-4-producing Th2 cells *in vitro* and *in vivo* (Ghoreschi et al., 2011). Furthermore, *in vivo* DMF treatment of MS patients leads to an alteration of circulating T helper cell subsets by decreasing the frequencies of Th1 cells and increasing the Th2 cell proportions (Gross et al., 2015). $CD4^+$ and $CD8^+$ memory T cells are also decreased with the use of DMF whereas the regulatory T cell population remains unaltered. Recent studies revealed that DMF influences B cell subsets of patients with RRMS, resulting in an increased number of B cells with regulatory functions (Lundy et al., 2016).

1.4. Aim of the study

The oral agent dimethyl fumarate (DMF) shows efficacy in the therapy of RRMS. It is assumed that DMF mainly acts via modulating the peripheral immune system and especially by reducing the pro-inflammatory properties of T cells (Gross et al., 2015; Mrowietz et al., 1998). Additionally, DMF treatment is suggested to exert neuroprotective effects through the activation of the transcription factor Nrf2 which in turn mediates the activation of ARE. Whether DMF can exert direct neuroprotective effects independent of the peripheral immune system is controversially discussed. Furthermore, it is still unknown if DMF has any direct immunomodulatory effects on B cells whose role in MS pathogenesis became increasingly important in the recent years.

In the first part of my thesis it was investigated if DMF exerts any CNS intrinsic effects independent of peripheral inflammation. DMF effects were analyzed on:

A1. Neurodegeneration including apoptosis of oligodendrocytes, demyelination and axonal damage as well as

A2. Neuroregeneration investigating remyelination, oligodendrocyte preservation and maturation.

In the second part of my thesis it was studied if DMF treatment is effective in a B cell-mediated EAE model. DMF effects were investigated on:

B1. Clinical course and histopathology of B cell-mediated EAE.

B2. Activation, functional properties and subtypes of B cells and T cells during the acute phase of EAE.

2. Material and Methods

2.1. Material

2.1.1. Reagents

Table 2: Reagents

REAGENT	SOURCE OF SUPPLY
Acetic Acid	Merck Millipore, Germany
Agarose	Starlab GmbH, Germany
BD FACS Clean™	BD Biosciences, USA
BD FACS Flow™	BD Biosciences, USA
BD FACS Rinse™	BD Biosciences, USA
BD FACS™ Lysing Solution, 10x	BD Biosciences, USA
BD Pharm Lyse™, 10x	BD Biosciences, , USA
Boric Acid	Merck Millipore, Germany
Crystal Violet	Sigma Aldrich, USA
Cytofix/Cytoperm™	BD Biosciences, , USA
Cytofix™	BD Biosciences, USA
Chloral Hydrate	Merck Millipore, Germany
Citric Acid	Merck Millipore, Germany
DAB (3,3'-Diaminobenzidine)	Sigma-Aldrich Chemie GmbH, Germany
DAPI (4',6-Diamidino-2-Phenylindole)	Sigma-Aldrich Chemie GmbH, Germany
DDSA (2-Dodecenylsuccinic Acid Anhydride)	Serva Electrophoresis GmbH, Germany
DEPEX	VWR International, Germany
DMF (Dimethyl Fumarate)	Biogen Idec, USA
DMSO (Dimethyl Sulfoxide)	Sigma Aldrich, USA
EDTA (Ethylenediamine Tetraacetic Acid Disodiumsalt Dihydrate)	Carl Roth, Germany

Ethanol, 100%	Merck Millipore, Germany
Ethidium Bromide	Sigma Aldrich, USA
Eosin G	Merck Millipore, Germany
FCS (Fetal Calf Serum)	Sigma Aldrich, USA
Foxp3 Fixation/Permeabilization Concentrate	Ebioscience, USA
Foxp3 Fixation/Permeabilization Diluent	Ebioscience, USA
Foxp3 Permeabilization Buffer, 10x	Ebioscience, USA
Generuler™, 100 Base Pairs (bp) DNA Ladder Plus	ThermoFisher Scientific, USA
Go-Taq® DNA Polymerase Buffer, 5x	Promega, USA
HCl (Hydrochloric Acid)	Merck Millipore, Germany
H_2O_2 (Hydroxic Peroxide), 30%	Merck Millipore, Germany
HPMC (Hydroxypropylmethylcellulose)	Biogen Idec, , USA
Ionomycin	Sigma Aldrich, USA
Isopropyl Alcohol	Merck Millipore, Germany
L-Glutamine, 200 Mm	Sigma Aldrich, USA
LPS (Lipopolysaccharide)	Sigma Aldrich, USA
Mayer's Hemalum	Merck Millipore, Germany
NaCl (Sodium Chloride), 0.9% Solution, Sterile	B. Braun Melsungen AG, Germany
$NaCO_3$ (sodium carbonate)	Merck Millipore, Germany
$NaHCO_3$ (sodium hydrogen carbonat)	Merck Millipore, Germany
NaF (sodium fluoride)	Merck Millipore, Germany
Paraffin Oil	Carl Roth, Germany
PBS (Phosphate Buffered Saline), 10x	Biochrom AG, Germany
PBS (Phosphate Buffered Salt Solution), Sterile	Sigma Aldrich, USA

Penicillin, 10,000 Units	Sigma Aldrich, USA
Perm/Wash™ Buffer, 10x	BD Biosciences, USA
PFA (Paraformaldehyde), Powder	Merck Millipore, Germany
PMA (Phorbol 12-Myristate 13-Acetate)	Sigma Aldrich, USA
RPMI-1640 (Roswell Park Memorial Institute-1640)	Sigma Aldrich, USA
Sodium Pyruvate, 100 mM	Sigma Aldrich, USA
TMB (3,3',5,5'-Tetramethylbenzidine) Substrate Solution	Ebioscience, USA
Tris (Tris(Hydroxymethyl)Aminomethane)	Carl Roth, Germany
Trypan Blue	Sigma Aldrich, USA
Tween	Merck Millipore, Germany
β-Mercaptoethanol	Sigma Aldrich, USA

2.1.2. Solutions, buffers and cell culture media

Table 3: Solutions, buffers and cell culture media

SOLUTION	COMPOSITION
Blocking Buffer for Immunohistochemistry	PBS 10% FCS
CFA (Complete Freund's Adjuvant)	Paraffin oil 15% mannide monooleate 6.7 mg/ml *Mycobacterium tuberculosis* H37RA
Chloral Hydrate, 14%	distilled water 14% chloral hydrate

Citric Acid Buffer, 10 Mm	2.1 g citric acid 1 l distilled water NaOH, adjust to pH 6
Coating buffer	8.4 g NaHCO3 3.5 g NaCO3 1 l distilled water Stir filter, adjust to pH 9.5
Cryo medium	60% $RPMI_{complete}$ 20% DMSO 20% FCS
3,3'-Diaminobenzidine Tetrachloride (Dab) Working Solution	PBS 0.5 mg/ml DAB add 20 µl 30% hydrogen peroxidase per 50 ml DAB solution before use
ELISA wash buffer	200 ml 10x PBS 1 ml Tween 1.8 l distilled water
ELISA stop solution	1 N H_2 SO_4 solution
1% Eosin	70% isopropyl alcohol 1% eosin G stir filter, before use add 0,5% acetic acid

FACS (Fluorescence-Activated Cell Sorting) Buffer	PBS, sterile 2% FCS
1% HCl	1% HCl absolute 70% ethanol
MACS (Magnetic-Activated Cell Sorting) Buffer	PBS, sterile 0.5% FCS 2 mM EDTA pH 7.2
Neutralization buffer	40 mM Tris 250 ml distilled water
10x PBS	95.5 g PBS 1 l distilled water
RD1 buffer (ELISA block buffer)	200 ml 10x PBS 20 g BSA 1.8 l distilled water
$RPMI_{complete}$	RPMI-1640 10% FCS 1 mM sodium pyruvate 50 µM β-Mercaptoethanol 100 units penicillin 2 mM L-glutamine
TAE (Tris, acetic acid, EDTA) buffer	40 mM Tris 20 mM acetic acid 1 mM EDTA 1 l distilled water (adjusted to pH 8)
Tail lysis buffer	25 mM NaOH 2 mM EDTA 250 ml distilled water

2.1.3. Antibodies, enzymes and proteins

Table 4: Proteins, enzymes and inhibitors

PROTEINS, ENZYMES, INHIBITORS	SOURCE OF SUPPLY
BSA (bovine serum albumin)	SERVA Electrophoresis GmbH, Germany
Recombinant mouse MOG-protein$_{1-117}$	Monash University, Australia
PTX (pertussis toxin)	List biological laboratories, USA
DNase I	Roche, Basel, Switzerland
Dreamtaq green PCR master mix (2x)	Thermo Fisher Scientific, USA
Proteinase K	Sigma Aldrich, USA
Trypsin, 0.05%	Gibco/Invitrogen, USA
Golgistop™	BD Biosciences, USA

Table 5: Monoclonal antibodies for flow cytometry

SPECIFICITY	FLUOROCHROME	CLONE	DILUTION	SOURCE OF SUPPLY
B220	FITC	RA3-6B2	1:100	BioLegend
B220	PE-Cy7	RA3-6B2	1:100	BD Biosciences
CD1D	Pacific Blue	1B1	1:100	BioLegend
CD4	BV510	GK1.5	1:100	BioLegend
CD4	PE	RM4-5	1:100	BioLegend
CD5	PerCP-Cy5.5	53-7.3	1:100	BioLegend
CD8a	FITC	53-6.7	1:100	BioLegend
CD19	APC-Cy7	6D5	1:100	BioLegend
CD19	FITC	HIB19	1:100	BD
CD23	APC	B3B4	1:100	BioLegend

CD25	APC	PC61	1:100	BD Biosciences
CD27	FITC	LG.3A10	1:100	BioLegend
CD37	PE	Duno85	1:100	BioLegend
CD40	APC	3/23	1:100	BD
CD40	PE	5C3	1:100	BioLegend
CD38	Pacific Blue	90	1:100	BioLegend
CD69	PerCP-Cy5.5	H1.2F3	1:100	BD Biosciences
CD80	APC	16-10A1	1:100	BD Biosciences
CD80	PerCP-Cy5.5	2D10	1:100	BioLegend
CD86	PE	GL1	1:100	BD Biosciences
CD95 (FAs)	PE	Jo2	1:100	BD Biosciences
CD138	BV-605	281-2	1:100	BioLegend
Foxp3	PE	FJK-16s	1:100	e-bioscience
GL-7	FITC	GL7	1:100	BioLegend
IFNΓ	APC	XMG1.2	1:100	BioLegend
IgM	FITC	RMM-1	1:100	BioLegend
IgD	PE	11-26c.2a	1:100	BD Biosciences
IL-17	PE	TC11-18H10	1:100	BD Biosciences
MHC-II	Pacific Blue	AF6-120.1	1:100	BioLegend

MHC-II	PE	AF6-120.1	1:100	BD Biosciences

Table 6: Monoclonal antibodies for antigen-independent activation of T cells in vitro

SPECIFITY	CLONE	SOURCE OF SUPPLY
LEAF™ purified anti-mouse CD3	145-2C11	BioLegend
LEAF™ purified anti-mouse CD28	37.51	BioLegend

Table 7: Primary antibodies for immunhistochemical staining

SPECIFICITY	SPECIES/CLONE	ANTIGEN RETRIEVAL/FIXATION	DILUTION	SOURCE OF SUPPLY
APP	mouse/MAB348	microwave, citric acid buffer	1:2000	Merck Millipore
B220	rat	microwave, citric acid buffer	1:200	BD Pharmingen
Casp3	rabbit/C92-605	Microwave, Tris-EDTA	1:150	BD Biosciences
CD3	rat/ CD3-12	microwave, citric acid buffer	1:200	Biorad
CNPase	Mouse/SMI-91R	microwave, citric acid buffer	1:200	Covance
GFAP	mouse	microwave, citric acid buffer	1:300	Synaptic Systems
GFAP	rabbit	none	1:1000	DAKO
MAC3	Rat/ M3/84	microwave, citric acid buffer	1:200	BD Pharmingen
MBP	rabbit/62301	none	1:1000	DAKO
NogoA	rabbit	microwave, Tris-EDTA	1:50	Santa Cruz

Olig2	rabbit	microwave, Tris-EDTA	1:300	IBL
PLP	mouse	microwave, citric acid buffer	1:500	Biozol

Table 8: Secondary antibodies for immunohistochemical staining

SECONDARY ANTIBODY	DILUTION	MANUFACTURER
Anti-mouse IgG, biotinylated	1:200	GE Healthcare Europe GmbH, Germany
Anti-rabbit IgG, biotinylated	1:200	GE Healthcare Europe GmbH, Germany
Anti-rat IgG, biotinylated	1:200	GE Healthcare Europe GmbH, Germany

Table 9: Applied Kits

KIT	SOURCE OF SUPPLY
$CD4^+$ T cell isolation kit II, mouse	Miltenyi Biotec, Germany
Cell lineage panel kit, mouse	Miltenyi Biotec, Germany
Dylight 405 Antibody labeling Kit	Thermo Fisher Scientific, USA

2.1.4. Oligonucleotide primers

Table 10: Primers

NAME	SEQUENCE	SOURCE OF SUPPLY
Ja18-2D2	5'-CCC GGG CAA GGC TCA GCC ATG CTC CTG-3'	Eurofins Scientific, Germany
Va3-2-2D2-M	5'-GCG GCC GCA ATT CCC AGA GAC ATC CCT CC-3'	Eurofins Scientific, Germany

2.1.5. Consumables

Table 11: Consumables

REAGENT	SOURCE OF SUPPLY
Bottle Top Filter, 0.2 µm	Sarstedt, Germany
Cell Culture Plates, Flat Bottom (6 Well, 24 Well, 96 Well)	Greiner bio-one, Austria
Cell Strainer (70 µm)	Greiner bio-one, Austria
FACS Tube, 5 ml	Sarstedt, Germany
LS Columns	Miltenyi Biotec, Germany
Needles	BD Biosciences, USA
Nunc™ Maxisorp® 96 Well ELISA Plate	Thermo Scientific, USA
96 Well Plate Round	Sarstedt, Germany
Pre-Separation Filters, 30 µm	Miltenyi Biotec, Germany
Syringes	BD Biosciences, USA
Serum Microtubes	Sarstedt, Germany
Tubes (50 ml, 15 ml, 10 ml, 2 ml, 1,5 ml, 0.2 ml)	Sarstedt, Germany

2.1.6. Technical devices

Table 12: Technical devices

DEVICE	SOURCE OF SUPPLY
Bx51 Olympus light microscope equipped with DP71 digital and XM10 monochrome camera	Olympus, Germany
Centrifuge 5415 R	Eppendorf, Germany
Centrifuge 5810 R	Eppendorf, Germany
FACS LSR II	BD Biosciences, USA
GentleMACS™ Dissociator	Miltenyi Biotec, Germany
Cell Incubator BBD6220	Thermo Scientific, USA
IMARK™ Microplate Reader	Bio-Rad, Germany
Microscope	Olympus
Microtome	Leica, Germany
Microwave	Bosch, Germany
Neubauer Chamber	Superior Marienfeld , Germany
QuadroMACS™ Separator	Miltenyi Biotec, Germany
T3 Thermocycler	Biometra, Germany
TP 1020 (Tissue Processor)	Leica, Germany

2.1.7. Software

Table 13: Software

SOFTWARE	APPLICATION	SOURCE OF SUPPLY
BD biosciences FACSDiva software 6.1.2	Data acquisition flow cytometry	BD Biosciences, USA
FlowJo 10.1	Data analysis flow cytometry	Tree Star Inc., USA

GraphpadPrism 6	Statistical analysis Graphs	GraphPad software Inc., USA
ImageJ 1.47d	Data analysis histology	National Institutes of Health, USA
PSremote 1.6.5	Gel documentation	Breeze systems limited, UK

2.2. Patients

Blood samples were obtained from non-treated and DMF-treated MS patients. MS patients receiving DMF were treated for at least six months.

Table 14: Clinical characteristics of MS patients

	Non-treated	**DMF-treated**
Age (years)	36 ± 10	36 ± 14
Sex	4 female, 2 male	5 female, 1 male
Disease duration (years)	7 ± 6	5 ± 5
Therapy duration (month)	-	6.5 ± 1
EDSS	1.3 ± 0.4	0.8 ± 1.0

2.3. Animals

C57Bl/6 mice

8-12 week old female C57BL/6J mice were obtained from Charles River laboratories, Germany. Each experimental group contained 5-8 mice and each experiment was performed at least twice. All experiments were approved by the Lower Saxony authorities for animal experimentation.

2D2 mice

2D2 animals were generated and characterized by Bettelli and colleagues in 2003. 90-95% of the CD4+ T cells in 2D2 mice express the MOG35-55-specific T cell receptor Vα3.2/ Vβ11 (Bettelli et al., 2003). 2D2 CD4+ T cells were used as reporter cells in several proliferation assays.

Nrf2 k.o. mice

A homozygous Nrf2 k.o. breeding pair was obtained from Jackson laboratory. Nrf2 k.o. animals were generated in 1996 by Chan and colleagues (Chan et al., 1996). In Nrf2 k.o. mice the genetic function of the transcription factor Nrf2 is abolished. 9-10 week old Nrf2 k.o. mice were cuprizone fed and used for further experiments.

Breeding

All transgenic mice were bred in the central animal facility of the University Medical Center Goettingen.

Housing

The mice were held under conventionally and specific pathogen free (SPF) conditions, they had access to food and water ad libitum and a 12h/12h light/dark cycle. Mice were allowed to adapt to the new environment for seven days before each experiment.

2.4. Methods

2.4.1. Genotyping

For the genotyping of 2D2 mice, tissue was obtained via a tail biopsy. After DNA extraction, transgenes were amplified with specific primers and separated by agarose gel electrophoresis as described below. All genotyping was performed by Ms. Katja Grondey, Mr. Jan Einar Albin and Mr. Julian Koch (Department of Neuropathology, University Medical Center Germany).

DNA extraction

DNA was isolated from tail biopsies of 2D2 mice. The tissue was digested in 100 µl lysis buffer at 99°C for 30 min. Afterwards 100 µl neutralization buffer was added.

PCR reaction

Each reaction sample contained 1 µl genomic DNA, 10 µl Dream Taq® PCR Mix 2x, 1 µl of each primer and 7 µl water (nuclease free).

Primer 1: 5'-CCC GGG CAA GGC TCA GCC ATG CTC CTG-3'

Primer 2: 5'-GCG GCC GCA ATT CCC AGA GAC ATC CCT CC-3'

PCR conditions

- Initial denaturation: 94°C, 2 min
- 35 cycles: Denaturation: 94°C, 1 min

Annealing: 58°C, 1 min

Extension: 72°C, 1 min

- Final extension: 72°C, 10 min

Agarose gel electrophoresis

For the analysis of PCR products, 5 µl of the sample were loaded on an agarose gel (2%(w/v) in TAE buffer) containing 3 µl ethidium bromide/GelRed. Electrophoresis was performed in a Sub-Cell GT Agarose Gel Electrophoresis System at 120V for 45 min. Evaluation of PCR products was done by visualization and documentation by UV-light in a gel-documentation device.

2.4.2. Cuprizone treatment

Mice received cuprizone at a 0.25% dosage ad libitum. Therefore 2.5 g cuprizone were mixed with 1000 g ground mouse chow. Mice were treated for one week or two weeks with cuprizone to analyze the apoptosis of oligodendrocytes and for six weeks to investigate the demyelination of the corpus callosum (CC). Body weights of the animals were measured weekly and transformed into percentage of initial weight. Therefore the mean of the initial body weights of each group was set to a hundred percent.

To investigate the effects on remyelination, mice were fed with cuprizone for 5 weeks, then the cuprizone diet was stopped and mice were treated with either DMF or control for one week or three days.

2.4.3. EAE induction

Mice were subcutaneously injected with 100 µg recombinant mouse MOG protein$_{1-117}$ emulsified in complete Freund's adjuvant. Directly and 48h after immunization mice were intraperitoneally injected with 200 ng Pertussis toxin. Mice were scored daily according to a 0-5 scale score as described by (Weber et al., 2010). The rMOG$_{1-117}$ was provided by the group of Claude C. Bernard (Monash University, Australia).

2.4.4. DMF treatment

Dimethyl fumarate (BG12) was synthesized at Biogen Idec. The compound was dissolved in a 0.8% hydroxypropyl methylcellulose solution (HPMC). The solution was stored at 8°C and used within a week. Cuprizone mice were treated twice daily with 15 mg/kg DMF or once daily with 100 mg/kg DMF. DMF was administered via oral gavage at a volume of 10 µl/g body weight. Control animals received 0.8% HPMC solution (control) as sham treatment.

EAE mice were treated twice daily with 15 mg/kg DMF or control. Preventive treatment started two days prior to immunization. When mice were treated therapeutically, treatment started when mice showed an EAE score of two or higher. For clinical analysis mice were treated until day 50 or 60 post immunization, for immunological analysis animals were treated until day 12 p.i.

2.4.5. Extraction of mouse plasma

Mice received 0.25% cuprizone and DMF or control for one week or for six weeks. To measure MMF levels, mice were sacrificed at the end of the experiment and blood samples were collected in a tube containing 4µl NaF solution (250 mg/ml in dH_2O). Samples were centrifuged latest 10 min after collection. The plasma was stored at – 80°C and later analyzed by mass spectrometry.

To measure the level of anti-MOG antibodies of mice during EAE, blood was collected from the facial vein into sera tubes and centrifuged at room temperature for 5 min at 10.0000 rpm. The plasma samples were stored at -20°C.

2.4.6. Analysis of monomethyl fumarate (MMF) in plasma and brain

MMF measurements were performed by the lab of Rob Scannevin (Biogen, Cambridge, USA). Therefore, 25 µL of either plasma or tissue homogenate samples were extracted by protein precipitation with acetonitrile containing 4C13-MMF as the internal standard. The aliquots of homogenization solution (plasma with 12.5 mg/mL of NaF) were added to the tissue samples. The tissue samples were homogenized at 6.5 m/s for 60 s on a Fast Prep Tissue Homogenizer prior to protein precipitation. The concentrations of MMF in plasma and brain samples were determined using qualified LC-MS/MS assays in the respective matrices. Data collections and integrations were accomplished using an API 5500 triple quadrupole mass spectrometer with a turbo ion spray interface (AB Sciex, Foster City, CA), and Analyst software (version 1.6.1). The peak area ratios of MMF relative to its internal standard were used to construct a standard curve using a quadratic regression with a 1/x2 weighting.

2.4.7. Detection of anti-MOG antibodies

For the measurement of anti-MOG Ab levels, a 96 well plate was coated with $rMOG_{1-117}$ diluted 1:200 (stock 2 mg/ml) over night at 4°C. The next day the plate was washed 3x with wash buffer and blocked with 200 µl/° RD1 buffer for 1h at RT shaking on a shaker plate (500 rpm). During this incubation time mouse plasma samples were diluted 1:40,500. Afterwards plates were washed 3x with wash buffer and 100 µl sample per well were added and incubated for 1.5 h at RT shaking on a shaker plate. Plates were washed 3x with wash buffer and 100 µl of a mixture including detection Ab (IgG mouse 2 mg/ml, diluted 1:6000 in RD1) und Streptavidin (diluted 1:40 in RD1) were added into each well and incubated for 1 h at RT in the dark. Plates were washed 4x with wash buffer and 100 µl of TMB solution were added and incubated until wells turned blue (15-20 min). 4x wachen. The reaction was stopped with ELISA stop buffer. The OD was determined at 450 nm with 540 nm wavelength correction using the iMark™ microplate reader.

2.4.8. Analysis of immune cells ex vivo

For the immunological readout, spleen and inguinal lymph nodes were isolated from control- or DMF-treated animals. After preparing a single cell suspension, immune cells were investigated ex vivo via flow cytometry.

2.4.8.1. Preparation of single cell suspensions

Single cell suspensions were prepared from spleen and lymph node for further investigation. Therefore, cells were disrupted by mechanical force through a sterile 70 µm cell strainer. After two washing steps, splenocytes and lymphocytes were further processed dependent on the following experiment. Centrifugation steps with tubes were performed for 10 min at 300 x g and 4°C and with plates for 8 min at 300 x g and 4°C. Cells were washed with PBS, FACS or MACS buffer depending on the further analysis. For a direct flow cytometric analysis of B and T cells, splenocytes and lymphocytes were washed with FACS buffer and transferred to a 96 well plate. For further isolation of B cells and T cells by magnetic-activated cell sorting (MACS), splenocytes were washed twice with 20 ml of MACS buffer. Cell numbers were determined prior to further analyses (see 2.4.7.4).

2.4.8.2. Preparation of peripheral blood leukocytes from mice

For analysis of the cell distribution in the blood under DMF treatment, blood samples were obtained by puncture of the facial vein. Several drops of blood were diluted in 300 µl PBS containing 1 mM EDTA and were transferred to a 5 ml FACS tube. 1 ml of FACS buffer was added and the tubes were centrifuged. Erythrocytes were lysed by resuspending the pellet in 1 ml of BD Biosciences Pharm lyse™ solution (pre-diluted 1:10 in bidistilled water). Lysis was performed for 3 min at RT and stopped by adding 3 ml of FACS buffer. FACS tubes with peripheral blood cells were centrifuged for 8 min at 300 x g at 4°C and the pellets were resuspended in 200 µl FACS buffer and transferred to a 96 well plate.

2.4.8.3. Preparation of human peripheral blood mononuclear cells (PBMCs)

To investigate the B cell frequency and activation under DMF treatment, blood samples were obtained from non-treated and DMF-treated MS patients. Afterwards, the collected blood was transferred into a 50 ml tube and 1:1 diluted with PBS. The blood/PBS mixture was carefully layered over 15 ml of Biocoll solution in a 50 ml tube and samples were centrifuged at 400 x g and 20°C for 35 min without acceleration and brake. The mononuclear cell layer is gathered at the interphase and was carefully removed with a 10 ml volumetric pipette in a new 50 ml tube. Then 50 ml $RPMI_{complete}$ were added and samples were centrifuged for 10 min at 300 x g and 4°C.

Afterwards this washing step was repeated twice. Cell were counted in the Neubauer chamber and stored at –80°C in cryo medium.

2.4.8.4. Cell counting

For the determination of cell numbers, a Neubauer chamber was used. The cell suspension was diluted 1:10 in trypan blue (pre-diluted 1:10 in PBS) prior to counting to exclude dead cells. Four squares with a surface of 1 mm^2 and a volume 0.1 µl each were counted for every sample. The concentration of cells in the original sample was calculated by the following formula:

Cells counted/4 * 10 * 10^4 = cells/ml

The total cell number was extrapolated to the sample volume.

2.4.9. Flow cytometry

The effects of DMF on different cell populations of the immune system were analyzed by flow cytometry. Single cell suspensions were stained with different combinations of fluorochrome-labeled antibodies and cell populations were analyzed using a FACS LSR II and the BD FACSDiva Software 6.1.2. The staining procedure was always performed in 96 well round bottom plates, plates were centrifuged for 8 min at 300 x g and 4°C and cells were washed with 200 µl FACS buffer.

2.4.9.1. FACS staining procedure of splenocytes, lymphocytes and peripheral blood leucocytes

Isolated cells were centrifuged and washed with FACS buffer. Cells were resuspended in 30 µl blocking buffer, consisting of anti-CD16/CD32 antibody diluted 1:100 in FACS buffer, and incubated for 10 min at 4°C. The fluorochrome-labeled antibodies per staining were diluted 1:50 in FACS buffer and 30 µl of this master mix was added to each well (final dilution 1:100). The samples were incubated for 15 min at 4°C in the dark. Following incubation, the wells were filled with 150 µl FACS buffer and plates were centrifuged. Cells were washed and resuspended in a mixture of 100 µl FACS buffer and 100 µl 4% PFA and incubated for 30 min. The fixed cells were then washed, resuspended in 200 µl FACS buffer and transferred to a 5 ml FACS tube. Fixed cells were analyzed by flow cytometry.

Thawed human PBMCs were counted in a Neubauer chamber and 1x10^6 cells were transferred to a 5 ml tube. The samples were washed twice with FACS buffer and afterwards stained with 50 µl of

a master mix containing fluorochrome-labeled antibodies (diluted 1:100 in FACS buffer). The samples were incubated for 15 min at 4°C in the dark and afterwards the samples were washed twice with 1 ml of FACS buffer. Finally cells were resuspended in 200 µl FACS buffer and analyzed by flow cytometry.

2.4.9.2. Intracellular detection of Foxp3

For the intracellular detection of Foxp3, splenocytes and lymphocytes were isolated as described above. Afterwards surface molecules were stained with the usual FACS staining procedure. But instead of the fixation step with PFA, cells were fixed in 100 µl Foxp3 fixation concentrate diluted 1:3 in dilution buffer overnight at 4°C. The next day, 100 µl Perm/Wash™ buffer were added to each sample and plates were centrifuged. Afterwards the samples were washed two times with 100 µl Perm/Wash™ buffer. The anti-Foxp3 antibody was diluted 1:100 in permeabilization buffer (prediluted 1:10 in bidistilled water) and 50 µl of the staining solution was added to each sample. Cells were incubated for 1 h at 4°C in the dark. After incubation, samples were washed two times with 100 µl of Perm/Wash™ buffer and once with FACS buffer. Finally, cells were resuspended in 150 µl FACS buffer and transferred to FACS tubes. Samples were analyzed by flow cytometry.

2.4.9.3. Intracellular detection of cytokines

To investigate the effects of DMF on the frequency of IL-17- and IFNγ-producing T cells, splenocytes and lymphocytes were isolated from immunized mice, treated with control or DMF *in vivo*. 500,000 cells were seeded per well of a 96 well round bottom plate and stimulated with 200 µl $RPMI_{complete}$ supplemented with ionomycin (0.5 µg/ml) and PMA (0.05 µg/ml) for 5 h at 37 °C and 5% CO2. After 3 hours, 100 µl supernatant was collected and 1 µl GolgiStop™ was added to each sample. Afterwards, a surface staining was performed as described above. Cells were fixed in Cytofix/Cytoperm™ over night at 8°C. The next day, cells were washed twice with 100 µl Perm/Wash™ buffer (10x) diluted 1:10 in bidistilled water. Anti-IL-17 and anti-IFNγ antibodies were diluted 1:50 in Perm/Wash™ buffer and 50 µl of the staining solution was added to each well. Cells were incubated with the staining antibodies for 1 h at 4°C in the dark. Afterwards, the cells were washed twice with 150 µl of Perm/Wash™ buffer and plates were centrifuged. Cells were washed once with FACS buffer, resuspended in 150 µl of FACS buffer and analyzed by flow cytometry.

2.4.10. Co-culture experiments

2.4.10.1. Purification of CD4$^+$ T cells and B cells

For co-culture and ex-vivo experiments, CD4$^+$ T cells or B cells were isolated from spleens of naïve C57BL/6 and 2D2 mice using MACS. Therefore, splenocytes were isolated as described above, but were washed immediately two times with 20 ml of MACS buffer and counted in a Neubauer Chamber. CD4$^+$ T cells were purified using the CD4$^+$ T cell isolation kit II (mouse, BD), B cells were purified using the Lineage panel (mouse, BD). LS columns and the QuadroMACS^{TM} separator were used for separation of cells following the manufacturer's instructions. After the purification, cells were washed in RPMI$_{complete}$ and. The specific cell number was either directly put into culture, CFSE labeled for further experiments (see 2.4.9.3) or co-cultured with B cells.

2.4.10.2. rMOG binding assay

To analyze the antigen-binding capacity of control-or DMF-treated B cells, 500,000 purified B cells were transferred into each well and incubated with 20 µg/ml rMOG$_{1-117}$ labeled with DyLight^{TM} 405 for 2h at 37°C and 5% CO_2. The rMOG$_{1-117}$ was previously labeled with the use of the DyLight^{TM} 405 Antibody labeling kit following the manufacturer's instructions. The labeling was performed by Ms. Elke Pralle (Department of Neuropathology, Göttingen). After the incubation, B cells were washed with 200 µl FACS buffer, afterwards resuspended in 200 µl FACS buffer and immediately analyzed by flow cytometry.

2.4.10.3. Analysis of T cell proliferation by CFSE dilution

The effect of DMF-treated B cells on T cell proliferation *in vitro* was assessed by CFSE-staining of CD4$^+$ T cells and subsequent flow cytometric analysis of CFSE dilution. CFSE can penetrate the intact cell membrane and binds irreversibly to intracellular proteins. Upon proliferation, the cytoplasm is shared between the two daughter cells and therefore the fluorescence intensity of CFSE is halved at each cell division. The CFSE profile of dividing cells can be analyzed by flow cytometry (Parish, 1999). CD4$^+$ T cells were isolated from the spleen of naïve C57Bl/6J or 2D2 mice and purified by MACS separation (see 2.4.9.1). CD4$^+$ T cells were counted in a Neubauer chamber (see 2.4.7.4) and cells were resuspended in 1 ml PBS. The CFSE stock solution (5 mM) was diluted 1:1,000. Afterwards 200 µl of the CFSE solution was mixed with 800 µl of the cell suspension. Cells were then incubated for 15 min at 37°C in the dark. The staining reaction was stopped by addition of 20 ml cold RPMI$_{complete}$ and cells were centrifuged for 10 min at 1250 rpm and 4°C.

The supernatant was discarded and cells were washed again in 20 ml of $RPMI_{complete}$. Finally, cells were resuspended in $RPMI_{complete}$ and counted in a Neubauer chamber (see 2.4.7.4). The appropriate number of CFSE-labeled $CD4^+$ T cells was then used in cultures for different proliferation experiments. T cell proliferation was analyzed by measuring the CFSE dilution using flow cytometry.

2.4.10.4. Co-culture of B cells with $CD4^+$ T cells

To investigate the effect of DMF on the antigen-presenting function of B cells, co-culture assays were performed. Therefore, mice were immunized with $rMOG_{1-117}$, treated with DMF or control until d12 p.i. *in vivo* and B cells were purified as described above. Splenic T cells were purified (see 2.4.9.1) from 2D2 mice and labeled with CFSE (see 2.4.9.3). 500,000 B cells and 20,000 CFSE-labeled T cells were seeded in 200 µl $RPMI_{complete}$ per well of a 96 well flat bottom plate. The co-culture was then stimulated with 0, 25 or 50 µg/ml $rMOG_{1-117}$. Cells were cultured for 72 h (37°C, 5% CO_2) and stained for T cell and B cell markers (see 2.4.8.1). Finally, T cell proliferation and expression of activation markers was measured by flow cytometry.

2.4.11. In vitro stimulation of cytokine secretion

To investigate effects of DMF on the proliferation of T cells *ex-vivo*, splenocytes were isolated from naïve animals treated with DMF or control for 19 days *in vivo*. T cells were purified by MACS separation and stained with CFSE as described above. Afterwards 20,000 T cells were transferred to each well of a 96 flat bottom well plate. This plate was previously coated with different concentrations of anti-CD3 and anti-CD28 antibodies over night at 8°C. T cells were incubated for 72 h at 37°C and 5% CO_2. T cell proliferation was investigated by FACS.

2.4.12. Detection of cytokines using ELISA

T cells are potent producers of a variety of cytokines. To analyze the DMF effects on this effector function, cytokine concentrations in the supernatant of stimulated single- and co-cultures were measured by ELISA.

T cells were stimulated as described in 2.4.10 and IFNγ and GM-CSF secretion was analyzed. ELISA was performed using the Mouse IFNγ or GM-CSF ELISA MAX™ standard set. All standards and samples were run as duplicates. The capture antibody was diluted 1:200 in coating buffer and the 96 well plate was coated with 100 µl/well over night at 4°C.

The next day the plate was washed 3x with wash buffer and blocked with 200 µl/well RD1 buffer for 1h at room temperature shaking on a shaker plate (500 rpm). While the plate was being blocked standard solutions were prepared as described in the manufacturer's instruction. Afterwards plates were washed 3x with wash buffer and 30 µl/well samples and standard dilutions were added and incubated over night at 4°C. The next day plates were washed 3x with wash buffer and 100 µl detection antibody (diluted 1:100 in RD1 buffer) were added. The plates were incubated for 2 h at room temperature with shaking (500 rpm). After incubation plates were washed 3x with wash buffer and 100 µl Avidin-HRP solution was added to each well, plate incubated for 30 min shaking (500 rpm) in the dark. Thereafter, plates were washed 4 times with wash buffer and 100 µl TMB substrate solution were added and incubated until wells turned blue in color (20-30 min). The reaction was stopped with ELISA stop buffer. The OD was determined at 450 nm with 540 nm wavelength correction using the iMark™ microplate reader.

2.4.13. Histology

Sample preparation, histochemical and immunohistochemical stainings were performed by Ms. Katja Grondey, Mr. Jan Einar Albin and Ms. Mareike Gloth (Department of Neuropathology, University Medical Center Germany).

2.4.13.1. Perfusion, tissue collection and sample preparation

At the end of the in vivo experiments, mice were injected with a lethal dose of 14% chloral hydrate solution. After mice were checked for loss of consciousness and protective reflexes, the perfusion was performed by puncturing the left heart ventricle and rinsing the blood system first with PBS followed by a solution of 4% PFA. Brains, spleen and a part of the liver were collected and stored in 4% PFA at 8°C for 2 days post-fixation. Afterwards the samples were transferred to PBS and stored at 8°C for 24 h.

For the cuprizone experiments, brains were sliced in 4 transverse sections. For EAE Experiments, the spinal cord was collected additionally and dissected into 10 to 12 sections.

Before the paraffin embedding, the tissue was washed in water and then gradually dehydrated overnight. This was done by an automated tissue processor which is performing a graded alcohol/xylene/paraffin series. Paraffin blocks were sliced in 1 µm thick sections using a sliding microtome, and then mounted on glass slides.

Prior to the start of the staining procedure, the sections had to be deparaffinized. Therefore the slices were incubated for at least 30 min at 54 °C and then rehydrated using the following steps.

4x 10 min xylol

1x 5 min isoxylol

2x 5 min 100% isopropyl alcohol (IPA)

1x 5 min 90% isopropyl alcohol (IPA)

1x 5 min 70% isopropyl alcohol (IPA)

1x 5 min 50% isopropyl alcohol (IPA)

Distilled water

After finishing the staining, the stained tissue sections were dehydrated by performing the described series above in reverse order. This time the incubation time was only 2-3 min to avoid a weakening of the staining. As a final step the stained sections were mounted in DePex medium.

2.4.14. Histochemical staining

Hematoxylin and eosin (HE) staining

To obtain a general overview of the tissue, a HE staining was performed. This staining was used to analyze inflammation and apoptosis. Hematoxylin stains basophilic nucleoproteins which results in blue colored cell nuclei. Eosin is binding acidophilic and basic extra- and intracellular proteins and marks thereby the parenchyma red. For the staining, sections were deparaffinized and rehydrated as described above. Slides then were incubated in Mayer's hemalaun for 5 min. Afterwards tissue sections were rinsed with dH_2O. The sections were differentiated by shortly dipping them in 1% HCL-alcohol (1% HCl-alcohol in 90% isopropyl alcohol). The sections were then blued by rinsing them under tap water. For the staining of the parenchyma the slides were incubated in 1% eosin for 5 min (1% eosin in 70% isopropyl alcohol + 10 drops glacial acetic acid). Finally the sections were rinsed with dH_2O, dehydrated and mounted in DePex medium.

Luxol Fast Blue/Periodic Acid Schiff (LFB/PAS staining)

LFB/PAS staining was performed to visualize myelin. Myelin is stained deep blue by LFB through the binding to lipoproteins. In contrast, PAS colors demyelinated parenchyma and also grey matter

in pink. At first, the sections were deparaffinized and rehydrated till the 90% IPA. Following the 90% IPA, the slides were put directly into the LFB solution over night at 60°C. The next day, the slides were washed in 90% IPA and differentiated by shortly dipping them into 0.05% lithium carbonate solution followed by a short dip into 70% IPA and a rinsing step with dH_2O. Then the sections were incubated in 1% periodic acid for 5 min and rinsed for 5 min under flowing tap water. Slides were shortly washed with dH_2O and afterwards incubated in Schiff's solution for 20 min. Slides were washed under tap water for 5 min and incubated in Mayer's hemalaun for 2 min. Slides were shortly dipped in dH_2O and afterwards differentiated in 1% HCl-alcohol (1% HCl-alcohol in 90% isopropyl). Sections were blued by rinsing under tap water for 10 min. Finally the tissue was dehydrated and mounted in DePex medium.

Bielschowsky silver impregnation

The Bielschowsky silver staining was used to analyze the axonal density. In this staining the axons appear black and the parenchyma yellow/ brownish. For this staining, the sections were deparaffinized and rehydrated. Slides were washed 3 times in dH_2O and then incubated for 20 min in a 20% silver nitrate solution. The slides were washed with ddH_2O and a 32% ammonium hydroxide solution was added dropwise to the used silver nitrate solution until the brownish solution becomes clear. The slides were incubated in the cleared silver nitrate/ammonium hydroxide solution for 15 min in the dark. After incubation, slides were transferred into ddH_2O containing 3 drops of ammonium hydroxide. 10 drops of a developer solution were added to the silver nitrate/ammonium solution and slides were incubated until the sections showed a deep brown color and transferred into dH_2O. The sections were incubated with a thiosulfate solution for 2 min and subsequently rinsed with tap water. Slides were rehydrated and mounted in DePex.

2.4.15. Immunohistochemical staining

For the detection of specific cell markers, immunohistochemical stainings with antibodies were used. The signal visualization was performed with the avidin biotin method. Therefore, the tissue was incubated with specific primary antibodies specific for the antigen of interest. Afterwards a further incubation step followed with a biotin conjugated secondary antibody directed against the primary antibody.

For a detailed list of the antibodies used for mouse tissue see Table 7.

The visualization of the signal is obtained by the binding of the avidin coupled peroxidase (POX) and the oxidation of DAB by POX in the presence of H_2O_2. The fixation of the tissue can influence the binding efficacy of several antibodies. For a better antigen retrieval heat, acid or protease treatments were used.

The immunohistological stainings were performed as follows: At first, the tissue was deparaffinized, rehydrated and rinsed 3x with dH_2O. For the antigen retrieval with citric acid- or Tris-EDTA buffer, the slides were placed in polystyrene cuvettes. Those cuvettes were filled with 1mM citric acid buffer (pH 6) or 1mM Tris-EDTA buffer (pH 9) and boiled 5 times in a microwave at 800W for 3 min.

The cuvettes were alternately filled with buffer or dH_2O after each of the boiling steps.

For the antigen retrieval with the proteinase solution the slides were incubated in a 37°C warm proteinase solution for 10 min and rinsed two times with dH_2O.

The slides were washed with PBS and incubated with 3% H_2O_2 for 20 min at 4°C to block endogenous peroxidase and reduce unspecific signals. Afterwards the slides were rinsed 3 times with PBS. The slides were pre-incubated with 10% FCS (in PBS) for 20 min at RT in a humidified chamber to prevent unspecific antibody binding. The slides were then incubated with the primary antibody (diluted in 10% FCS/PBS) over night at 4 °C in a humidified chamber. The slides were rinsed 3 times with PBS and incubated with biotin conjugated secondary antibody (diluted in 10% FCS/PBS) for 1 h at RT in a humidified chamber. The slides were rinsed with PBS for 3 times and incubated with 0.1% POX (diluted in 10% FCS/PBS) for 1 h at RT in a humidified chamber. Afterwards, the slides were again rinsed with PBS 3 times. For the signal development, the slides were put into DAB solution for several minutes and then rinsed 3 times with PBS. For the detection of mouse CD3 positive cells, the DAB signal was amplified with 2% copper sulfate in 0.9 % sodium chloride for 10 min. The slides were washed with dH_2O. The nuclei were counterstained with Meyer's hemalaun solution for 30 sec followed by a short dip (1 s) in dH_2O and a short wash step in dH_2O. The differentiation was performed by a short dip into 1 % HCl-alcohol (1% HCl-alcohol in 90% isopropyl alcohol). The blueing of the tissue was done by rinsing the slides under tap water for 10 min. The slides were dehydrated and mounted in DePex medium.

2.5. Morphometry

Cuprizone: The number of cells stained with the corresponding antibodies was determined over the whole corpus callosum defined by an ocular morphometric grid at a 400x magnification and shown as cells/mm². For the determination of demyelinated areas of the corpus callosum, myelinated as well as demyelinated area of the corpus callosum was measured after LFB/PAS, PLP or MBP staining using ImageJ software. The percentage of demyelinated area was calculated relative to the whole area of the corpus callosum.

EAE: The number of cells stained with the corresponding antibodies was determined in at least 6 spinal cord sections defined by an ocular morphometric grid at a 400x magnification and shown as cells/mm². Inflammatory infiltrates were analyzed via a semi quantitative score (0 = no inflammation, 1 = slight inflammation, 2 = moderate inflammation, 3 = strong inflammation) after H&E staining in at least 6 spinal cord sections. To determine the white matter demyelination, myelinated and demyelinated areas were measured in at least 6 spinal cord cross sections after LFB-PAS staining using ImageJ software. The percentage of demyelinated area was calculated relative to the whole white matter area.

2.6. Data analysis and statistics

The software BDDiva and FlowJo 10.1 were used to analyze all flow cytometric data.

Statistics were calculated using the software GraphPad Prism 6. Data were tested for normal distribution with the help of the D'Agostino & Pearson omnibus normality test. To compare two experimental groups, unpaired t-tests were used for parametric data and Mann-Whitney U tests for non-parametric data. For comparison of more than two experimental groups one way ANOVA with Sidak post test was used. Statistical significance was defined as $p<0.05$. Data in text and figures are presented as mean ± SD and EAE Scores and antibody titer as mean ± SEM.

3. Results

3.1. DMF treatment in the cuprizone model

The oral agent DMF has beneficial effects on the relapse rate and different MRI parameters in RRMS patients (Fox et al., 2012; Gold et al., 2012). Several *in vitro* studies demonstrated the immunomodulatory effects of DMF and its metabolite MMF on peripheral immune cells like T cells, B cells and dendritic cells (Litjens et al., 2004a; Mrowietz and Asadullah, 2005; Treumer et al., 2003; Zhu and Mrowietz, 2001). Besides its immunomodulatory effects, the question if DMF exerts direct neuroprotective functions is unclear and the mode of action is still not fully understood (Moharregh-Khiabani et al., 2010; Scannevin et al., 2012b). To address the question if DMF has CNS intrinsic neuroprotective effects, independent of the peripheral immune system, the cuprizone model was used.

3.1.1. DMF effects after short-term cuprizone intoxication

Initial experiments were performed using two different dosages of DMF, 15 mg/kg twice daily and 100 mg/kg once a day (data not shown), to determine the most appropriate treatment dosage in regard to efficacy. Data evaluation revealed that treatment with 15 mg/kg DMF twice a day was more effective and therefore only this dosage was used in subsequent experiments. The DMF short-term treatment was studied using 9 to 10 week old C57BL/6 mice which were fed with 0.25% cuprizone and simultaneously treated with control (HPMC) or 15 mg/kg DMF twice a day for 7 days or 2 weeks. Clinical and histological analyses were performed to assess control- and DMF-treated mice.

3.1.1.1. DMF treatment decreased the cuprizone-induced weight loss of C57BL/6 mice

Mice which are fed with cuprizone show a profound body weight loss during the first two weeks of cuprizone exposure. Furthermore, DMF is known to exert gastrointestinal side effects, like abdominal pain, which may lead to a decreased feed uptake by mice. For these reasons, body weight of control- and DMF-treated mice was evaluated every day of cuprizone treatment. After 4 days of 0.25% cuprizone treatment, control-treated mice lost significantly more weight compared to DMF-treated mice which persisted till 6 days after cuprizone treatment (Figure 1). The body weight of DMF-treated mice (day 4: 92.7% ± 1.46 %, day 5: 92.7% ± 1.2%, day 6: 93.1% ± 1.6%) remained significantly higher than the body weight of control-treated animals (day

4: 87.4% ± 1.2%, p<0.05; day 5: 86.5% ± 1.8%, p<0.01; day 6: 86.4% ± 2.6%,p<0.05). No further weight loss was detectable at later time points (data not shown).

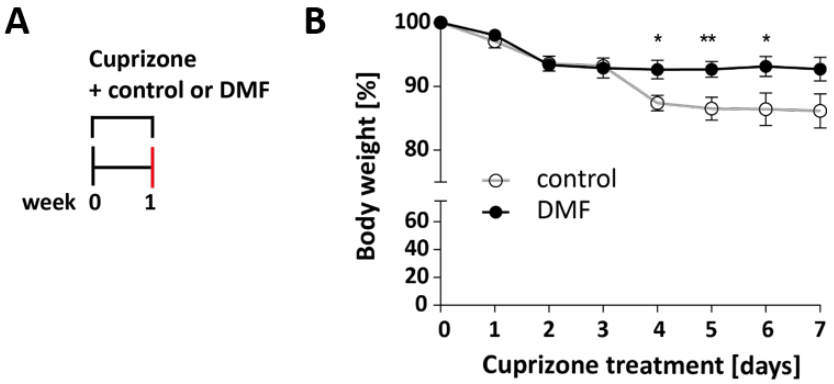

Figure 1: Effect of DMF treatment on cuprizone induced weight loss. (A) Schematic representation of cuprizone and control or DMF treatment. C57BL/6 mice were fed with 0.25% cuprizone for 1 week and simultaneously treated with control or 15 mg/kg DMF twice a day. (B) Mice were daily monitored for body weight. DMF treatment significantly reduced the cuprizone-induced weight loss compared to controls. Data are represented as mean± SEM (n=12, *p<0.05, **p<0.01, unpaired t-test).

3.1.1.2. Apoptotic cell death of oligodendrocytes is decreased by DMF treatment

The apoptosis of oligodendrocytes begins shortly after the initiation of the cuprizone diet. Therefore, histological evaluations were performed after 7 days of cuprizone exposure (Hesse et al., 2010a). The number of apoptotic oligodendrocytes was analyzed after staining for caspase-3 (Casp3), a marker for apoptotic cell death, and by morphological analysis (condensed and/or fragmented nuclei) of H&E (haematoxilin and eosin) stained sections (Figure 2). DMF treatment significantly decreased the number of apoptotic oligodendrocytes after 7 days of cuprizone exposure compared to control treated animals. The mean number of caspase-3 positive cells in the CC decreased from 106 ± 31 cells/mm^2 in controls to 38 ± 13 cells/mm^2 in DMF-treated animals (p<0.0001). Furthermore, the number of cells showing morphological signs of apoptosis was also significantly reduced from 87 ± 25 cells/mm^2 in control- to 38 ± 14 cells/mm^2 in DMF-treated animals (p<0.0001).

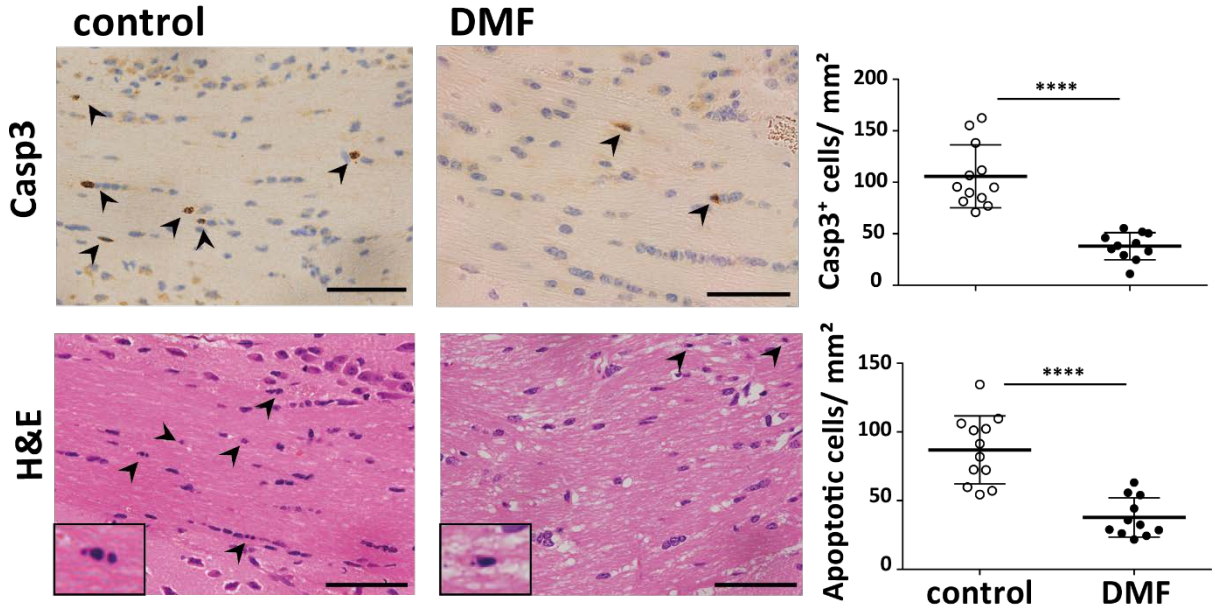

Figure 2: DMF treatment reduces cuprizone-induced apoptosis of oligodendrocytes in the CC. For the analysis of DMF effects on the apoptosis of oligodendrocytes C57BL/6 mice were fed with 0.25% cuprizone for 1 week and simultaneously treated with control or 15 mg/kg DMF twice a day. Apoptotic cells in the CC were identified after caspase-3 staining and by morphological criteria in H&E staining. Representative sections of the CC are shown on the left and quantifications of cells on the right. Histological evaluation revealed that DMF treatment significantly decreases the apoptosis of oligodendrocytes under cuprizone diet. Data are represented as mean± SD (****p<0.0001, unpaired t-test). Inserts show an apoptotic cell in higher magnification. Scale bar = 50 µm

3.1.1.3. Higher numbers of oligodendrocytes were present with DMF treatment

Since DMF treatment significantly reduced the apoptosis of oligodendrocytes after 7 days of cuprizone treatment, it was investigated if DMF also influences the oligodendrocyte populations. The total number of oligodendrocytes including progenitor cells was analyzed after IHC staining for Olig2 and the number of mature oligodendrocytes after IHC staining for NogoA (Figure 3). DMF-treated mice showed a significantly higher number of $Olig2^+$ cells (235 ± 35 cells/mm^2) in the CC compared to controls (156 ± 43 cells/mm^2) ($p<0.001$). The number of $NogoA^+$ cells was not significantly altered by application of DMF.

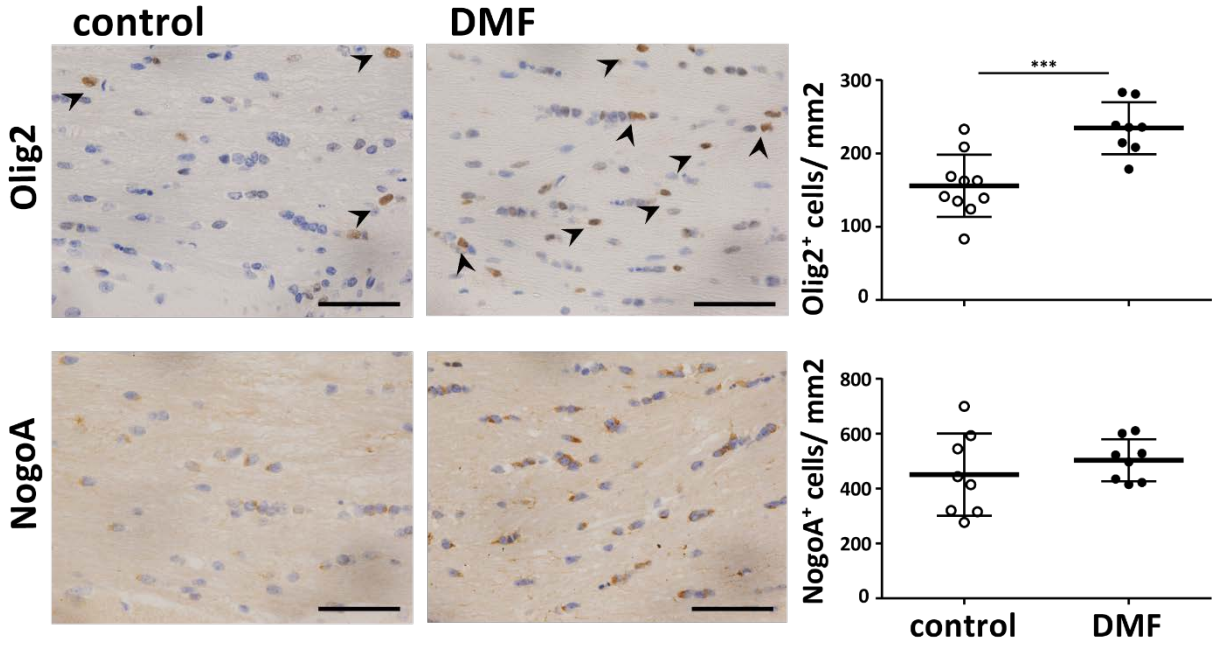

Figure 3: DMF treatment increases number of oligodendrocytes after 7 days of cuprizone exposure. C57BL/6 mice were fed with 0.25% cuprizone and simultaneously treated with control or 15 mg/kg DMF twice a day for 7 days. The number of oligodendrocytes including progenitor cells (Olig2$^+$) and mature oligodendrocytes (NogoA$^+$) in the CC was analyzed after IHC staining. Representative sections of the CC are shown on the left and quantifications of cells on the right. The number of Olig2$^+$ oligodendrocytes is significantly higher after DMF treatment whereas the number of mature oligodendrocytes is not altered. Data are represented as mean± SD (**p<0.01, unpaired t-test). Scale bar = 50 µm

3.1.1.4. DMF application reduced the acute axonal damage after 7 days of cuprizone exposure

Brain sections from control- or DMF-treated mice were stained for amyloid precursor protein (APP, a marker for acute axonal damage), reactive astrocytes (GFAP) and microglia/macrophages (Mac3) (Figure 4). After 7 days of cuprizone diet, almost no acute axonal damage, represented by the number of APP$^+$ spheroids, was detectable in the CC of DMF-treated mice (0 ± 0.6 cells/mm^2) compared to controls (6 ± 6 cells/mm^2) ($p<0.05$). The number of GFAP$^+$ cells and Mac3$^+$ cells was slightly reduced by DMF treatment, but this effect was not statistically significant when compared to controls.

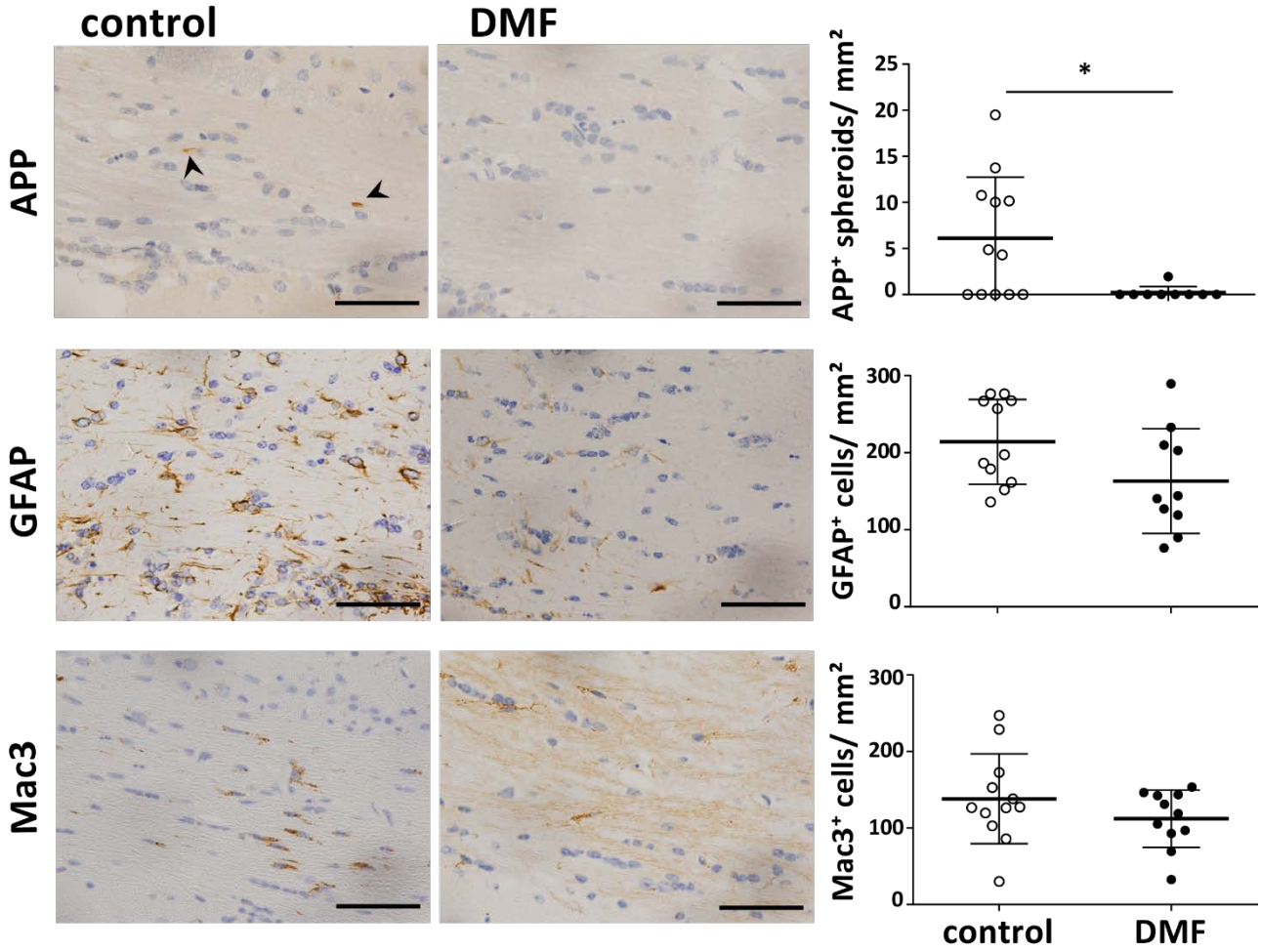

Figure 4: DMF treatment reduces the acute axonal damage induced by cuprizone diet. C57BL/6 mice were fed with 0.25% cuprizone for 7 days and simultaneously treated with control or 15 mg/kg DMF twice a day. IHC of brain sections was performed to investigate the acute axonal damage (APP), number of reactive astrocytes (GFAP) and number of microglia/macrophages (Mac3) in the CC. Representative sections of the CC are shown on the left and quantifications of axonal spheroids and cells on the right. DMF treatment significantly reduces cuprizone-induced acute axonal damage compared to controls. The number of reactive astrocytes and microglia/macrophages were not significantly altered by DMF application. Data are represented as mean± SD (*p<0.05, Mann-Whitney U test). Scale bar = 50 µm

3.1.1.5. Anti-apoptotic effect of DMF was not detectable after 2 weeks of cuprizone exposure

The number of apoptotic oligodendrocytes was significantly reduced by DMF application after 7 days of cuprizone diet. To investigate if this effect persists over a longer period of time, C57BL/6 mice were fed with 0.25% cuprizone and simultaneously treated with control or 15 mg/kg DMF twice a day for 2 weeks. Apoptosis of oligodendrocytes was morphologically analyzed in H&E staining and the number of mature oligodendrocytes was evaluated after NogoA staining

(Figure 5). DMF treatment slightly diminished the number of apoptotic cells after 2 weeks of cuprizone diet, but this effect was not statistically significant. The number of mature oligodendrocytes was comparable between control- and DMF-treated mice. In addition, DMF-treated mice showed a higher number of $Olig2^{+}$ cells, but in contrast to the results received after 7 days of cuprizone exposure this effect was not statistically significant (data not shown).

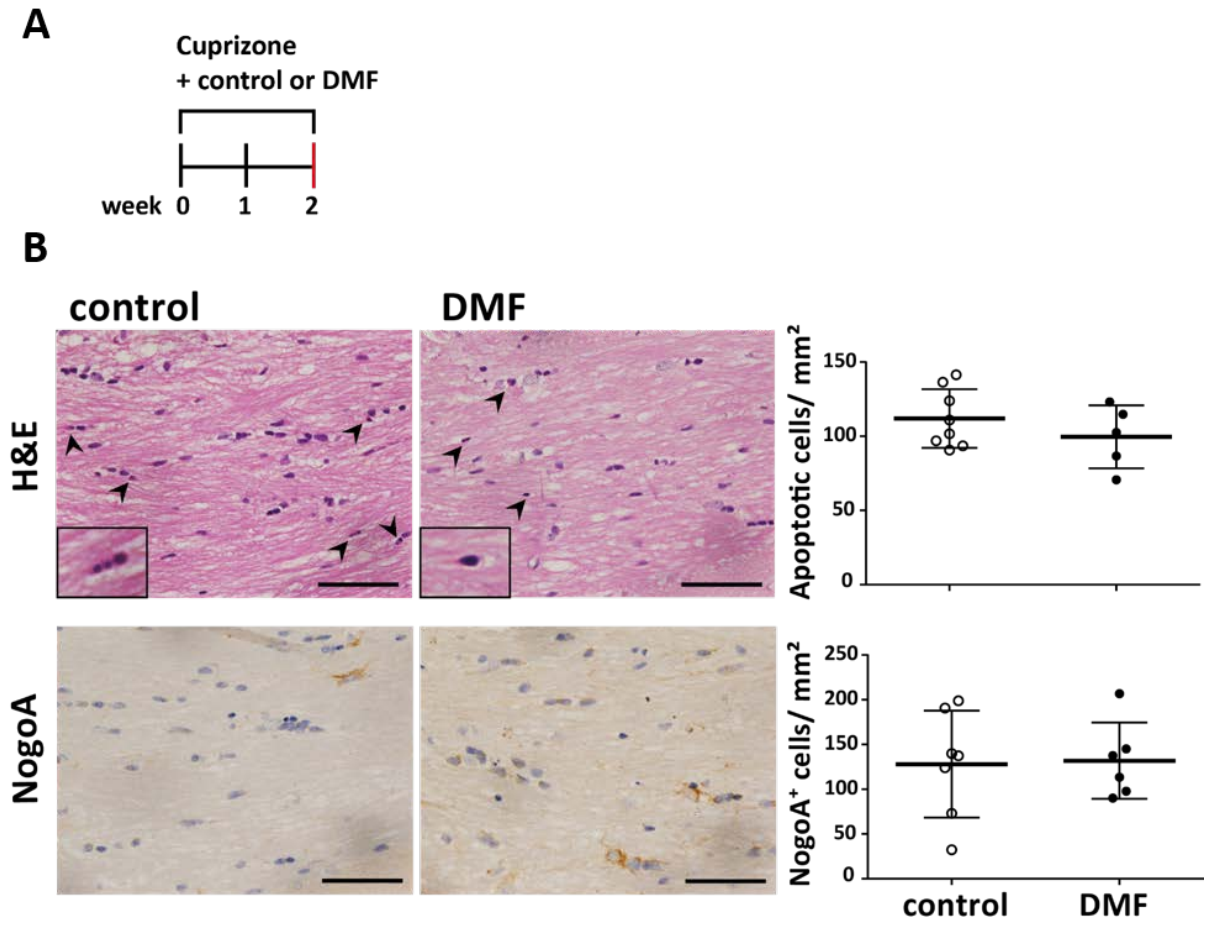

Figure 5: DMF treatment does not prevent apoptosis of oligodendrocytes in the CC after 2 weeks of cuprizone diet. The DMF effect on the apoptosis of oligodendrocytes was additionally analyzed after 2 weeks of cuprizone treatment. (A) Schematic representation of cuprizone and control or DMF treatment. C57BL/6 mice were fed with 0.25% cuprizone for 2 weeks and simultaneously treated with control or 15 mg/kg DMF twice a day. (B) Histological staining was performed to analyze the number apoptotic cells (H&E) and number of mature oligodendrocytes (NogoA) in the CC. Representative sections of the CC are shown on the left and quantification of cells on the right. Histological evaluation revealed that DMF treatment does not significantly alter the apoptosis of oligodendrocytes and the number of mature oligodendrocytes after 2 weeks of cuprizone feeding. Data are represented as mean± SD. Inserts show an apoptotic cell in higher magnification. Scale bar = 50 µm

3.1.2. Long-term effects of DMF in the cuprizone mouse model

DMF-treated mice showed reduced numbers of apoptotic oligodendrocytes and higher numbers of $Olig2^+$ oligodendrocytes after 7 days of cuprizone exposure leading to the suggestion that DMF might also reduce cuprizone-induced demyelination of the CC. As the acute axonal damage was reduced by DMF after short term treatment, we were also interested in the axonal damage after long-term DMF treatment in the cuprizone model. To address this question, 9 to 10 week old C57BL/6 mice were fed with 0.25% cuprizone and simultaneously treated with control or 15 mg/kg DMF twice a day for 6 weeks to study DMF effects on the demyelination of the CC as well as to analyze the axonal damage. Body weight of control- and DMF-treated mice was evaluated every week of cuprizone treatment (data not shown). However, the DMF effects seen on the body weight after one week of cuprizone treatment did not last in the long term therapy.

3.1.2.1. Cuprizone-induced demyelination was not affected by DMF treatment

Brain sections of control- and DMF-treated mice were examined and analyzed for demyelination of the CC after LFB-PAS and PLP (proteolipid protein) staining (Figure 6). The myelin in the LFB-PAS staining appears in blue and in PLP staining in brown. First, the area of the whole CC was measured and afterwards only the demyelinated regions. The demyelinated area is then indicated as percentage of the total CC. The LFB-PAS staining showed that the myelin appeared to be better preserved in the medial part of the CC of DMF-treated mice, but this effect did not reach statistical significance when compared to controls. The extent of demyelination in the PLP staining was similar between both groups. DMF effects on the cortical demyelination were also examined in DMF- and control-treated mice. However, the extent of demyelination was comparable between both groups (data not shown).

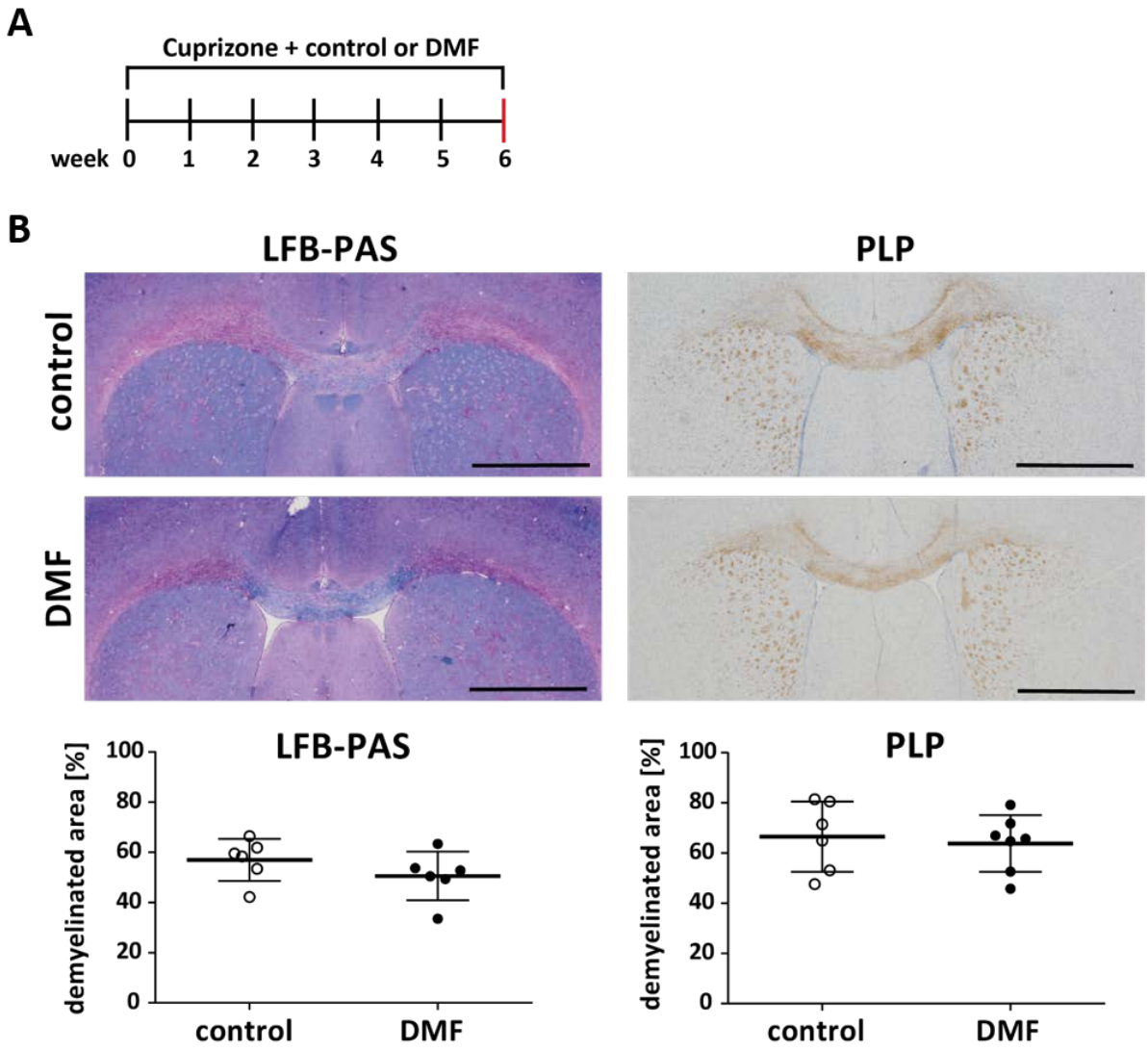

Figure 6: DMF application does not reduce demyelination in the CC. The demyelination of the CC was investigated after long-term cuprizone diet. (A) Schematic representation of cuprizone and control or DMF treatment. C57BL/6 mice were fed with 0.25% cuprizone and simultaneously treated with control or 15 mg/kg DMF twice a day for 6 weeks. (B) LFB/PAS and PLP stainings were performed to measure the demyelinated area of the CC. Representative sections of the CC are shown above and the corresponding quantifications below. Demyelination is not significantly decreased by DMF treatment after 6 weeks of cuprizone exposure. Data are represented as mean± SD. Scale bar = 1000 µm

3.1.2.2. DMF treatment did not significantly reduce the acute axonal damage, astrogliosis and microglia/macrophages after 6 weeks of cuprizone intoxication

Cuprizone-mediated demyelination leads to an increased accumulation of microglia/macrophages, acute axonal damage and higher numbers of astroglia. Mac3, APP and GFAP immunohistochemistry was used to assess the number of microglia/macrophages, acute axonal

damage and the number of activated astrocytes (Figure 7). DMF treatment did not significantly alter the number of Mac3$^+$ cells compared to controls. Additionally, the number of APP$^+$ spheroids and GFAP$^+$ cells was not significantly reduced by DMF treatment compared to controls. Nevertheless, a trend for less acute axonal damage and lower numbers of reactive astrocytes and macrophages/microglial cells was observed in DMF-treated animals after 6 weeks of cuprizone diet.

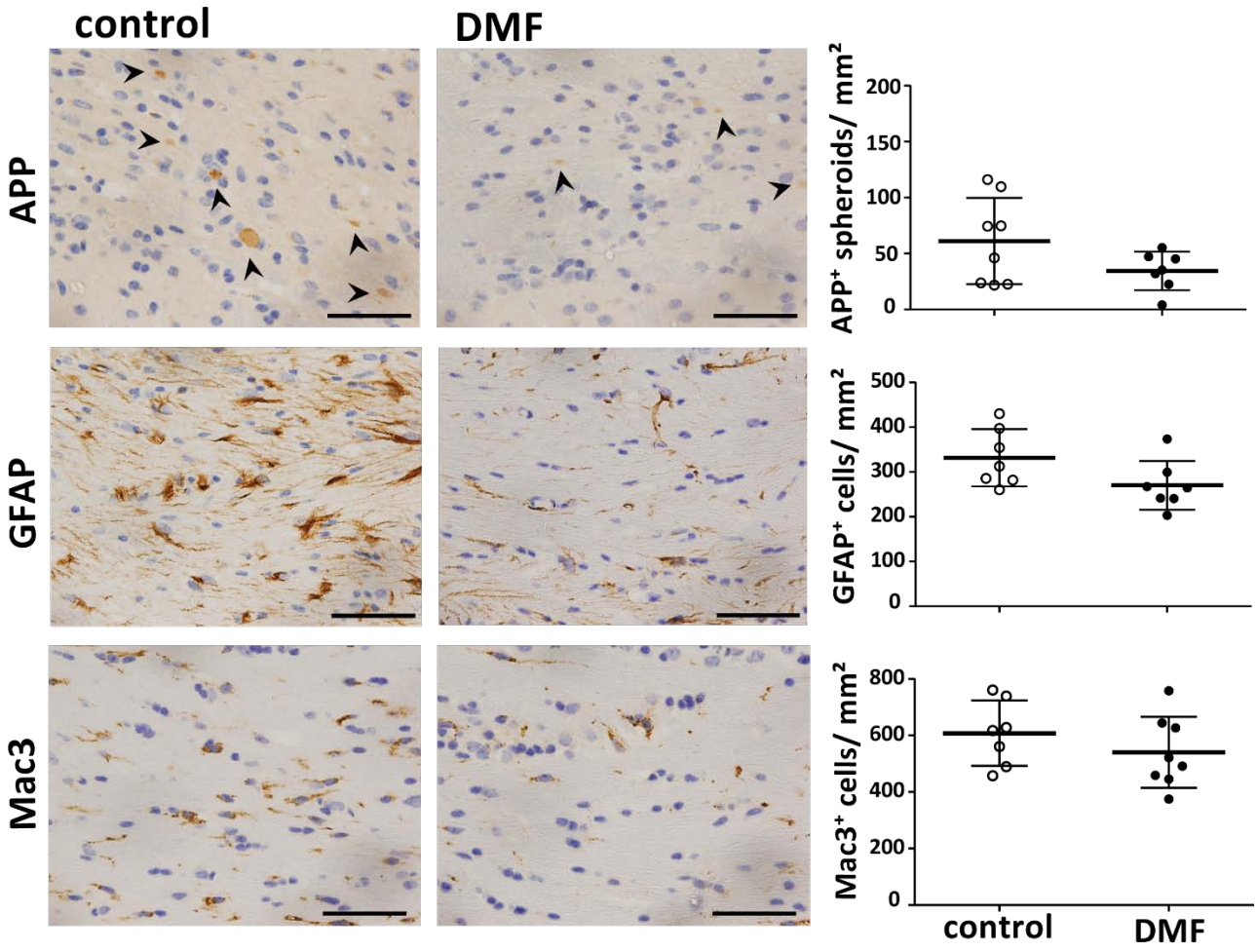

Figure 7: No significant effect of DMF on acute axonal damage, astrogliosis and macrophage/microglial numbers after long-term cuprizone treatment. IHC staining for microglia/macrophages (Mac3), acute axonal damage (APP) and reactive astrocytes (GFAP) was performed of brain sections from C57BL/6 mice fed with 0.25% cuprizone and simultaneously treated with control or 15 mg/kg DMF twice a day for 6 weeks. Representative sections of the CC are shown on the left and quantifications of cells on the right. The number of microglia/macrophages (Mac3), acute axonal damage and the number of reactive astrocytes are not significantly reduced by DMF application after 6 weeks of cuprizone diet. Data are represented as mean± SD. Scale bar = 50 µm

3.1.2.3. Axonal density was not significantly higher after DMF treatment

In addition to the evaluation of the acute axonal damage, DMF effects were analyzed on the axonal density during cuprizone intoxication. Therefore a Bielschowsky staining was performed and axons were counted across the width of the CC under the cingulum bundle as depicted in Figure 8. The axonal density in the CC was tended to be higher in DMF-treated mice, but this effect did not reach statistical significance.

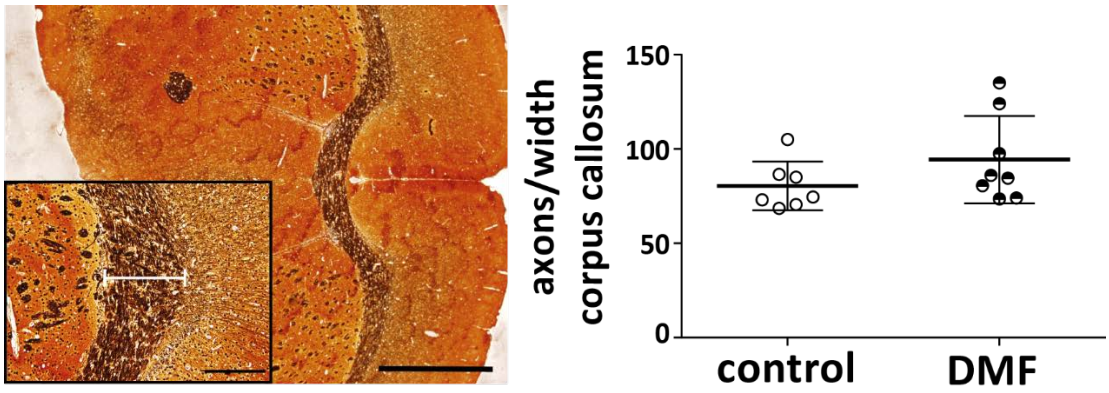

Figure 8: DMF treatment shows no significant effect the axonal density. C57BL/6 mice were fed with 0.25% cuprizone and simultaneously treated with control or 15 mg/kg DMF twice a day for 6 weeks. The number of axons in the CC was analyzed by Bielschowsky staining. Axons were counted over the width of the CC (white bar) under the cingulum bundle. Representative sections of the CC are shown on the left and quantification of axons on the right. The number of axons is not altered by DMF treatment. Data are represented as mean± SEM. Scale bar = 1000 µm, scale bar insert = 200 µm

3.1.2.4. DMF treatment enhanced the number of mature oligodendrocytes after 6 weeks of cuprizone

Olig2$^+$ oligodendrocytes (including progenitor cells) were preserved by DMF treatment after 7 days of cuprizone diet whereas no difference in the number of Olig2$^+$ oligodendrocytes and mature oligodendrocytes was observed after 2 weeks. To examine the number of mature oligodendrocytes after 6 weeks of cuprizone exposure, an IHC staining for NogoA was performed (Figure 9). Histological evaluation showed that the number of NogoA$^+$ cells was significantly lower in controls (110 ± 38 cells/mm^2) compared to DMF-treated animals (146 ± 21 cells/mm^2) ($p<0.05$). The total number of oligodendrocytes (Olig2$^+$ cells) was not altered by DMF treatment after 6 weeks of cuprizone (data not shown).

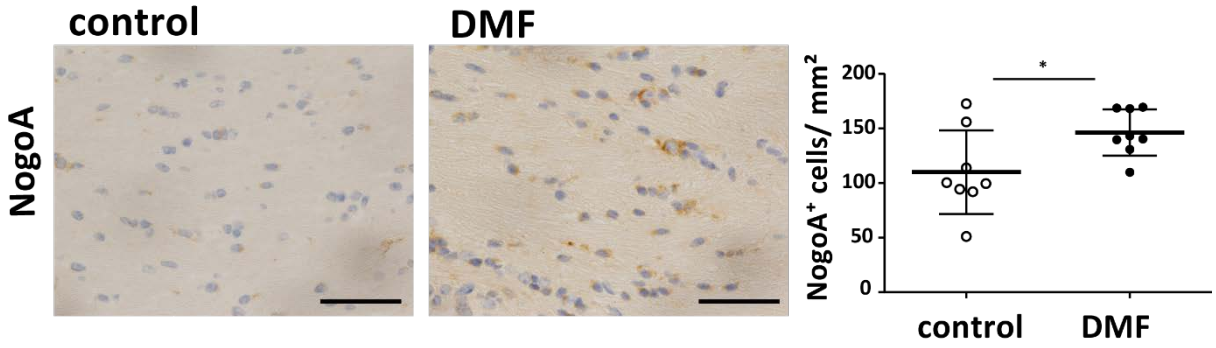

Figure 9: Higher numbers of mature oligodendrocytes after 6 weeks of cuprizone exposure with DMF treatment. C57BL/6 mice were fed with 0.25% cuprizone and simultaneously treated with control or 15 mg/kg DMF twice a day for 6 weeks. The number of mature oligodendrocytes (NogoA) in the CC was analyzed after IHC staining. Representative sections of the CC are shown on the left and quantification of cells on the right. The number of mature oligodendrocytes is significantly higher after DMF treatment. Data are represented as mean± SD (*p<0.05, unpaired t-test). Scale bar = 50 µm

3.1.3. DMF effects after cuprizone withdrawal

For the analysis of remyelination, C57BL/6 mice were fed with 0.25% cuprizone for 5 weeks to induce demyelination of the CC. This time point was chosen because endogenous remyelination already starts after 5 weeks of cuprizone exposure. After 5 weeks, cuprizone diet was stopped and mice were fed with normal chow and treated therapeutically with control or 15 mg/kg DMF twice a day for 3 days. Next to remyelination, analyses focused on the axonal damage and accumulation of microglia/macrophages.

3.1.3.1. Remyelination was not enhanced by DMF treatment

Naturally, the removal of cuprizone leads to rapid remyelination of the CC of mice. In the first experiment, remyelination was analyzed after 7 days of cuprizone withdrawal and control or DMF treatment (data not shown). Since remyelination was already far advanced at this time point, a shorter treatment period was chosen for further analyses. To investigate the potential of DMF to increase remyelination, C57BL/6 mice were fed with 0.25% cuprizone for 5 weeks to induce demyelination. Afterwards cuprizone diet was stopped and mice were treated with control or 15 mg/kg DMF twice a day for 3 days. Remyelination was investigated after LFB-PAS staining (Figure 10). Both groups still showed the same extent of demyelination in the lateral region of the CC illustrating that DMF treatment could not increase the remyelination of the CC compared to controls. Additionally, the extent of remyelination in the CC was analyzed in sections stained for

PLP, MBP and CNPase. No significant difference between control- and DMF-treated animals was observed for these three myelin proteins (data not shown). The number of mature oligodendrocytes (NogoA$^+$ cells) and the total number of oligodendrocytes (Olig2$^+$ cells) was not altered by 3 days of DMF treatment after cuprizone withdrawal (data not shown).

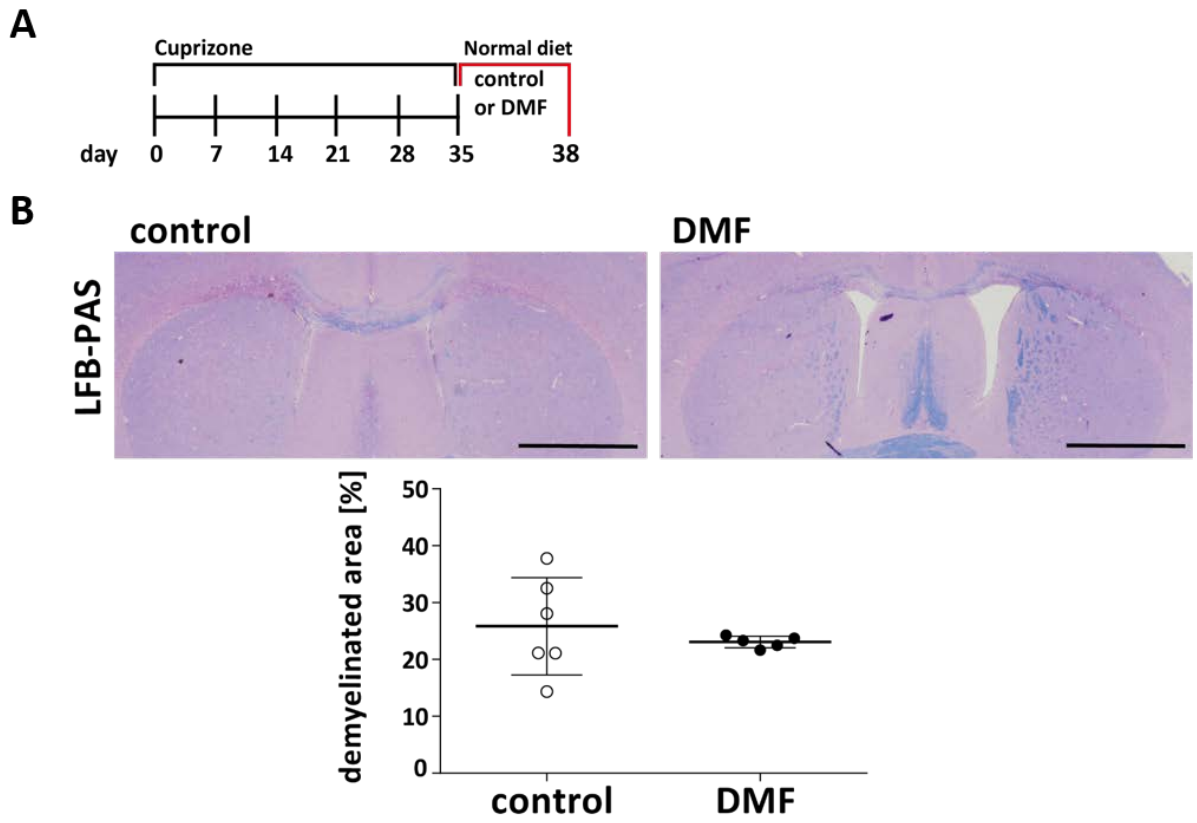

Figure 10: DMF has no effect on the remyelination of the CC. (A) Schematic representation of cuprizone and control or DMF treatment. C57BL/6 mice were fed with 0.25% cuprizone for 5 weeks. Afterwards cuprizone diet was stopped and mice were treated with control or 15 mg/kg DMF twice a day for 3 days. (B) LFB/PAS staining was performed to measure the demyelinated area of the CC. Representative sections of the CC are shown above and the corresponding quantification below. Remyelination is not significantly increased by 3 days of DMF treatment after cuprizone withdrawal. Data are represented as mean± SD. Scale bar = 1000 µm

3.1.3.2. Acute axonal damage was diminished by DMF after 3 days of cuprizone withdrawal

The effects of DMF on acute axonal damage and numbers of microglia/macrophages after cuprizone removal were investigated after IHC staining of brain sections from control- or DMF-treated mice. Acute axonal damage was investigated by counting APP$^+$ spheroids and phagocyte accumulation by counting Mac3$^+$ cells (Figure 11). The number of APP$^+$ spheroids was significantly

decreased by DMF (84 ± 53 cells/mm^2) when compared to controls (190 ± 78 cells/mm^2) ($p<0.05$). The accumulation of microglia/macrophages was comparable between both groups.

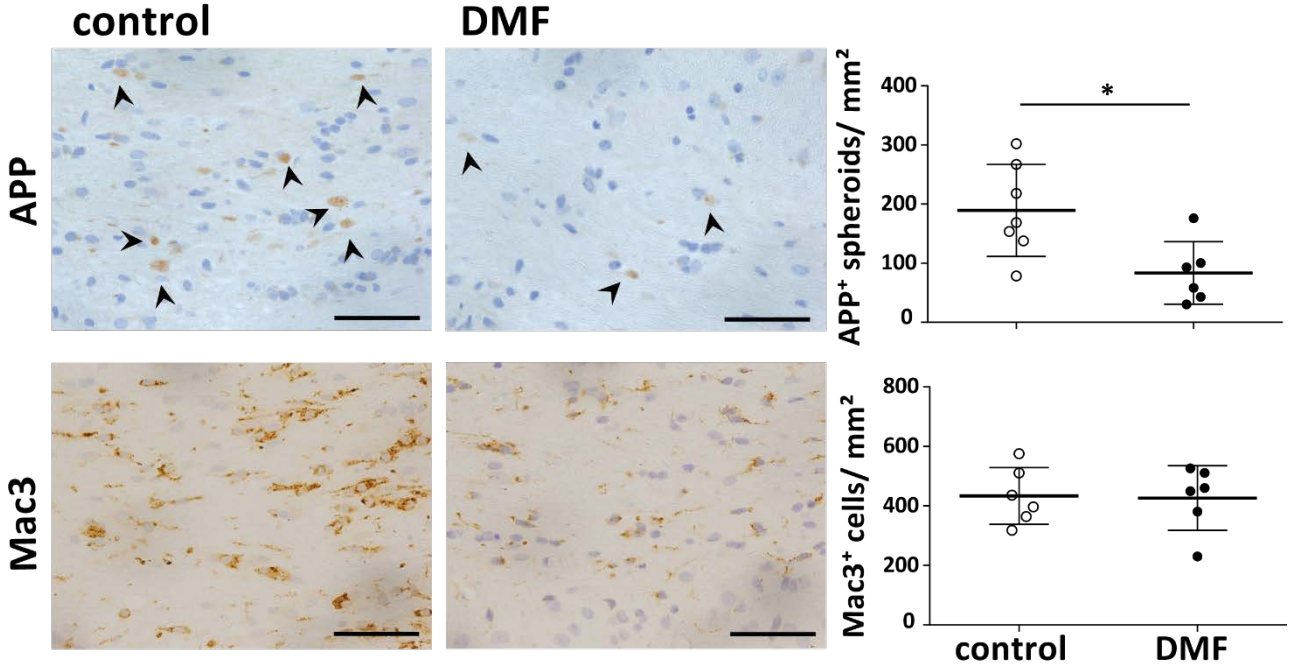

Figure 11: DMF treatment decreases acute axonal damage after cuprizone withdrawal. C57BL/6 mice were fed with 0.25% cuprizone for 5 weeks. Afterwards cuprizone diet was stopped and mice were treated with control or 15 mg/kg DMF twice a day for 3 days. IHC staining for acute axonal damage (APP) and the number of microglia/macrophages was performed. Representative sections of the CC are shown on the left and quantification of cells on the right. Acute axonal damage is significantly reduced by 3 days of DMF treatment after cuprizone withdrawal. Data are represented as mean± SD (*$p<0.05$, unpaired t-test). Scale bar = 50 µm

3.1.4. MMF was detectable in the brain of DMF-treated mice

An important feature of the cuprizone mouse model is the intact blood brain barrier (BBB) which allows the investigation of CNS intrinsic effects without the influence of the peripheral immune system. To analyze if DMF can pass the BBB and reaches the CNS, its metabolite MMF was measured in plasma and brain samples of control- and DMF-treated mice by mass spectrometry. MMF could be detected in the plasma and brain samples of DMF-treated mice after 7 days and was even slightly increased after six weeks of therapy (Figure 12). No MMF was found in the plasma and brain of controls. Mass spectrometry analysis was kindly performed by the lab of Rob Scannevin (Biogen Idec, Cambridge).

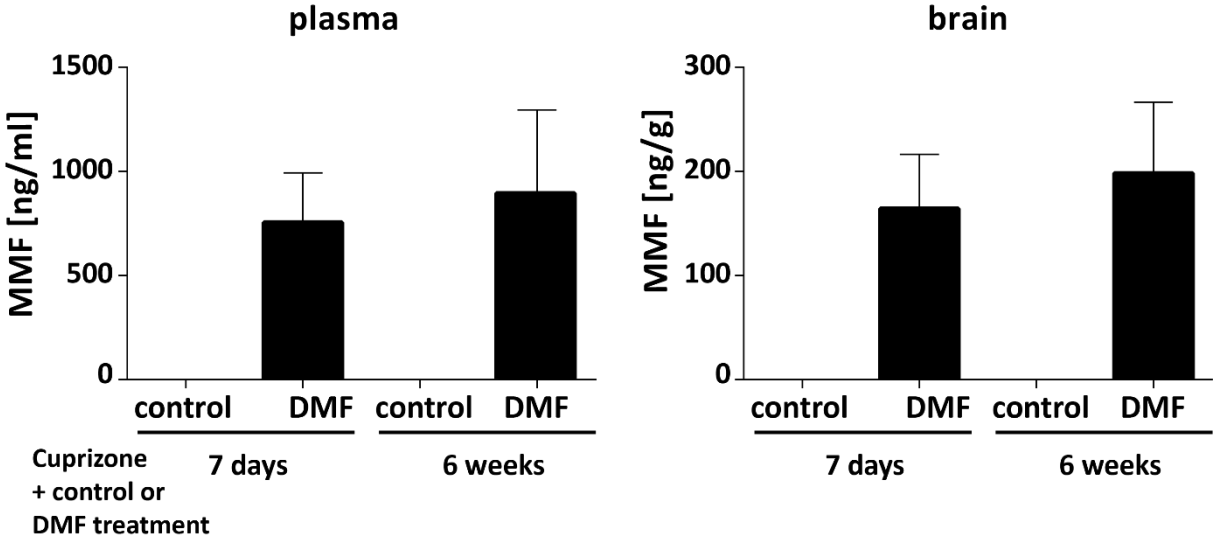

Figure 12: MMF, the active metabolite of DMF, is present in the brain of DMF-treated mice. C57BL/6 mice were fed with 0.25% cuprizone and simultaneously treated with control or 15 mg/kg DMF twice a day for 7 days or 6 weeks. The amount of the DMF metabolite MMF was analyzed by mass spectrometry in plasma and brain. MMF can be detected in the plasma and brain of DMF-treated mice after 7 days and 6 weeks whereas in control-treated mice MMF is not detectable. Data are represented as mean± SD (7 days n=6, 6 weeks n=4).

3.1.5. DMF did not reduce apoptosis of oligodendrocytes in Nrf2 k.o. mice

It is assumed that DMF exerts protective functions via the activation and stabilization of the transcription factor Nrf2, which activates antioxidant response pathways and thereby leads to a better protection of cells against oxidative stress (Linker et al., 2011; Scannevin et al., 2012c; Thiessen et al., 2010). To investigate if the DMF-mediated reduction of apoptotic oligodendrocytes after 7 days of cuprizone is dependent on Nrf2, apoptosis of oligodendrocytes was examined in Nrf2 k.o. mice. Similar to the first experiments, Nrf2 k.o. mice were fed with 0.25% cuprizone for 7 days and simultaneously treated with control or 15 mg/kg DMF twice a day. Apoptosis of oligodendrocytes was analyzed in H&E stained tissue (Figure 13). Histological evaluation revealed that control-treated Nrf2 k.o. mice already showed reduced numbers of apoptotic cells when compared to C57BL/6 mice (Figure 2). The number of apoptotic cells was similar in control- and DMF-treated Nrf2 k.o. mice.

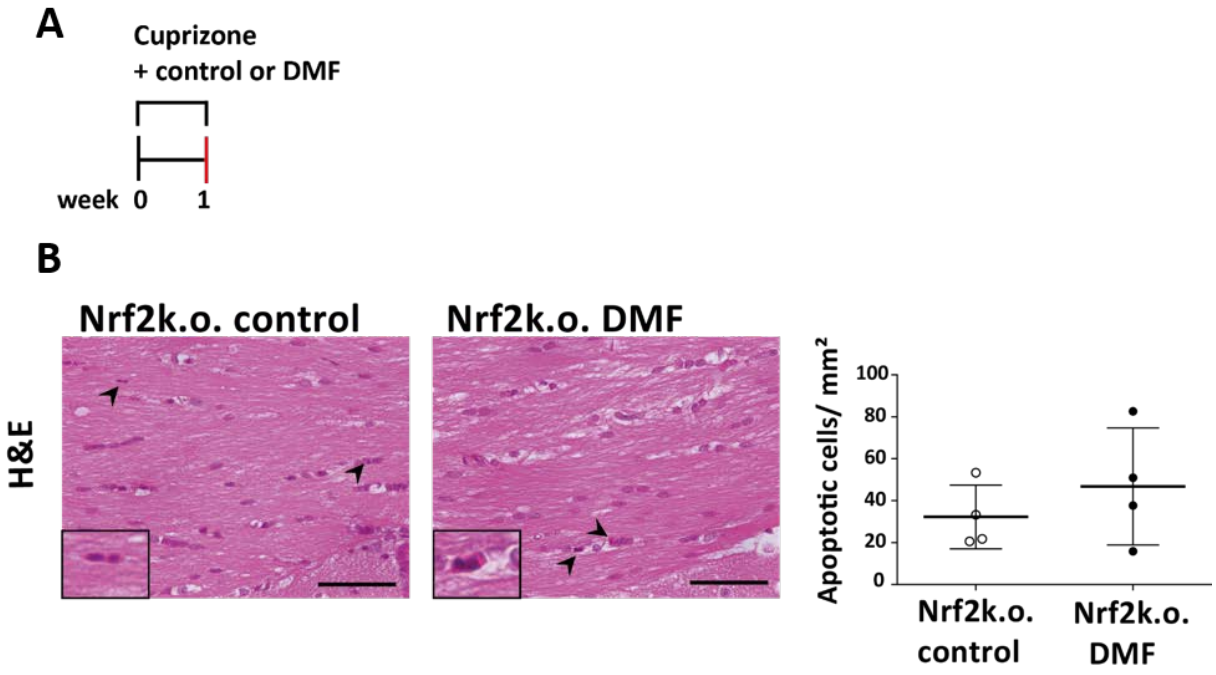

Figure 13: DMF treatment does not decrease apoptosis of oligodendrocytes in the CC of Nrf2 k.o. mice. (A) Schematic representation of cuprizone and control or DMF treatment. Nrf2 k.o. mice were fed with 0.25% cuprizone for 7 days and simultaneously treated with control or 15 mg/kg DMF twice a day. (B) Apoptotic cells in the CC were identified by morphology in H&E staining. Representative sections of the CC are shown on the left and quantification of cells on the right. Histological evaluation revealed that the number of apoptotic oligodendrocytes is not reduced in Nrf2 k.o. mice by DMF treatment. Data are represented as mean± SD. Inserts show an apoptotic cell in higher magnification. Scale bar = 50 µm

In summary, although DMF did not profoundly alter the extent of demyelination and remyelination, the number of oligodendrocytes was increased in DMF-treated animals over time. Whereas after short-term cuprizone exposure the overall number of oligodendrocytes including OPCs was increased with DMF treatment, after 6 weeks of cuprizone diet the number of mature oligodendrocytes was higher in DMF-treated animals compared to controls.

DMF treatment reduced the acute axonal damage after 7 days of cuprizone treatment. Although this effect was not significant after 6 weeks of cuprizone diet, a trend towards less acute axonal damage in DMF-treated animals was observed. Nevertheless, therapeutic DMF treatment significantly decreased the number of damaged axons after 3 days of treatment following cuprizone withdrawal.

3.2. DMF effects in a B cell-mediated EAE model

Besides the analysis of CNS intrinsic effects, further studies focused on peripheral effects mediated by DMF treatment. Therefore, DMF was analyzed in a B cell-mediated EAE model.

The beneficial effects of the B cell-depleting agent rituximab in the therapy of RRMS emphasized the pathological role of B cells in the disease pathogenesis (Hauser et al., 2008b). Previous studies investigated the effects of DMF in more T cell-dependent EAE models, induced by immunization with MOG peptide. In this model, B cells do not extensively contribute to the disease pathogenesis demonstrated by the detrimental effects of rituximab in this EAE (Weber et al., 2010). Therefore, the present study aimed to examine the effects of DMF on adaptive immune cells in an EAE model, induced by immunization with MOG protein, in which B cells contribute in a pathogenic manner.

For the investigation of DMF-mediated effects, mice were treated once in a preventive setting, starting 2 or 7 days before immunization, or in a therapeutic regimen starting when mice showed an EAE score of 2 (hind limb weakness) or higher (Figure 14).

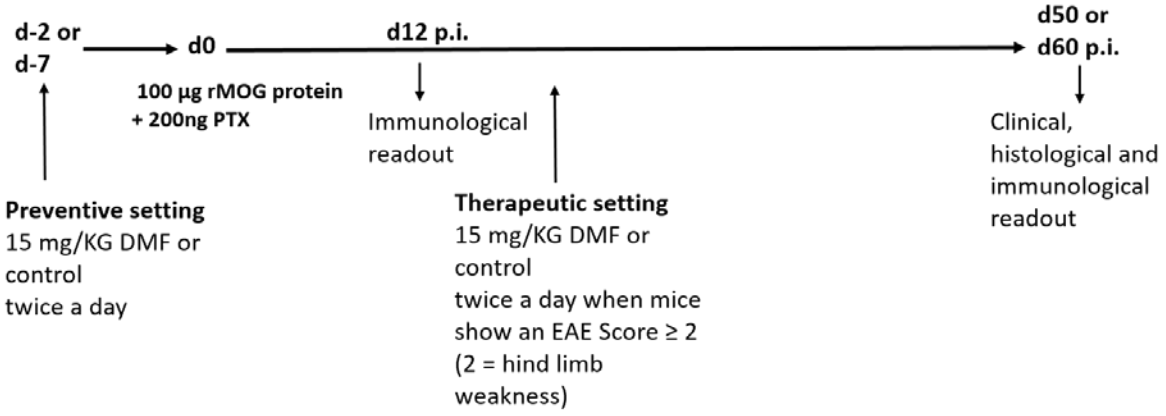

Figure 14: Schematic representation of the experimental setup. C57BL/6 mice were immunized with 100 µg $rMOG_{1-117}$ and treated with 15 mg/kg DMF or control twice a day. Preventive treatment started 2 or 7 days prior to immunization, therapeutic treatment when mice showed an EAE Score of 2 (hind limb weakness) or higher. For immunological evaluations mice were treated until day 12 and for clinical and histological evaluations until day 60.

3.2.1. DMF treatment decreased EAE severity and demyelination of the spinal cord

To investigate the efficiency of DMF to improve B cell-mediated chronic EAE, C57BL/6 mice were immunized with $rMOG_{1-117}$ and received oral treatment with either 15 mg/kg DMF or control twice a day. In the preventive setting, mice were treated until d60, in the therapeutic regimen until d50 p.i. (Figure 14). Clinical, histological and immunological analyses were performed to examine DMF-mediated alterations of adaptive and innate immunity.

3.2.1.1. Preventive and therapeutic DMF treatment ameliorated the clinical course of EAE

The initial experiments focused on the clinical effects mediated by DMF application. Hence, EAE score and body weight (data not shown) of immunized mice were monitored daily (Figure 15). Animals of the preventively treated groups showed an overall lower EAE severity compared to therapeutically treated animals. Data evaluations revealed that both preventive and therapeutic DMF treatment significantly ameliorated the disease course of mice (*p<0.05, **p<0.01).

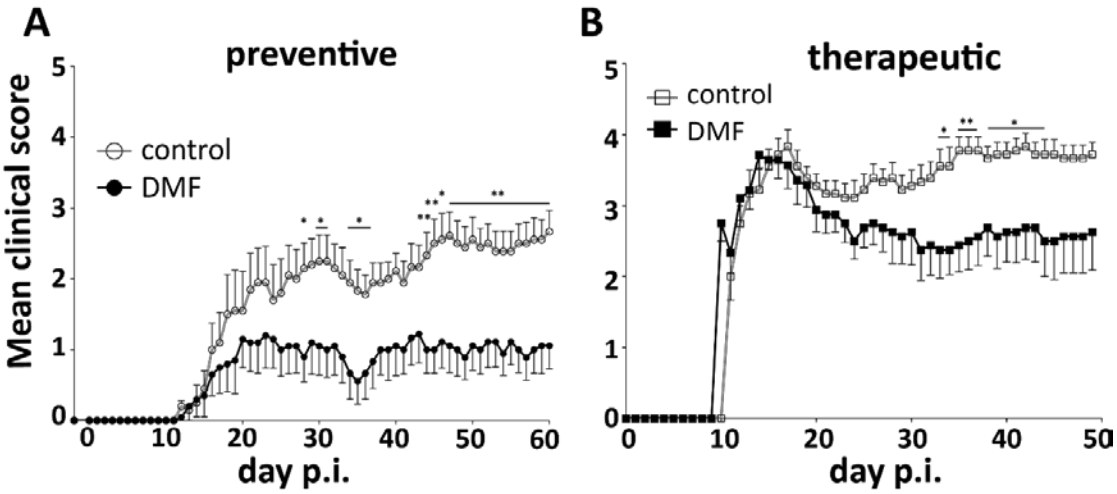

Figure 15: Clinical course of EAE is ameliorated by preventive and therapeutic DMF treatment. Clinical disease scores of chronic EAE in C57BL/6 mice, immunized with $rMOG_{1-117}$ and treated with 15 mg/kg DMF (black) or control (grey) twice a day. (A) Preventive DMF treatment significantly ameliorates the disease course as compared to control. Mice were treated from d-2 until d60. Data are represented as mean ± SEM (n=10 per group, *p<0.05, **p<0.01, Mann-Whitney U test). (B) Therapeutic DMF treatment started when mice showed an EAE Score of 2 (hind limb weakness) or higher. Therapeutic application of DMF significantly ameliorates the course of disease compared to control. Data are represented as mean ± SEM (control n=9 per group, DMF n=8 per group, *p<0.05, **p<0.01, Mann-Whitney U test).

3.2.1.2. Anti-MOG Ab titers were not altered by DMF application

To evaluate the effects of DMF treatment on the humoral immune response, production of anti-MOG Ab levels in the serum of $rMOG_{1-117}$ immunized mice treated with 15 mg/kg DMF or control was determined weekly until day 42 p.i. (Figure 16). Animals which were treated with DMF preventively showed slightly increased Ab levels whereas the Ab level was slightly reduced in animals after the start of therapeutic DMF therapy compared to controls. Neither preventive nor therapeutic DMF application could significantly change the amount of anti-MOG Abs at any time point.

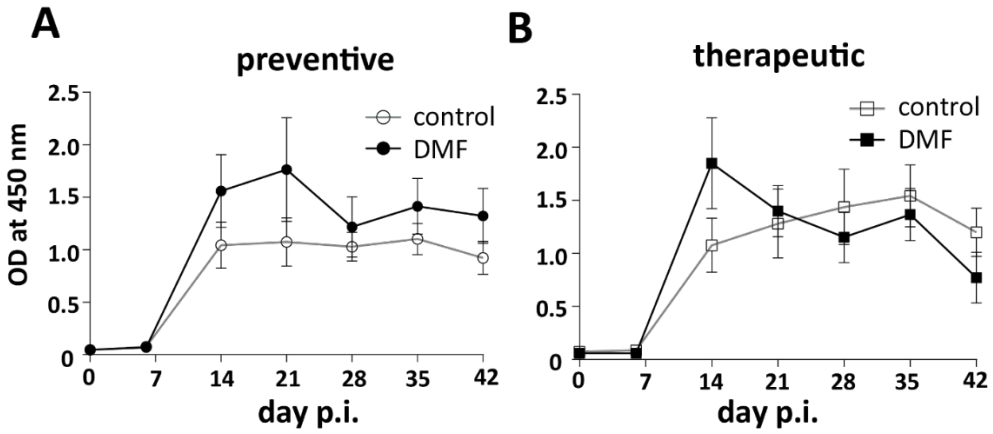

Figure 16: Anti-MOG Ab serum levels remain constant under preventive and therapeutic DMF treatment. C57BL/6 mice were immunized with $rMOG_{1-117}$ and treated with 15 mg/kg DMF (black) or control (grey) twice a day. Anti-MOG Ab serum levels were weekly determined by ELISA until day 42 p.i. Before analysis serum samples were diluted 1:40,500. (A) Preventive and (B) therapeutic DMF treatment do not alter anti-MOG Ab levels compared to controls. Preventive DMF treatment started 2 days before immunization and therapeutic DMF treatment started when mice showed an EAE Score of 2 (hind limb weakness) or higher. Data are represented as mean ± SEM (preventive control and DMF n=10, therapeutic control n=9, therapeutic DMF n=8).

3.2.1.3. Demyelination and inflammation of the spinal cord was decreased by DMF

DMF could significantly reduce the EAE severity in the preventive setting as well as in the therapeutic regimen. To study if DMF could also diminish the damage of the CNS, spinal cord sections of control-or DMF-treated mice were analyzed for demyelination, inflammation and the number of infiltrated cells. LFB-PAS staining was performed to measure the demyelinated area and inflammation was analyzed in H&E staining (Figure 17).

Additionally, spinal cord sections were examined for infiltrating B cells (B220), T cells (CD3) and macrophages (Mac3). Mice which were preventively treated with DMF showed no significantly reduced demyelination, inflammation or number of infiltrating cells compared to their controls. In contrast, demyelination was reduced in therapeutically DMF-treated mice (4.7% ± 0.9 %) compared to controls (14.0% ± 2.4 %) ($p<0.05$). Furthermore, therapeutic application of DMF significantly decreased inflammation from a mean inflammation score of 1.6 ± 0.2 in controls to a mean score of 0.7 ± 0.2 ($p<0.01$). The number of infiltrating $Mac3^+$ cells was significantly diminished by therapeutic DMF treatment (217 ± 59 cells/mm^2) compared to controls (444 ± 102 cells/mm^2) ($p<0.05$). Infiltrating B cell and T cell numbers were not significantly altered by therapeutic DMF treatment.

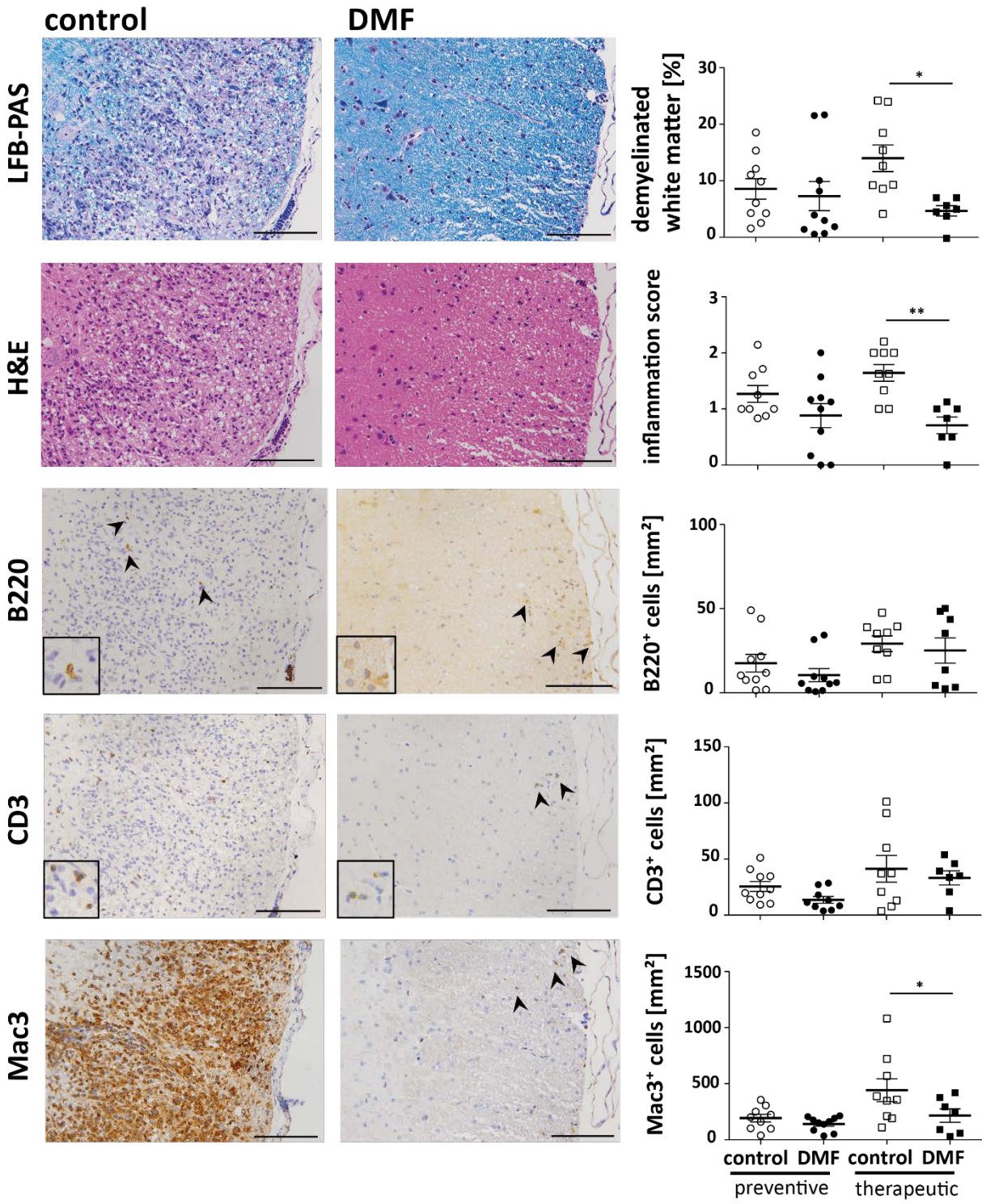

Figure 17: Spinal cord demyelination and infiltration is reduced after DMF treatment. Histological evaluation of C57BL/6 mice, immunized with $rMOG_{1-117}$ and preventive or therapeutically treated with 15 mg/kg DMF or control twice a day. Demyelination (LFB/PAS), inflammation (H&E) and immune cell infiltration of the spinal cord evaluated by B220-, CD3- and Mac3-immunohistochemistry 50 days (therapeutic) and 60 days (preventive) after immunization. Representative sections of therapeutic treated mice (left) and percentage of demyelinated white matter area, score of spinal cord inflammation (0 = no inflammation, 1 = slight inflammation, 2 = moderate inflammation, 3 = strong inflammation) and number of infiltrating immune cells/mm^2 spinal cord (right). Therapeutic DMF treatment significantly reduces spinal cord demyelination and infiltration of cells. Data are represented as mean ± SEM (*p<0.05, **p<0.01, one way ANOVA with Sidak post test). Inserts show $B220^+$ or $CD3^+$ cells in higher magnification. Scale bar = 100 µm

3.2.2. DMF had opposing effects on B cells and T cells during the early phase of EAE

DMF treatment ameliorated the clinical course of B cell-mediated chronic EAE and could also reduce the demyelination and inflammation of the spinal cord. To investigate if DMF-mediated effects already occur at the beginning of the disease, an earlier time point of EAE was chosen for immunological evaluations. Therefore, C57BL/6 mice were immunized with $rMOG_{1-117}$ and preventively treated with 15 mg/kg DMF or control 2 or 7 days prior to immunization until day 12, a day of the disease onset (Figure 14).

3.2.2.1. DMF treatment altered the activation and differentiation of T cells

Effects of DMF on the activation and differentiation of T cells were evaluated by analyzing T cell molecules which reflect their activation state and subpopulations.

3.2.2.1.1. DMF induced a shift in the local distribution of T cells

Lymphopenia is an abnormally low level of lymphocytes and a common side effect of DMF therapy in MS patients (Longbrake et al., 2015). Therefore DMF effects on the cell frequency of immunized mice were analyzed in blood, lymph node and spleen 12 days after immunization. The frequencies of $CD4^+$ T cells, $CD8^+$ T cells, $CD19^+$ cells (B cells) and $CD11b^+$ cells (including monocytes/macrophages, granulocytes, dendritic cells) were analyzed by flow cytometry (Figure 18). Data evaluation revealed a significant decrease in the frequency of $CD4^+$ T cells in DMF-treated animals (12.6% ± 1.5%) compared to control-treated animals (14.7% ± 1.8%). In contrast, the $CD4^+$ T cell frequency was significantly increased in lymph node and spleen by DMF treatment from a mean of 20.0% ± 2.7% and 12.8% ± 2.4% respectively in controls to a mean of 23.2% ± 3.0% and 15.4% ± 1.9% respectively in DMF-treated mice ($p<0.05$). The frequency of $CD8^+$ T cells was also increased in the spleen of DMF-treated mice (8.9% ± 1.3%) compared to controls (7.1% ± 1.8%) ($p<0.05$). In the blood the frequency of $CD8^+$ T cells was slightly decreased and in the lymph node slightly increased. The frequencies of $CD19^+$ cells and $CD11b^+$ cells were comparable between both groups in all analyzed compartments.

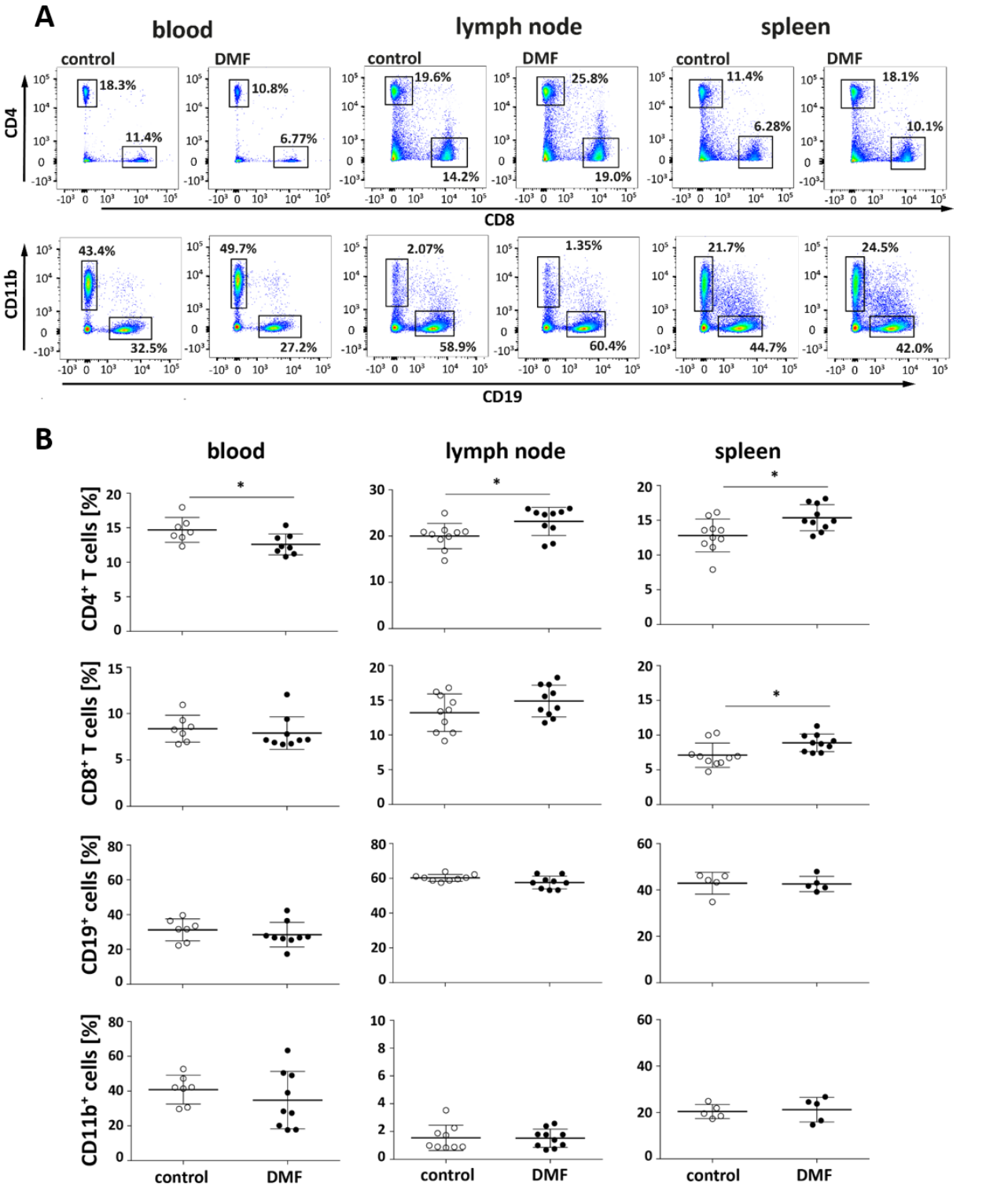

Figure 18: T cell frequencies in blood, lymph node and spleen are altered under DMF treatment at day 12 p.i. Cell frequencies of $CD4^+$ T cells, $CD8^+$ T cells, $CD19^+$ cells and $CD11b^+$ cells were analyzed by flow cytometry (A). C57BL/6 mice were immunized with $rMOG_{1-117}$ and treated with 15 mg/kg DMF or control twice a day from d-7 until d12 p.i. (B) *In vivo* DMF treatment significantly reduces the frequency of $CD4^+$ T cells in blood and increases the frequency of $CD4^+$ T cells in lymph node and the frequencies of $CD4^+$ T cells and $CD8^+$ T cells in spleen compared to controls. Data are represented as mean ± SD (*$p<0.05$, unpaired t-test).

3.2.2.1.2. Reduced T cell activation upon DMF treatment

Since DMF treatment significantly increased the T cell frequency in lymph node and spleen, the next experiment focused on the activation status of these T cells. DMF-induced changes in the activation of $CD4^+$ T cells and $CD8^+$ T cells were analyzed in lymph node and spleen from immunized mice treated with DMF or control until day 12 p.i. T cell activation was characterized by the expression of activation markers CD69 and CD25, samples were gated on $CD4^+$ T cells and $CD8^+$ T cells. The geometric mean fluorescence intensity (gMFI) of CD69 and CD25 was examined by flow cytometry (Figure 19). Data values were normalized to control (set 100%). The expression of CD69 on $CD4^+$ T cells was significantly downregulated in lymph node and spleen by DMF treatment from a mean of 100.0% ± 8.9% and 100.0% ± 5.0% in controls to a mean of 91.1% ± 4.5% and 92.2% ± 4.2% in DMF-treated mice ($p<0.05$, $p<0.01$). $CD4^+$ T cells of the lymph node from DMF-treated mice also showed a reduced expression of CD25 compared to controls (92.2% ± 7.5% vs. 100.0% ± 6.3%) ($p<0.05$). CD25 expression on splenic $CD4^+$ T cells remained unaltered by DMF. Furthermore, DMF treatment decreased the expression of CD69 on $CD8^+$ T cells in lymph node and spleen from a mean of 100.0% ± 11.3% and 100.0% ± 3.9% in controls to a mean of 89.1% ± 7.0% and 91.7% ± 6.0% in DMF-treated mice ($p<0.05$, $p<0.01$).

Next page →

Figure 19: DMF decreases the expression of activation markers on T cells. (A) The effects of DMF on the expression of CD69 on $CD4^+$ T cells and $CD8^+$ T cells and CD25 on $CD4^+$ T cells in lymph node and spleen were analyzed ex vivo by flow cytometry. C57BL/6 mice were immunized with $rMOG_{1-117}$ and treated with 15 mg/kg DMF or control twice a da y from d-7 until d12 p.i. (B) Application of DMF significantly reduces the expression of CD69 on $CD4^+$ T cells and $CD8^+$ T cells in lymph node and spleen and the expression CD25 on $CD4^+$ T cells in the lymph node. Data are normalized to control and represented as mean ± SD (*$p<0.05$, **$p<0.01$, unpaired t-test).

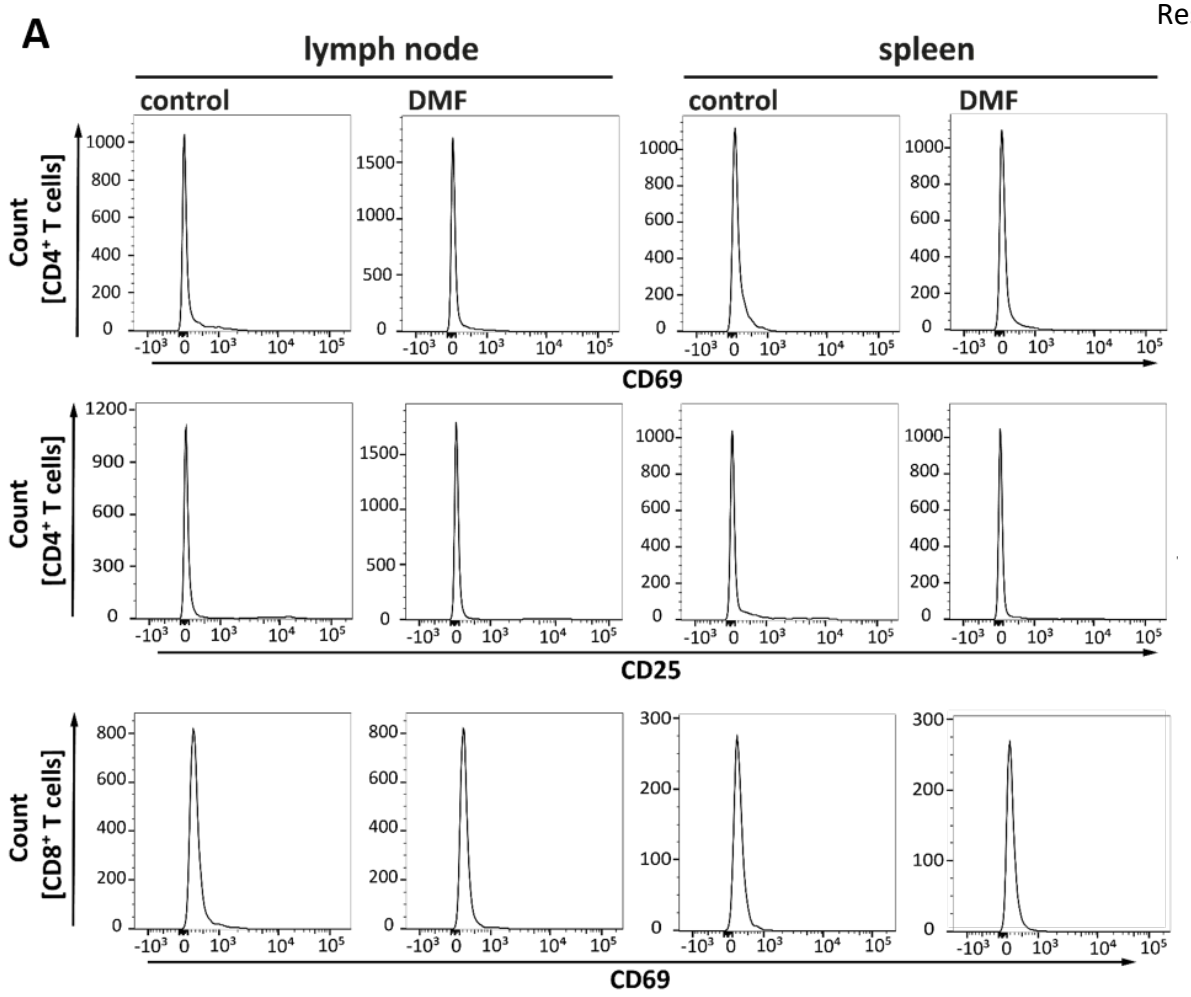
A
lymph node
spleen
control
DMF
control
DMF
Count [CD4+ T cells]
CD69
Count [CD4+ T cells]
CD25
Count [CD8+ T cells]
CD69

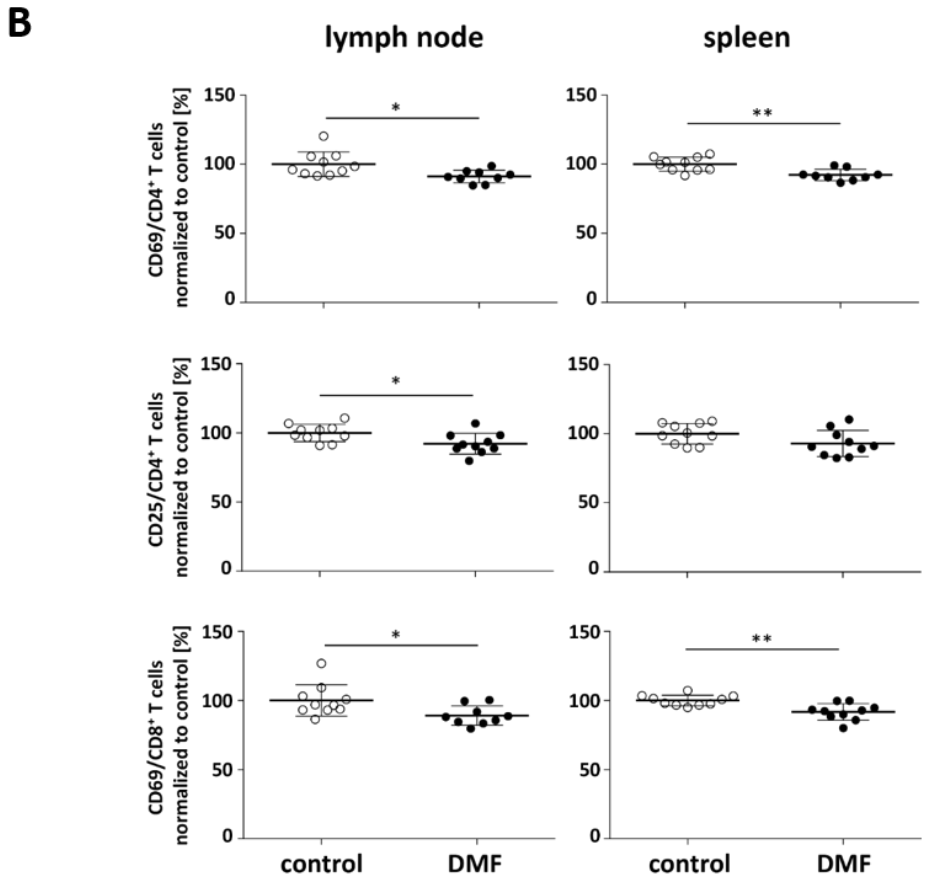
B
lymph node
spleen
CD69/CD4+ T cells normalized to control [%]
CD25/CD4+ T cells normalized to control [%]
CD69/CD8+ T cells normalized to control [%]
control
DMF
control
DMF

3.2.2.1.3. DMF affected the T cell activation marker CD44 on $CD4^+$ T cells and $CD8^+$ T cells

CD44 is an adhesion receptor and usually expressed on activated T cells and long-lived memory cells (Baaten et al., 2010a). It is involved in several biological processes like migration of cells and inflammation. To investigate the effects of DMF on the expression of CD44 on $CD4^+$ T cells and $CD8^+$ T cells, lymphocytes and splenocytes were isolated from immunized mice treated with DMF or control and were stained for CD4, CD8 and CD44. $CD4^+$ T cells and $CD8^+$ T cells were divided into CD44 high ($CD44^{hi}$), CD44 intermediate ($CD44^{int}$) and CD44 low ($CD44^{low}$) T cells (Figure 20, Figure 21).

The frequency of $CD44^{hi}$ $CD4^+$ T cells was significantly decreased in the spleen of DMF-treated mice (22.1% ± 1.8%) compared to controls (25.5% ± 4.1%) ($p<0.05$) whereas the frequencies of $CD44^{int}$ $CD4^+$ T cells and $CD44^{low}$ $CD4^+$ T cells remained unaltered by DMF application (Figure 20). DMF treatment did not significantly modify the frequencies of $CD44^{hi}$ $CD4^+$ T cells, $CD44^{int}$ $CD4^+$ T cells and $CD44^{low}$ $CD4^+$ T cells in the lymph node.

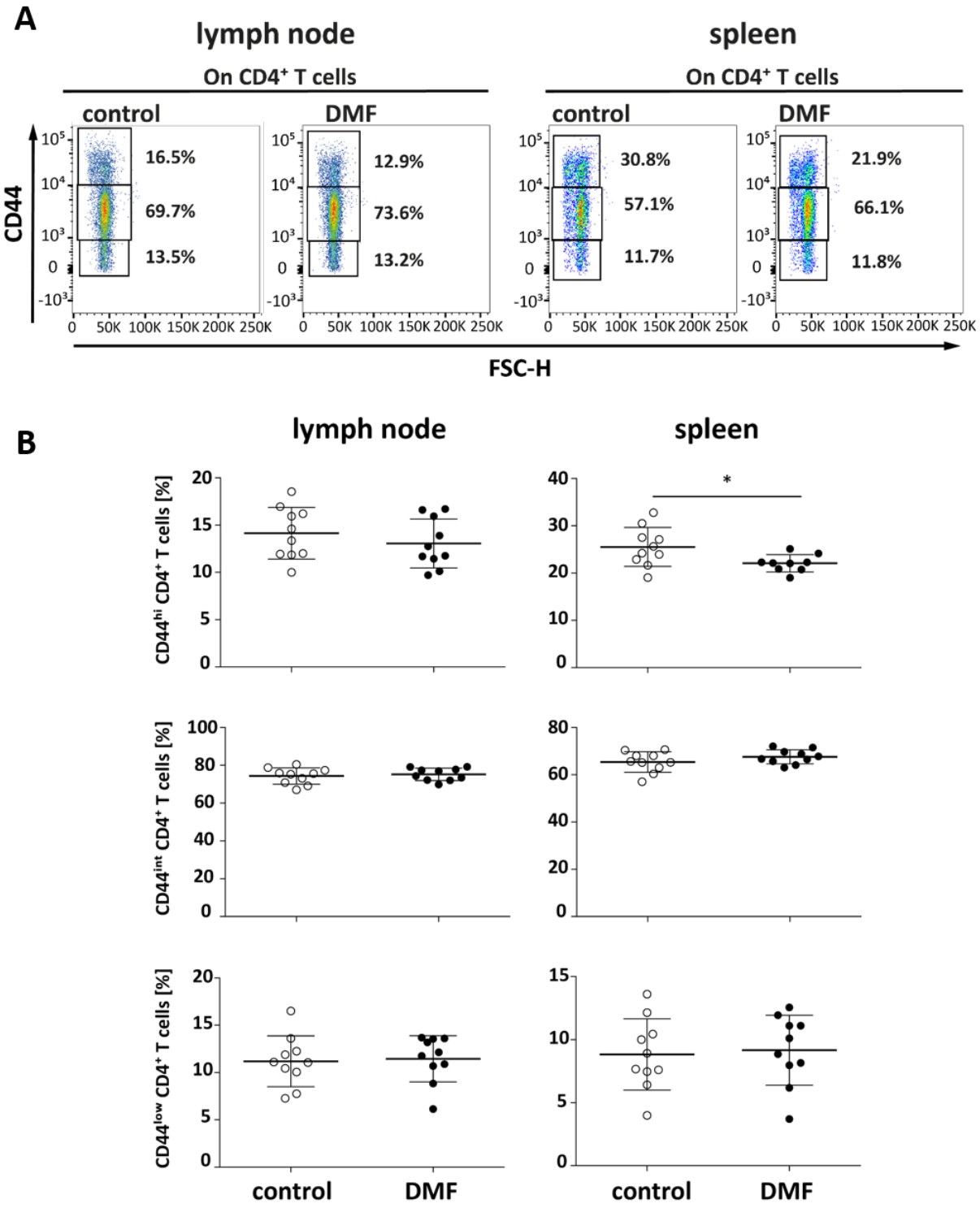

Figure 20: DMF decreases the frequency of CD44^{high} CD4^{+} T cells. The effects of DMF on CD44 expression were investigated in lymph node and spleen from rMOG$_{1-117}$-immunized C57BL/6 mice treated with 15 mg/kg DMF or control twice a day from d-7 until d12 p.i. (A) The expression of CD44 on the surface of CD4^{+} T cells was analyzed by flow cytometry. Subsets of CD4^{+} T cells were classified as follows: CD44 high (CD44^{hi}), CD44 intermediate (CD44^{int}) and CD44 low (CD44^{low}). (B) DMF treatment induces a shift in CD4^{+} T cell subpopulations towards fewer CD44 high cells in spleen. The frequencies of CD4^{+} T cell subpopulations in the lymph node remain unaltered under DMF treatment. Data are represented as mean ± SD (*p<0.05, unpaired t-test).

Besides the analysis of $CD4^+$ T cell subpopulations, DMF effects were also examined on subpopulations of $CD8^+$ T cells. The frequency of splenic $CD44^{hi}$ $CD8^+$ T cells was considerably reduced by DMF treatment (14.4% ± 2.0%) compared to controls (16.8% ± 1.8%) ($p<0.05$) whereas the frequencies of $CD44^{int}$ $CD8^+$ T cells and $CD44^{low}$ $CD8^+$ T cells were not altered by DMF application (Figure 21). DMF treatment did not significantly influence the frequencies of $CD44^{hi}$ $CD4^+$ T cells, $CD44^{int}$ $CD4^+$ T cells and $CD44^{low}$ $CD4^+$ T cells in the lymph node.

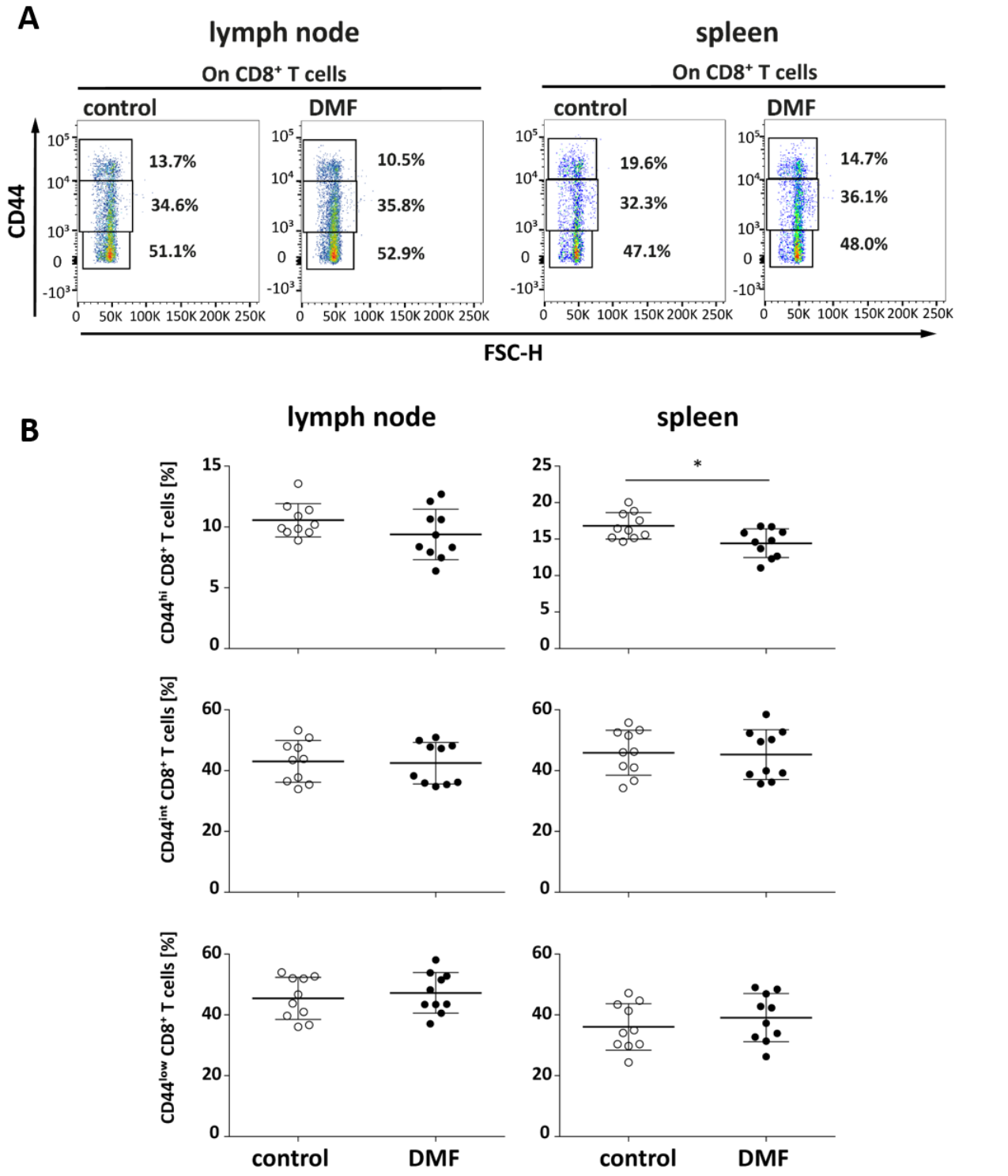

Figure 21: The frequency of CD44^{high} CD8^{+} T cells is reduced by DMF. The effects of DMF on CD44 expression were investigated in lymph node and spleen from rMOG$_{1-117}$-immunized C57BL/6 mice treated with 15 mg/kg DMF or control twice a day from d-7 until d12 p.i. (A) The expression of CD44 on the surface of CD8^{+} T cells was analyzed by flow cytometry. Subsets of CD8^{+} T cells were classified as follows: CD44 high (CD44^{hi}), CD44 intermediate (CD44^{int}) and CD44 low (CD44^{low}). (B) DMF treatment induces a shift in CD8^{+} T cell subpopulations towards fewer CD44 high cells in spleen. The frequencies of CD8^{+} T cell subpopulations in the lymph node remain unaltered under DMF treatment. Data are represented as mean ± SD (*p<0.05, unpaired t-test).

3.2.2.1.4. DMF decreased IFNγ-producing $CD4^+$ T cells numbers

After the characterization of DMF effects on the T cell activation, it was further analyzed if DMF treatment could directly affect the differentiation of pro-inflammatory T cells. Effects of DMF on the frequency of IFNγ-producing $CD4^+$ T cells and IL-17-producing $CD4^+$ T cells were investigated by *ex vivo* stimulation of lymphocytes and splenocytes, isolated from control- or DMF-treated mice, with ionomycin and PMA respectively. Cytokine secretion was blocked and intracellular IFNγ and IL-17 staining was analyzed by flow cytometry (Figure 22). $CD4^+$ T cells were investigated for IFNγ and IL-17 production. DMF significantly reduced the frequency of IFNγ-producing $CD4^+$ T cells in lymph node and spleen from a mean of 2.1% ± 0.9% and 6.8% ± 2.2% in controls to a mean of 1.0% ± 0.4% and 4.4% ± 0.9% in DMF-treated mice ($p<0.01$). DMF treatment slightly reduced IL-17-producing $CD4^+$ T cells compared to controls, but this effect was not statistically significant.

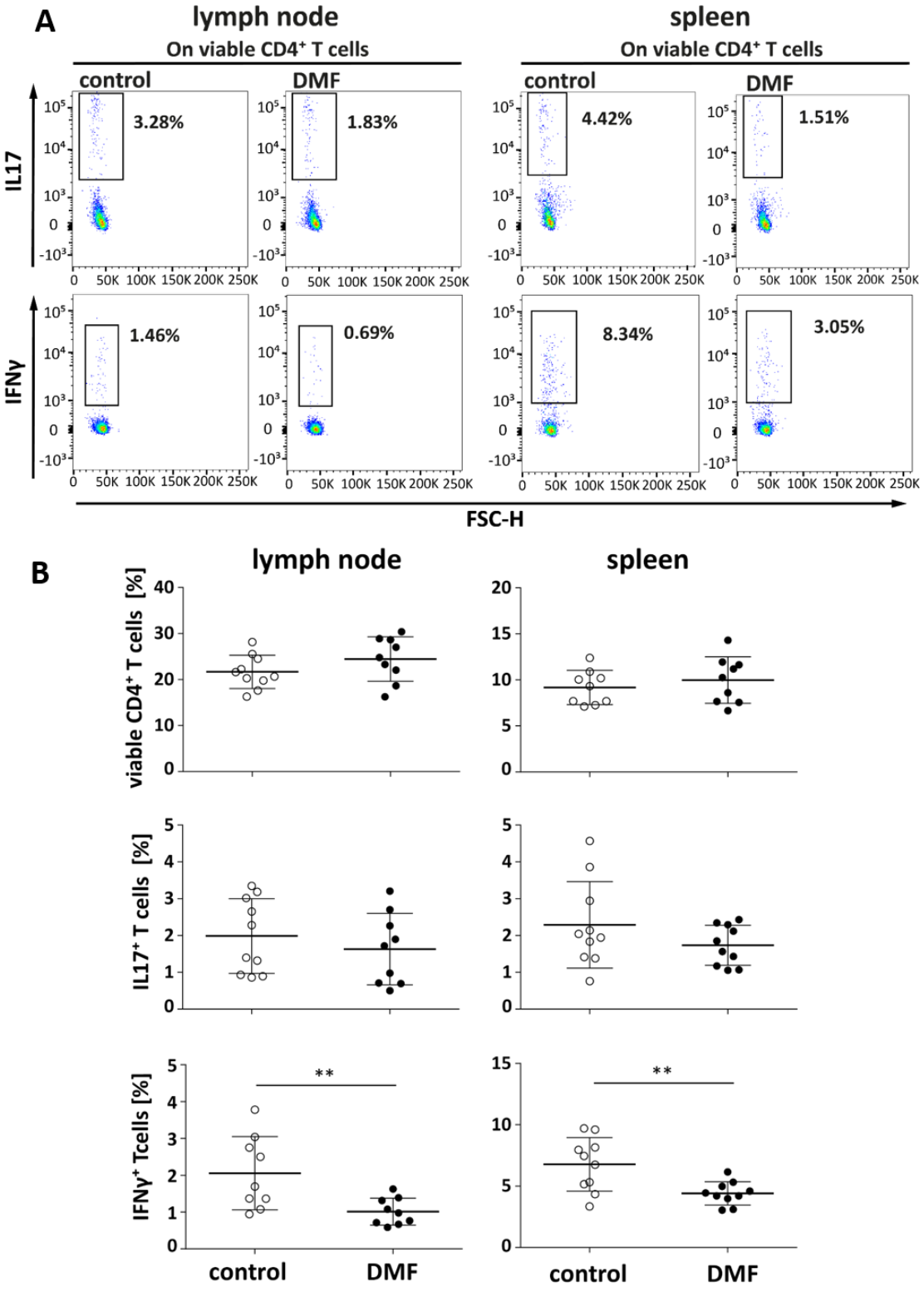

Figure 22: DMF treatment reduces the differentiation of IFNγ$^+$ T cells and IL17$^+$ T cells Splenocytes and lymphocytes were isolated from C57BL/6 mice immunized with $rMOG_{1-117}$ and treated with 15 mg/kg DMF or control twice a day from d-7 until d12 p.i. (A) After ex vivo stimulation with Ionomycin and PMA the proportions of IFNγ-producing (IFNγ$^+$) and IL17-producing (IL17$^+$) T cells were evaluated by intracellular cytokine staining and flow cytometry. (B) In vivo treatment with DMF significantly decreases the frequency of IFNγ$^+$ T cells in lymph node and spleen while the frequencies of viable CD4$^+$ T cells and IL17$^+$ T cells remain unaltered. Data are represented as mean ± SD (**p<0.01, unpaired t-test)

3.2.2.1.5. The frequency of regulatory T cells was not influenced by DMF treatment

For the investigation of DMF effects on anti-inflammatory T cells, the frequency of regulatory T cells among lymphatic and splenic $CD4^+$ T cells was determined in immunized mice treated with either DMF or control. Regulatory T cells are characterized by the expression of the transcription factor Foxp3 and additionally by the surface marker CD25 (Hori et al., 2003). Thus, surface staining for CD4, CD25 and intracellular staining of Foxp3 was performed and the frequencies of $Foxp3^+$ and $Foxp3^+$ $CD25^+$ cells within the population of $CD4^+$ T cells were analyzed via flow cytometry. As seen in Figure 23, data analysis revealed that DMF treatment did not majorly affect the frequency of regulatory T cells.

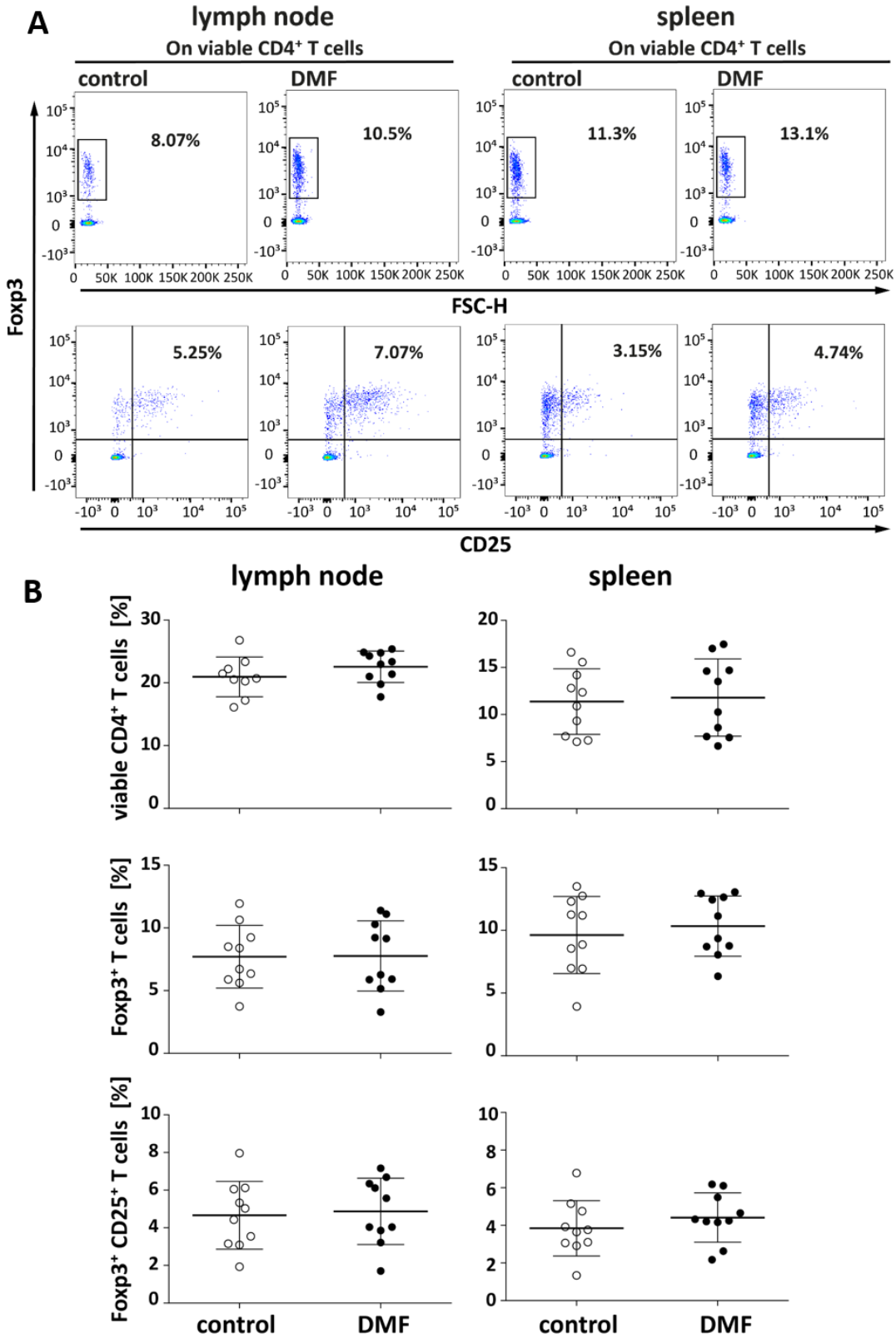

Figure 23: DMF treatment does not alter regulatory T cell frequencies. Splenocytes and lymphocytes were isolated from C57BL/6 mice immunized with $rMOG_{1-117}$ and treated with 15 mg/kg DMF or control twice a day from d-7 until d12 p.i. The frequencies of $Foxp3^+$ T cells and $Foxp3^+$ $CD25^+$ T cells were assessed by intracellular and surface staining and flow cytometry. *In vivo* treatment with DMF does not alter the frequencies of $Foxp3^+$ T cells and $Foxp3^+$ $CD25^+$ T cells in lymph node and spleen. Data are represented as mean ± SD.

3.2.2.1.6. *In vivo* DMF-treated T cells showed reduced proliferation upon antigen-independent activation *in vitro*

To investigate whether DMF treatment *in vivo* could alter the functional properties of T cell activation and proliferation *in vitro*, T cells were isolated from **naïve** C57BL/6 mice treated with 15 mg/kg DMF or control for 19 days. The purified T cells were labeled with the fluorescent dye CFSE and stimulated with anti-CD3/CD28 in an antigen-independent manner. CFSE fluorescence intensity is halved with each cell division and by analyzing the CFSE profile of T cells by flow cytometry, the number of cell divisions can be measured (Parish, 1999).

Proliferation of $CD4^+$ T cells and $CD8^+$ T cells was divided in following proliferation rates: low proliferation, intermediate proliferation and high proliferation (Figure 24B). The total proliferation of *in vivo* DMF-treated $CD4^+$ T cells, stimulated with 0.125 µg/ml anti-CD3, was significantly reduced compared to controls (76.4% ± 3.8% vs. 89.2% ± 2.7%) ($p<0.001$). This reduced proliferation was also demonstrated by the number of cell divisions. DMF-treated $CD4^+$ T cells showed an increased frequency of cells with low proliferation rate compared to controls (DMF: 38.3% ± 3.5% vs. control: 22.7% ± 7.0%) ($p<0.01$) and reduced frequency of cells with high proliferation rate (DMF: 13.9%± 3.7% vs. control: 36.9% ± 12.3%) ($p<0.001$). DMF-treated $CD4^+$ T cells, stimulated with 0.25 µg/ml anti-CD3, showed only a significant reduction in the frequency of cells with high proliferation rate (DMF: 30.6% ± 12.9% vs. control: 46.4% ± 10.7%) ($p<0.01$). The frequency of $CD4^+$ T cells with low proliferation rate, stimulated with 0.25 µg/ml anti-CD3, and the frequencies $CD4^+$ T cells with intermediate proliferation rate, stimulated with 0.125 µg/ml anti-CD3 or 0.25 µg/ml anti-CD3, were not significantly altered by DMF treatment.

In vivo DMF treatment also reduced the total proliferation of $CD8^+$ T cells, stimulated with 0.125 µg/ml anti-CD3, when compared to control-treated $CD8^+$ T cells (86.9% ± 3.4% vs. 94.6% ± 0.9%) ($p<0.0001$) (Figure 24B). This decreased proliferation was also demonstrated by the number of cell divisions. DMF-treated $CD8^+$ T cells showed an increased frequency of cells with low proliferation rate compared to controls (DMF: 27.5% ± 5.6% vs. control: 9.6% ± 4.6%) ($p<0.05$) and reduced frequency of cells with high proliferation rate (DMF: 28.1% ± 8.4% vs. control: 61.3%± 12.4%) ($p<0.0001$). The frequency of $CD8^+$ T cells with intermediate proliferation rate, stimulated with 0.125 µg/ml anti-CD3, was not significantly altered by DMF treatment.

Proliferation of $CD8^+$ T cells, stimulated with 0.25 µg/ml anti-CD3, was neither changed totally nor in single proliferation rates by DMF treatment.

Besides the analysis of proliferation, T cell differentiation of proliferating T cells was analyzed by the production of IFNγ and GM-CSF measured by ELISA (Figure 24C). DMF-treated T cells, stimulated with 0.125 µg/ml anti-CD3, secreted significantly less IFNγ when compared to controls (DMF: 2844 ± 578 pg/ml vs. control: 3851 ± 845 pg/ml) ($p<0.05$). *In vivo* DMF treatment of T cells also significantly reduced the production of GM-CSF *in vitro* from mean secretion of 3553 ± 796 pg/ml by control-treated T cells to a mean secretion of 2404 ± 1194 pg/ml by DMF-treated T cells ($p<0.05$). *In vitro* IFNγ production of T cells stimulated with 0.25 µg/ml anti-CD3 and GM-CSF production of T cells stimulated with 0.125 µg/ml anti-CD3 was not altered by DMF application *in vivo*.

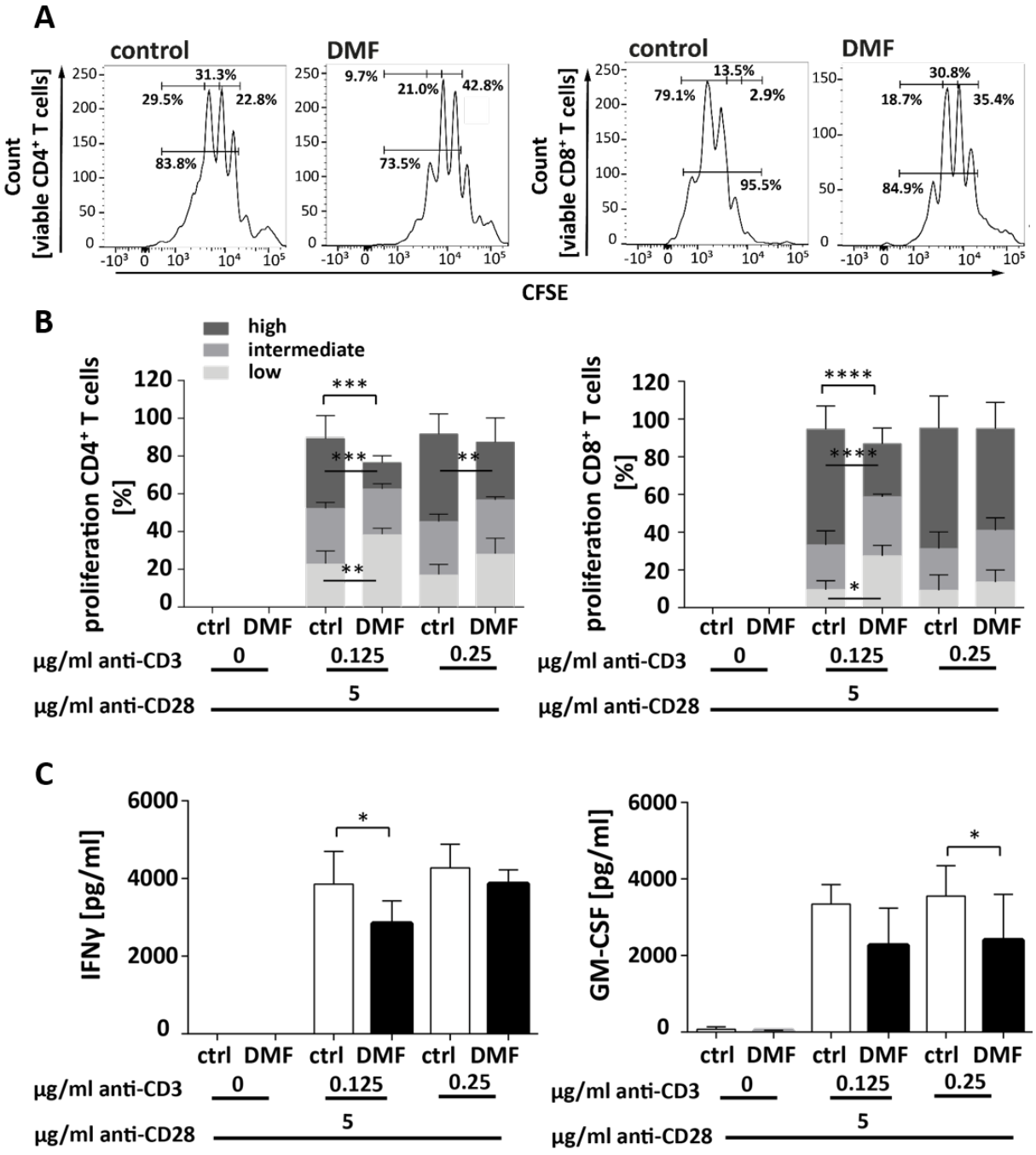

Figure 24: Proliferation of *in vivo* DMF-treated T cells is decreased after antigen-independent stimulation. T cells were purified from the spleens of naïve C57BL/6 mice treated with 15 mg/kg DMF or control twice a day for 19 days. *In vitro*, these T cells were stimulated with 0, 0.125 or 0.25 µg/ml anti-CD3 and 5µg/ml anti-CD28 to induce T cell proliferation. (A) Proliferation of $CD4^+$ T cells and $CD8^+$ T cells was analyzed by flow cytometry. Representative FACS plots for $CD4^+$ T cells and $CD8^+$ T cells stimulated with 0.125 µg/ml anti-CD3 and 5 µg/ml anti-CD28 are shown. (B) In vivo DMF-treated T cells proliferate significantly less after antigen-independent stimulation compared to controls. Data are represented as mean ± SD (n=4, *p<0.05, **p<0.01, ***p<0.001, ****p<0.0001, one-way ANOVA with Sidak post test, two-way ANOVA with Turkey multiple comparison test) (C) IFNγ and GM-CSF production by control- or DMF treated T cells stimulated with 0, 0.125 or 0.25 µg/ml anti-CD3 and 5 µg/ml anti-CD28 was determined by ELISA. T cells treated with DMF produce significantly less IFNγ and GM-CSF compared to control-treated T cells. Data are represented as mean ± SD (n=5, *p<0.05, one-way ANOVA with Sidak post test).

3.2.2.2. DMF treatment increased the antigen-presenting function of B cells

After the investigation of DMF effects on T cells, it was analyzed how DMF influences pathogenic B cells which contribute to the disease pathogenesis in this EAE model. The activation, function and phenotype of B cells were investigated via flow cytometry and co-culture experiments.

3.2.2.2.1. DMF application increased MHC-II expression on B cells

The next set of experiments investigated DMF-induced alterations in B cell subpopulations, activation state and effector functions. Therefore, $rMOG_{1-117}$ immunized mice received daily oral treatment with either 15 mg/kg DMF or control from d-7 until d12 p.i. The activation state of B cells was analyzed *ex vivo* via the expression of MHC-II and the co-stimulatory molecules CD80, CD86 and CD40 in lymph node and spleen by flow cytometry (Figure 25). MHC-II expression was significantly enhanced on B cells in lymph nodes of DMF-treated mice from a mean of 3653 ± 714 gMFI in controls to a mean of 4538 ± 620 gMFI in DMF-treated animals. The expression of CD80, CD86 and CD40 on lymphatic and splenic B cells as well as MHC-II expression on splenic B cells was not significantly changed by DMF application.

Next page →

Figure 25: MHC-II expression on B cells is increased after DMF treatment. For the analysis of DMF effects on B cell activation, splenocytes and lymphocytes were isolated from C57BL/6 mice immunized with $rMOG_{1-117}$ and treated with 15 mg/kg DMF or control twice a day from d-7 until d12 p.i. (A) The expression of MHC-II and co-stimulatory molecules CD80, CD86 and CD40 on B cells ($B220^+$ $CD19^+$) was analyzed by flow cytometry. (B) Data evaluation revealed that DMF significantly increases the expression of MHC-II on B cells of the lymph node whereas the co-stimulatory molecules remain mostly unaltered. Data are represented as mean ± SD (**p<0.01, unpaired t-test).

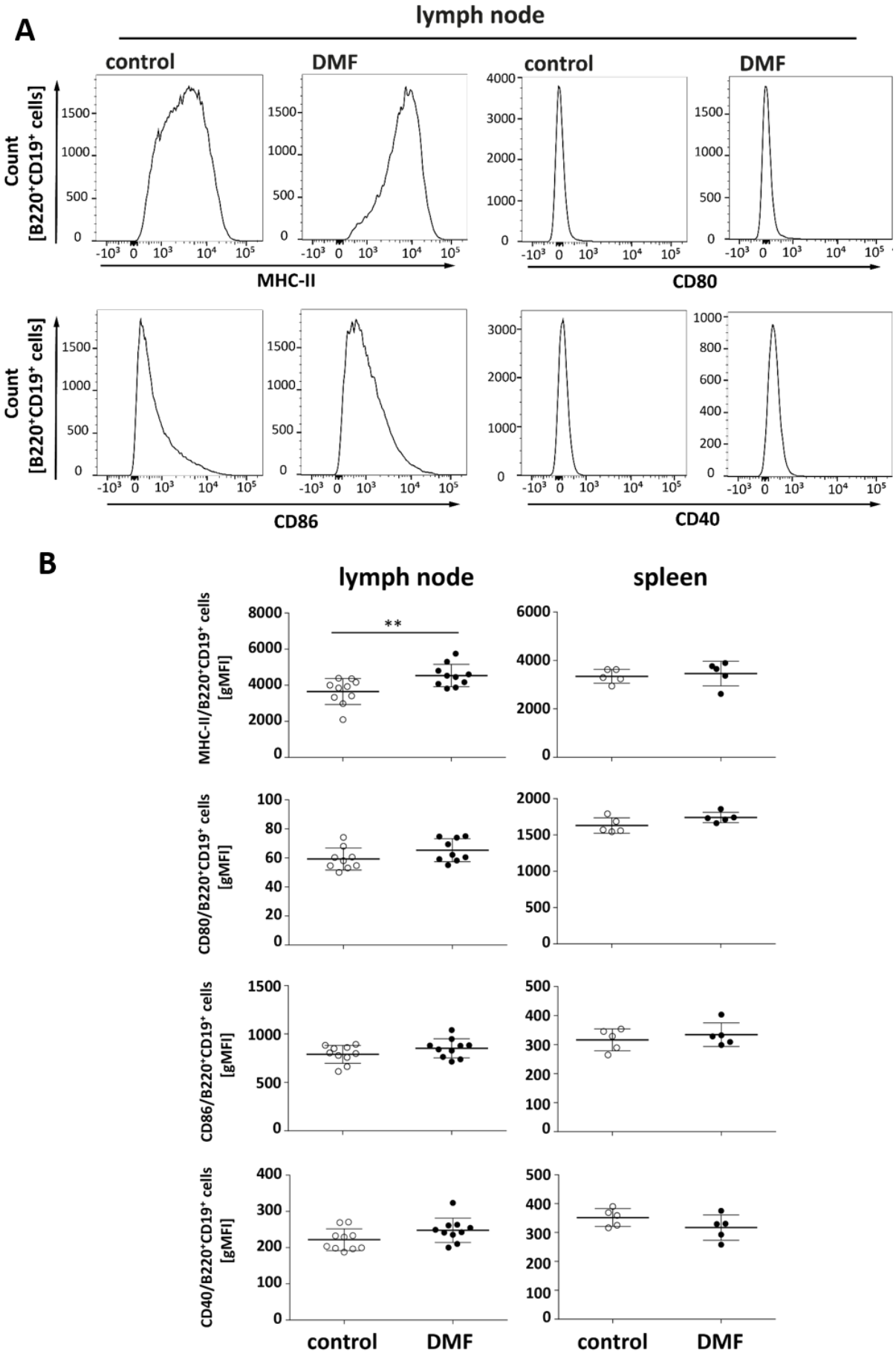
A
lymph node
control
DMF
control
DMF
Count [B220+CD19+ cells]
MHC-II
CD80
CD86
CD40
B
lymph node
spleen
MHC-II/B220+CD19+ cells [gMFI]
CD80/B220+CD19+ cells [gMFI]
CD86/B220+CD19+ cells [gMFI]
CD40/B220+CD19+ cells [gMFI]
**
control
DMF
control
DMF

3.2.2.2.2. The expression of activation markers was not influenced by DMF treatment

To further investigate the DMF effect on B cell activation, the expression of the activation markers CD69 and CD25 as well as the expression of the antigen-specific activation marker Fas (CD95) were measured on B cells from DMF- or control-treated mice. Therefore lymph nodes and spleen were isolated from immunized mice treated with either 15 mg/kg DMF of control and B cell activation markers were analyzed by flow cytometry (Figure 26). The expression of CD69, CD25 and Fas on B cells isolated from lymph node and spleen was comparable between DMF-treated and control-treated mice.

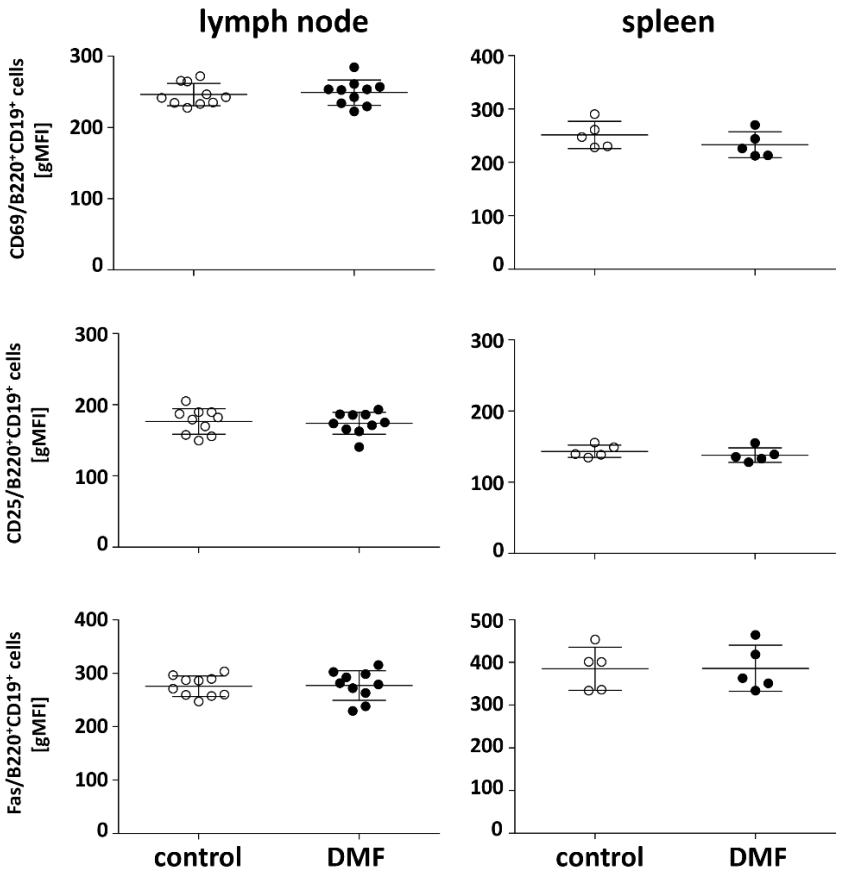

Figure 26: Expression levels of activation markers on B cells remain constant after DMF treatment. For the analysis of DMF effects on B cell activation, splenocytes and lymphocytes were isolated from C57BL/6 mice immunized with $rMOG_{1-117}$ and treated with 15 mg/kg DMF or control twice a day from d-7 until d12 p.i. The expression of activation marker CD69, CD25 and Fas (CD95) on B cells ($B220^+$ $CD19^+$) was analyzed by flow cytometry. DMF treatment does not significantly alter the expression of activation markers on B cells. Data are represented as mean ± SD.

3.2.2.2.3. DMF treatment shifted B cell subsets towards more CD21^{int} B cells

After DMF effects were investigated on B cell activation, it was further analyzed if DMF also affects specific subpopulations of B cells. Murine B cells can be divided by distinct expression pattern of the surface molecules CD21 and CD23. Using flow cytometry, CD21^{hi} CD23^{+} B cells can be distinguished from CD21^{int} CD23^{+} B cells and CD21^{-} CD23^{-} B cells (Shen and Fillatreau, 2015). CD21^{hi} CD23^{+} B cells, CD21^{int} CD23^{+} B cells and CD21^{-} CD23^{-} B cells will be further referred to as transitional, follicular and immature B cells, respectively, in this work.

To examine the effects of DMF on B cell subpopulations in spleen and bone marrow, the proportion of transitional, follicular and immature B cells were analyzed within the proportion of B220^{+} CD19^{+} B cells by flow cytometry (Figure 27). DMF treatment profoundly altered B cell subpopulations in immunized mice. DMF mediated a shift towards more follicular B cells and fewer transitional B cells in spleen, whereas the immature B cells in the bone marrow remained constant. Transitional B cells were decreased in DMF-treated animals (12.9% ± 2.5%) when compared to controls (14.9% ± 0.9%) ($p<0.05$). Follicular B cells were increased in DMF-treated mice (74.6% ± 2.5%) compared to control-treated animals (72.6% ± 1.1%) ($p<0.05$).

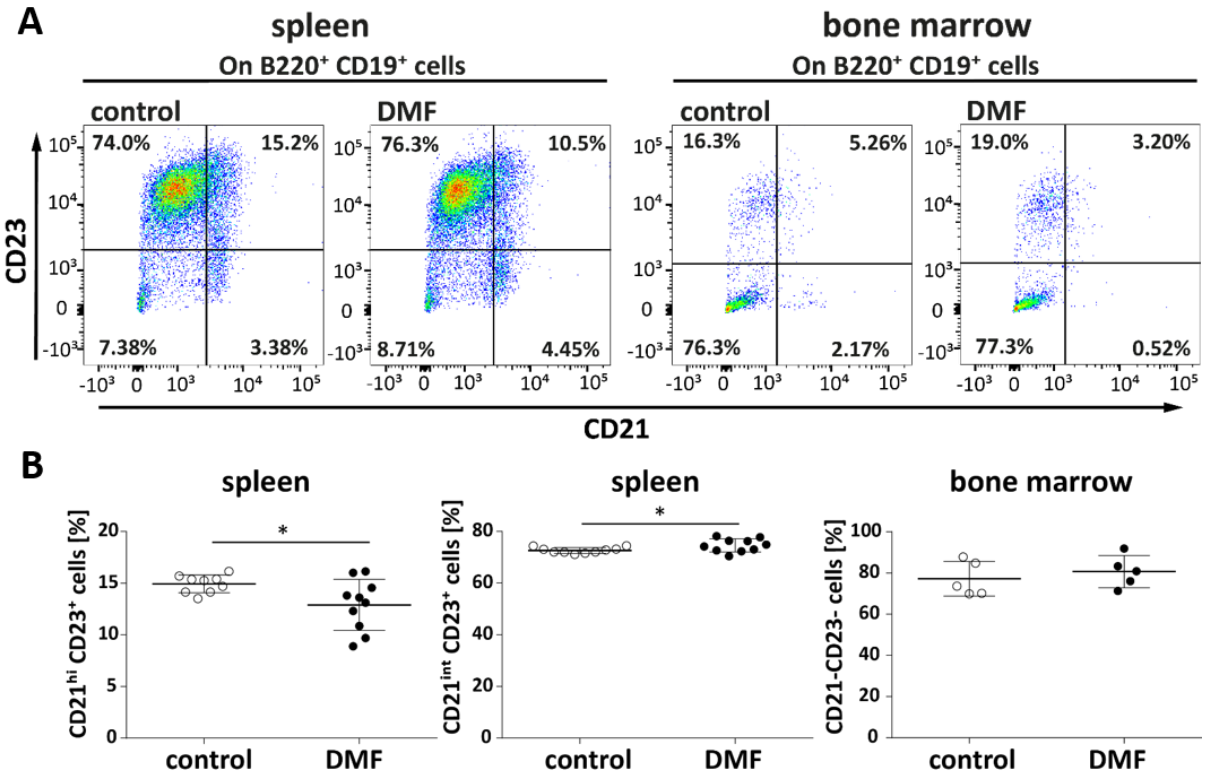

Figure 27: DMF induces a shift in B cell subpopulations. The effects of DMF B cell subpopulations were investigated in spleens from rMOG$_{1-117}$-immunized C57BL/6 mice treated with 15 mg/kg DMF or control twice a day from d-7 until d12 p.i. The expression of CD21 and CD23 on the surface of B cells (B220$^+$ CD19$^+$) was analyzed by flow cytometry. Subsets of B cells were classified as follows: CD21^{hi} CD23$^+$ B cells (transitional B cells), CD21^{int} CD23$^+$ B cells (follicular B cells) and CD21$^-$ CD23$^-$ B cells (immature B cells). DMF treatment induces a shift in B cell subpopulations towards fewer transitional and more follicular B cells in spleen. Data are represented as mean ± SD (*p<0.05, unpaired t-test).

3.2.2.2.4. B cell phenotypes were not altered under DMF treatment

Investigation of DMF effects on B cell subpopulations revealed that DMF treatment enhanced the frequency of follicular B cells, which reside in lymphoid follicles inside the spleen. Additionally, B cells can be divided in more specific phenotypes. Figure 28 shows the DMF effects on the following B cell phenotypes: immature naïve B cells (CD23$^-$, IgM$^+$, IgD$^-$), mature naïve B cells (CD23$^+$, CD38, IgM$^-$, IgD$^+$), memory B cells (B220^{high}, CD38$^+$, IgD$^-$), regulatory B cells (CD1d^{high}, CD5$^+$), germinal center B cells (CD37$^+$, GL7$^+$) and antigen-activated B cells (CD27$^+$, CD69$^+$, CD80$^+$, MHC-II^{high}).

To analyze whether DMF treatment *in vivo* could affect specific phenotypes of B cells, B cells were isolated from the spleen of immunized C57BL/6 mice treated with 15 mg/kg DMF or control from

d-7 until d12 p.i. The purified B cells were analyzed and phenotypes distinguished by flow cytometry using the surface markers described above (Figure 28). DMF-treated animals displayed slightly lower frequencies of immature naïve and germinal center B cells. The frequencies of antigen-activated and regulatory B cells were slightly increased by DMF treatment. Nevertheless, these effects did not reach any statistically significance. The frequencies of mature naïve and memory B cells remained unaltered by DMF.

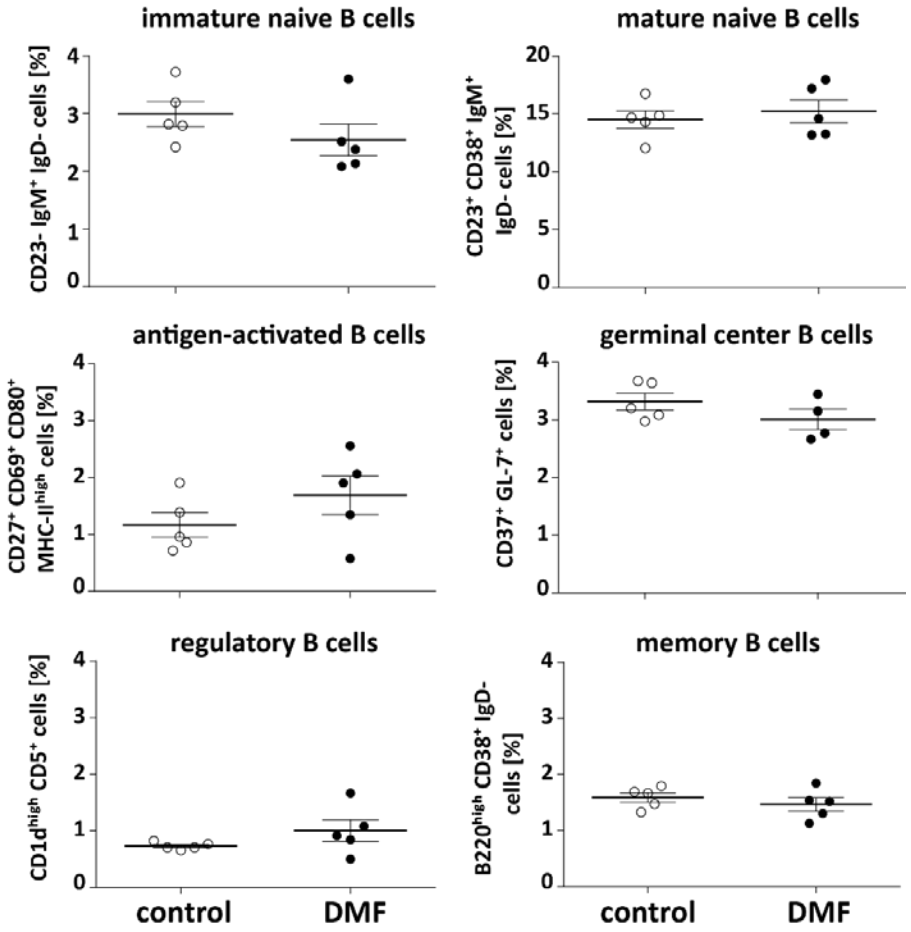

Figure 28: B cell phenotypes are not significantly affected by DMF treatment. B cells were purified from the spleens of C57BL/6 mice immunized with $rMOG_{1-117}$ and treated with 15 mg/kg DMF or control twice a day from d-7 until d12 p.i. The expression of B220, CD1d, CD5, CD23, CD27, CD37, CD38, CD69, CD80, GL-7, IgD, IgM and MHC-II on the surface of B cells was analyzed by flow cytometry. Subsets of B cells were classified as follows: immature naïve B cells ($CD23^-$, IgM^+, IgD^-), mature naïve B cells ($CD23^+$, CD38, IgM^-, IgD^+), memory B cells ($B220^{high}$, $CD38^+$, IgD^-), regulatory B cells ($CD1d^{high}$, $CD5^+$), germinal center B cells ($CD37^+$, $GL7^+$) and antigen-activated B cells ($CD27^+$, $CD69^+$, $CD80^+$, $MHC\text{-}II^{high}$). FACS evaluation revealed that these B cell phenotypes are not significantly influenced by DMF application in vivo. Data are represented as mean ± SD.

3.2.2.2.5. DMF did not alter the frequency of rMOG$_{1-117}$-binding B cells

As a first functional analysis of *in vivo* control- or DMF-treated B cells, an rMOG-binding assay was performed to examine the antigen-binding capacity of B cells. Purified B cells of control- or DMF-treated mice were then incubated with fluorescence-labeled rMOG for 2 hours and the frequency of B cells which had bound to rMOG was analyzed by flow cytometry (Figure 29). Data evaluation revealed that *in vivo* DMF treatment did not significantly alter the rMOG-binding capacity of B cells *in vitro.*

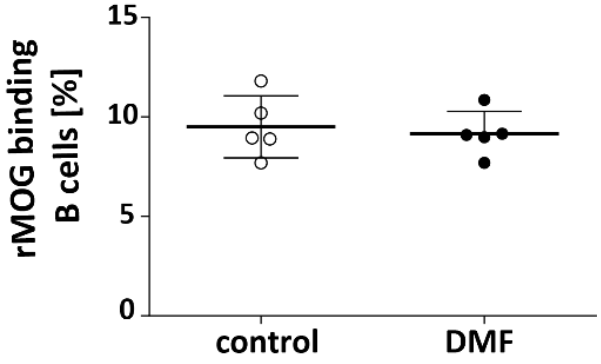

Figure 29: DMF has no effect on the rMOG$_{1-117}$-binding capacity B cells. B cells were purified from the spleens of C57BL/6 mice immunized with rMOG$_{1-117}$ and treated with 15 mg/kg DMF or control twice a day from d-7 until d12 p.i. *In vitro*, these B cells were incubated with fluorescence-labeled rMOG$_{1-117}$ and frequency of rMOG-binding B cells was evaluated by flow cytometry. *In vivo* treatment with DMF does not influence the antigen-binding capacity of B cells. Data are represented as mean ± SD.

3.2.2.2.6. *In vivo* DMF-treated B cells promoted antigen-dependent T cell proliferation *in vitro*

In a next experiment it was investigated how DMF affects the antigen-presenting functions of B cells. Therefore a co-culture experiment with control- or DMF-treated B cells and 2D2 T cells was performed to analyze B cell-mediated effects on T cell proliferation and T cell differentiation *in vitro*. Immunized C57BL/6 mice were treated with 15 mg/kg DMF or control from d-2 until day12 p.i. B cells were purified from the spleens of control- or DMF-treated C57BL/6 mice. Afterwards, these purified B cells were co-cultured with unlabeled or CFSE-labeled T cells isolated from **naïve** 2D2 mice and stimulated with rMOG$_{1-117}$. T cell proliferation and differentiation were analyzed by flow cytometry.

The first co-culture experiment investigated whether DMF treatment *in vivo* could alter the antigen-presenting functions of B cells. Therefore *in vivo* control- or DMF-treated B cells were co-cultured with CFSE-labeled 2D2 T cells and stimulated with 0, 25 or 50 µg/ml $rMOG_{1-117}$. B cells with a more potent antigen-presenting function induce a higher activation and proliferation of 2D2 T cells. Figure 30 illustrates the DMF-mediated effects on the antigen-presenting function of B cells measured indirectly by T cell proliferation after 65 h.

To acquire a more detailed analysis of DMF-induced effects, the proliferation of 2D2 T cells was divided in different proliferation rates. A low proliferation rate would therefore indicate a weak antigen-presenting function of B cells whereas high proliferation rate would indicate a more potent antigen-presenting function of B cells. The impact of DMF treatment on the antigen-presenting function of B cells and thereby on 2D2 T cell proliferation is shown in Figure 30B. The total proliferation of 2D2 T cells co-cultured with *in vivo* DMF-treated B cells was significantly enhanced compared to controls (25 µg/ml $rMOG_{1-117}$: ctrl 13.6% ± 2.5% vs. DMF 18.7% ± 4.4%, 50 µg/ml $rMOG_{1-117}$: ctrl 16.8% ± 3.6% vs. DMF 24.2% ± 4.2%) ($p<0.05$, $p<0.01$). When compared to control, DMF-treated B cells increased the frequency of 2D2 T cells with low proliferation rate (50 µg/ml $rMOG_{1-117}$: ctrl 5.6% ± 0.5% vs. DMF 6.2% ± 0.7%, $p<0.05$), the frequency of 2D2 T cells with intermediate proliferation rate (50 µg/ml $rMOG_{1-117}$: ctrl 5.8% ± 1.6% vs. DMF 8.2% ± 1.1%, $p<0.05$) and the frequency of 2D2 T cells with high proliferation rate (25 µg/ml $rMOG_{1-117}$: ctrl 4.4% ± 0.7% vs. DMF 7.4% ± 2.1%, $p<0.001$; 50 µg/ml $rMOG_{1-117}$: ctrl 5.4% ± 1.6% vs. DMF 8.2% ± 2.3%, $p<0.01$). The frequencies of 2D2 T cells with low and intermediate proliferation rate stimulated with 25 µg/ml $rMOG_{1-117}$ were not significantly altered by DMF-treated B cells when compared to 2D2 T cells co-cultured with control-treated B cells.

Additionally to the analysis of 2D2 T cell proliferation, co-cultured B cells were analyzed for MHC-II expression by flow cytometry (Figure 30C). In accordance with the *ex vivo* staining of B cells (Figure 25), MHC-II expression was slightly increased on DMF-treated co-cultured B cells, stimulated with 25 µg/ml $rMOG_{1-117}$, when compared to control-treated B cells. Nevertheless, this effect did not reach statistically significance.

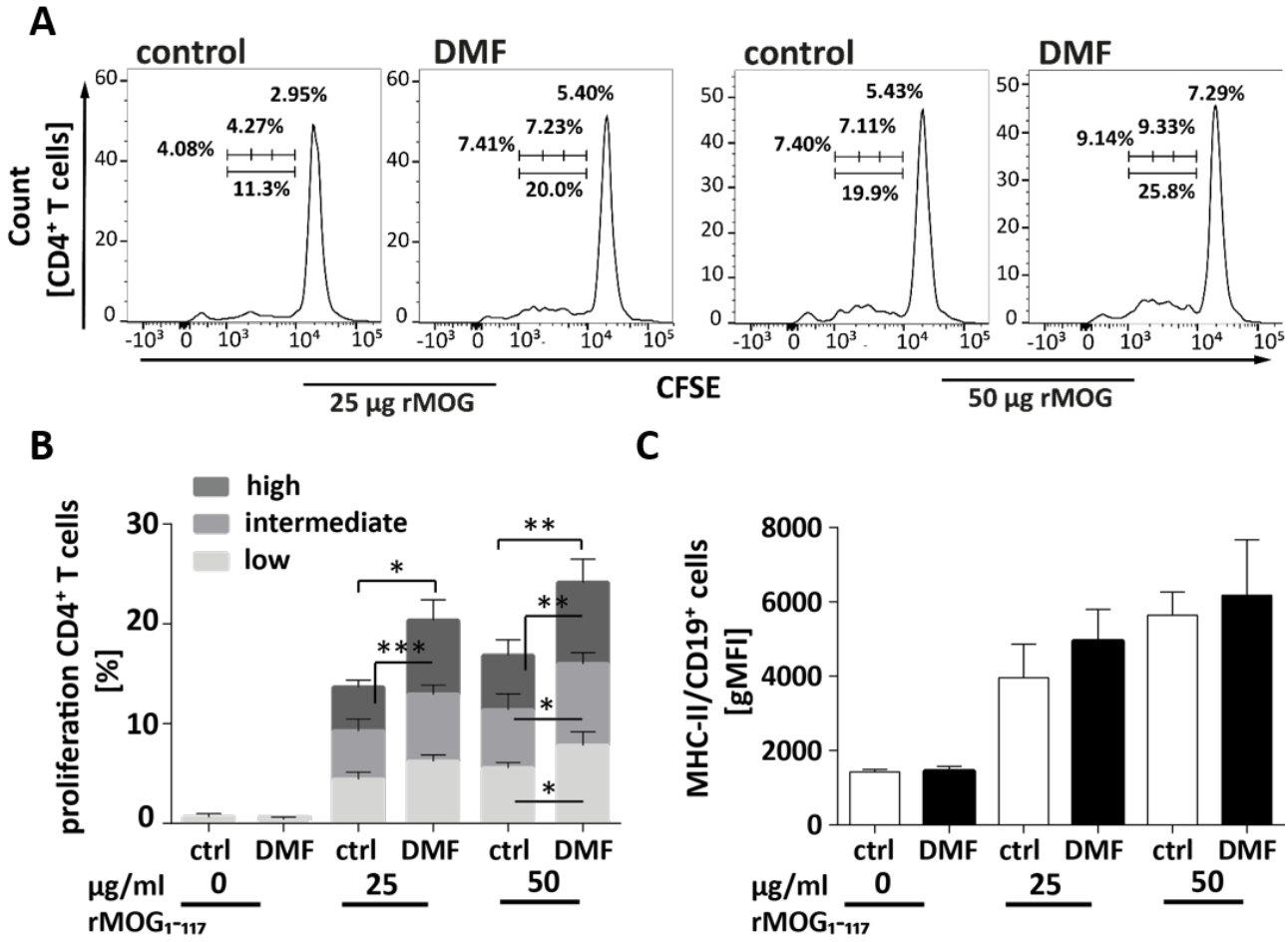

Figure 30: In vivo DMF treatment enhances the antigen-presenting function of B cells. To investigate the effects of DMF on the antigen-presenting function, B cells were purified from C57BL/6 mice immunized with $rMOG_{1-117}$ and treated with 15 mg/kg DMF or control twice a day from d-2 until d12 p.i. These isolated B cells were then co-cultured with CFSE-labeled 2D2 T cells and stimulated with 0, 25 or 50 µg/ml $rMOG_{1-117}$. (A,B) The proliferation was analyzed by flow cytometry in the presence of either control- or DMF-treated B cells. Proliferation of 2D2 T cells is significantly increased when these are co-cultured with DMF-treated B cells. (C) Simultaneously, MHC-II expression was analyzed on co-cultured B cells via flow cytometry. MHC-II is not significantly upregulated on B cells isolated from DMF-treated mice. Data are represented as mean ± SD (n=5, *p<0.05, **p<0.01, ***p<0.001, two-way ANOVA).

3.2.2.2.7. *In vivo* DMF-treated B cells do not influence differentiation of IFNγ-producing T cells

The first co-culture experiment demonstrated that 2D2 T cell proliferation could be amplified by *in vivo* DMF treatment of B cells. Hence, it was interesting to further analyze the fate of these high proliferating 2D2 T cells. To address this question, the differentiation of 2D2 T cells *in vitro* was analyzed in another co-culture system. The co-culture assay was performed as described in sections 2.4.10.4 and 3.2.2.2.6, except for the CFSE labeling of 2D2 T cells.

After 65 hours, 2D2 T cells were treated with ionomycin and PMA, cytokine secretion was blocked and intracellular IFNγ staining was analyzed by flow cytometry. As depicted in Figure 31, there was no difference in the frequency of IFNγ$^+$ T cells between 2D2 T cells which were co-cultured with control- or DMF-treated B cells.

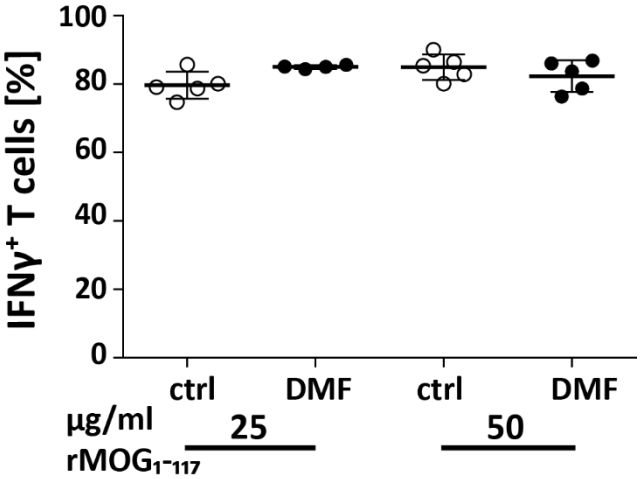

Figure 31: In vivo DMF-treated B cells do not alter T cell differentiation in vitro. B cells were purified from C57BL/6 mice immunized with $rMOG_{1-117}$ and treated with 15 mg/kg DMF or control twice a day from d-2 until d12 p.i. These isolated B cells were then co-cultured with CFSE-labeled 2D2 T cells and stimulated with 25 or 50 µg/ml $rMOG_{1-117}$. The differentiation of IFNγ-producing (IFNγ$^+$) T cells was analyzed by intracellular staining and flow cytometry in the presence of either control- or DMF-treated B cells. The frequency of IFNγ$^+$ T cells is not altered in the presence of DMF-treated B cells. Data are represented as mean ± SD.

3.2.3. DMF effects on human B cells

We could observe that DMF treatment induced profound alterations of B cell functions in mice. To study if these DMF effects could also partly be seen on human B cells, a FACS analysis of B cells from non-treated MS patients (MS control) and DMF-treated MS patients (MS DMF) was performed.

3.2.3.1. DMF treatment enhanced MHC-II expression on human B cells

For the analysis of B cells, PBMCs isolated from MS patients were stained for CD19, MHC-II, CD80 and CD40 analyzed via flow cytometry (Figure 32). MHC-II expression was significantly increased on B cells from DMF-treated MS patients when compared to non-treated MS patients (MS DMF

13078 ± 2199 gMFI vs. MS control 10592 ± 1428 gMFI) ($p<0.05$). The frequency of B cells and expression of CD80 and CD40 was comparable between DMF- and non-treated MS patients.

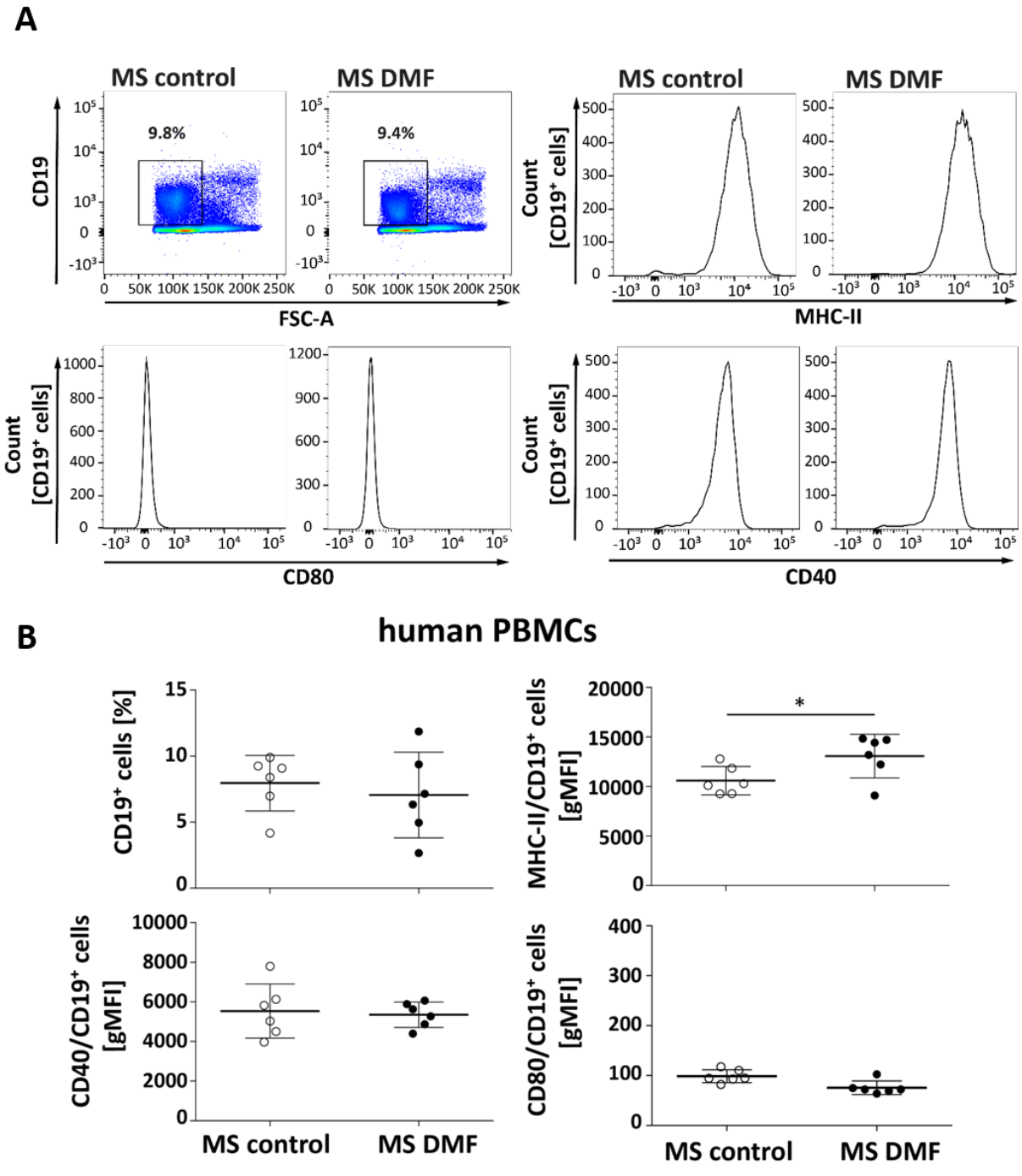

Figure 32: DMF effects on B cells of MS patients. PBMCs were isolated from non-treated (control) or DMF-treated MS patients. The frequency of B cells and expression of MHC-II and co-stimulatory molecules CD80 and CD40 on B cells ($CD19^+$) was analyzed by flow cytometry (A). Data evaluation revealed that DMF significantly increases the expression of MHC-II on B cells of DMF-treated MS patients whereas the B cell frequency and expression of co-stimulatory molecules remain mostly unaltered (B). Data are represented as mean ± SD (*$p<0.05$, unpaired t-test).

In summary, DMF treatment in a B cell-mediated EAE model significantly ameliorated the disease course and reduced demyelination and inflammation of the spinal cord. Furthermore, T cell activation, pro-inflammatory T cell differentiation and antigen-independent proliferation of T cells was significantly decreased under DMF treatment during the early phase of EAE. In contrast, DMF increased MHC-II expression, the frequency of follicular B cells and antigen-presenting properties of B cells. These results could also partly be observed in DMF-treated MS patients whose B cells also showed an increased expression of MHC-II.

4. Discussion

The oral agent dimethyl fumarate (DMF) has been approved for the therapy of RRMS. Besides its beneficial effects on relapse rate and MRI lesion formation, DMF and its metabolite MMF have been shown to exert several immunomodulatory functions on cells of the adaptive immune system (Moharregh-Khiabani et al., 2009). This includes the ability to induce apoptosis of activated T cells and the downregulation of the transcription factor NF-κB in T cells, DCs and endothelial cells which results in a reduced production of inflammatory cytokines, chemokines and adhesion molecules (de Jong et al., 1996; Stoof et al., 2001; Treumer et al., 2003). In EAE and cell culture, DMF was described to have neuroprotective functions mediated by the activation of the transcription factor Nrf2 which lead to an increased protection of cells against reactive oxygen species (ROS) (Linker et al., 2011; Scannevin et al., 2012c). Nevertheless, it is still unknown if DMF treatment has any direct effects on the CNS which are not mediated via the modulation of peripheral immune cells.

The present study aimed to analyze if DMF has CNS intrinsic effects independent of the peripheral immune system. Therefore, the cuprizone mouse model was used to study the effects of DMF on CNS cells, demyelination and remyelination as well as axonal damage. Histological evaluation revealed that DMF showed neuroprotective and possibly neuroregenerative effects within the CNS.

In the second part of this study DMF effects were investigated in a B cell-mediated EAE model. So far, DMF was only analyzed in mainly T cell-mediated EAE models and direct effects of DMF on B cells have not been reported. Clinical, histological and immunological analyses were performed to study the DMF effects in this animal model and revealed B cell altering properties of DMF.

4.1. DMF shows neuroprotective and potentially regenerative effects in the cuprizone mouse model

MS is an inflammatory and demyelinating disease of the CNS with focal lesions in which myelin, myelin-forming cells (oligodendrocytes) and axons are damaged (Trapp and Nave, 2008). The histopathology of MS is heterogeneous, with lesion patterns characterized by immune-mediated demyelination but also patterns which suggest a primary oligodendrogliopathy (Lucchinetti et al., 2000; Rone et al., 2016). The oral agent DMF has been shown to exert beneficial effects in the therapy of RRMS. So far, it is assumed that the successful treatment is mainly mediated via DMF

effects on the peripheral immune system (e.g. reduction of pro-inflammatory T cells and DCs) whereas direct effects of DMF on the central nervous system are still controversially discussed (Ghoreschi et al., 2011; Litjens et al., 2006; Moharregh-Khiabani et al., 2009; Scannevin et al., 2012c). We investigated the DMF effects on the CNS in the cuprizone model in which the BBB remains intact and an influence of peripheral immune cells can be majorly excluded (Bakker and Ludwin, 1987; McMahon et al., 2002). Different time points were examined to analyze the treatment effects on oligodendrocyte apoptosis, axonal damage as well as demyelination and remyelination.

4.1.1. DMF exerts neuroprotective effects during short-term cuprizone treatment

One feature of MS lesions is the loss of myelin-producing oligodendrocytes. Oligodendrocytes may show signs of apoptotic cell death, e.g. the upregulation of apoptosis-related proteins such as FAS, (Dowling et al., 1996; Lucchinetti et al., 2000). Thus, we aimed to analyze if DMF could influence the apoptosis of oligodendrocytes induced by cuprizone intoxication. Loss of oligodendrocytes is an early event during cuprizone treatment and therefore DMF effects on apoptosis were analyzed after one week of cuprizone diet (Figure 2) (Matsushima and Morell, 2001b). The number of apoptotic cells was significantly reduced by DMF treatment, which suggested that DMF may have a cytoprotective effect on oligodendrocytes (Figure 2). The exact mechanism of cuprizone-induced oligodendrocyte apoptosis is still unknown, but several studies suggest that cuprizone provokes mitochondrial dysfunction, such as the formation of giant mitochondria, and disturbances of the oligodendroglial metabolism which could contribute to the apoptosis of oligodendrocytes (Acs et al., 2013; Goldberg et al., 2013; Matsushima and Morell, 2001b). The formation of these megamitochondria mainly takes place in hepatic cells but could also be observed in oligodendrocytes (Acs et al., 2013; Biancotti et al., 2008). It is considered to be a protective mechanism of cells against oxidative stress, since it was demonstrated that mitochondria enlarge when exposed to elevated levels of ROS *in vitro* (Wakabayashi, 2002). These data may suggest that the cuprizone-mediated loss of oligodendrocytes could be caused by increased oxidative damage. It could already be demonstrated that oligodendrocytes show a high vulnerability to oxidative stress (Praet et al., 2014). One factor which contributes to this high vulnerability is the intrinsically low amount of glutathione (GSH) in oligodendrocytes, a molecule which is required as an electron donor for the glutathione peroxidase (GPx) (Juurlink et al., 1998; Witherick et al., 2010).

This enzyme reduces free hydrogen peroxide (H_2O_2) in order to protect cells from oxidative damage. Furthermore, cuprizone intoxication was shown to decrease the GSH content of hepatic cells as well as oligodendrocytes and could thereby increase susceptibility of oligodendrocytes to oxidative stress (Biancotti et al., 2008). Several *in vitro* and *in vivo* studies revealed that DMF can protect cells against oxidative damage via an increased activation of Nrf2 and increased production and recycling of GSH. Nrf2 elevates gene expression of several detoxification enzymes (e.g. GSH-dependent enzymes) and is normally located in the cytoplasm where it is sequestered to kelch-like erythroid cell-derived protein 1 (Keap1), a functional inhibitor of Nrf2 (Nguyen et al., 2009). Fumaric acid esters (FAEs), including DMF, can bind Keap1 by covalent binding to thiol groups and therefore promote the translocation of Nrf2 into the nucleus (Linker et al., 2011; Nguyen et al., 2005). A study in 1990 could show that *in vivo* DMF treatment induces the activity of GSH-dependent detoxification enzymes (e.g. NADPH oxidoreductase) in various murine tissues (Spencer et al., 1990). *In vitro*, DMF and its metabolite MMF elevated GSH levels in murine and human astrocytes and increased the viability of astrocytes and rat cortical neurons after oxidative challenge with H_2O_2 (Albrecht et al., 2012; Scannevin et al., 2012c). The DMF effect on cell viability after oxidative stress challenge was suggested to be Nrf2-dependent, since the effect was lost in cells lacking Nrf2. Additionally, *in vitro* treatment with MMF increased cellular ATP content and more importantly, enhanced mitochondrial membrane polarization which can antagonize mitochondrial dysfunction (Scannevin et al., 2012c). A recent study showed that *in vitro* DMF treatment increases the levels of antioxidant molecules including carnitine, ascorbic acid and GSH in human oligodendrocytes (Huang et al., 2015). Correspondingly, DMF could also protect oligodendrocytes against H_2O_2-mediated oxidative damage. Oxidative stress and mitochondrial injury are also assumed to contribute to oligodendrocyte loss in MS pathology (Bradl and Lassmann, 2010; Haider et al., 2011). A continuative study confirmed that mitochondrial injury occurs in active MS lesions and may contribute to the production of ROS (Fischer et al., 2012). Thus, the antioxidant impact of DMF may also exert beneficial effects leading to reduced oligodendrocyte loss in MS patients.

Besides the apoptosis of oligodendrocytes, it was also investigated if DMF influences the number of oligodendrocytes including oligodendrocyte precursor cells ($Olig2^+$ cells) and specifically mature oligodendrocytes ($NogoA^+$ cells) after 7 days of cuprizone exposure.

This study revealed that DMF treatment preserved a higher number of Olig2$^+$ cells whereas the number of NogoA$^+$ cells was only slightly increased by DMF treatment at this time point (Figure 3). The lowest numbers of Olig2$^+$ cells are observed after 10 days of cuprizone treatment whereas fewest numbers of NogoA$^+$ cells are observed on day 21 of cuprizone treatment (Hesse et al., 2010b). Interestingly, on day 21 numbers of Olig2$^+$ cells start to increase again suggesting a recruitment of oligodendroglial progenitor cells (OPCs) even with ongoing cuprizone treatment (Matsushima and Morell, 2001b). This phenomenon was also observed in our experiments, where Olig2$^+$ cells were decreased compared to NogoA$^+$ cells on day 7 of cuprizone treatment (Figure 3). Our data suggest that DMF might exert an early protective effect on oligodendrocytes which are majorly affected by cuprizone intoxication, specifically preserving Olig2$^+$ cells.

Furthermore, DMF also significantly reduced the number of acutely damaged axons compared to control treatment, investigated 7 days after cuprizone treatment (Figure 4). Acute axonal damage was analyzed by staining for amyloid precursor protein (APP), which is observed at sites of axonal injury (Koo et al., 1990). Although cuprizone treatment leads to axonal damage in mice, it is assumed that cuprizone has no direct toxic effect on axons and axonal damage is rather a secondary event following previous oligodendroglial damage (Irvine and Blakemore, 2006; Mason et al., 2001; Stidworthy et al., 2003). In murine EAE, DMF treatment could significantly increase axonal density in early and chronic disease stages (Linker et al., 2011; Reick et al., 2014). In a model of experimental autoimmune neuritis (EAN), DMF reduced the acute axonal damage in rats which correlated with a significant increase of Nrf2 in axons at this time point (Pitarokoili et al., 2015). Consequently, DMF-mediated Nrf2 activation is thought to lead to a better protection of axons. In MS, acute axonal damage mainly occurs during the early stages of disease and correlates with the extent of inflammation (Kuhlmann et al., 2002). Taken together, these data suggest that DMF treatment may reduce the acute axonal damage in MS patients by direct CNS effects in addition to the known axon-protective effect ascribed to the immunomodulatory mode of action of fumarates.

Cuprizone treatment of mice leads to an increased activation of microglia/macrophages and increased number of reactive astrocytes, features which also can be observed in MS lesions (Groebe et al., 2009; Hibbits et al., 2012; Hiremath et al., 1998). In our study DMF treatment only slightly decreased the number of microglia/macrophages (Mac3$^+$ cells) and reactive astrocytes

expressing GFAP (glial fibrillary acidic protein) after 7 days of cuprizone treatment (Figure 4). Although it was reported that DMF reduced microglial inflammation *in vitro*, only mild *in vivo* effects of DMF on the infiltration of macrophages were observed in several EAE or previous cuprizone experiments (Linker et al., 2011; Moharregh-Khiabani et al., 2009; Reick et al., 2014; Wilms et al., 2010). Therefore, DMF seems to have no major effect on the activation and accumulation of microglia/macrophages in these animal models. In contrast, DMF has been shown to reduce the number of activated astrocytes in the spinal cord of EAE mice (Linker et al., 2011). This observation could suggest that the DMF-induced decrease of astrogliosis is mainly mediated by peripheral immunomodulatory effects of DMF.

To analyze if the DMF effects on oligodendrocyte apoptosis could also be observed at a later time point after cuprizone exposure, the number of apoptotic cells and mature oligodendrocytes were analyzed after 2 weeks of cuprizone treatment. Since in later stages of cuprizone diet, oligodendroglial cell death is independent of caspase 3, apoptotic cells were analyzed by morphology (condensed and/or fragmented nuclei) (Hesse et al., 2010b). DMF treatment slightly reduced the number of apoptotic cells, but in contrast to day 7 this effect did not reach statistical significance (Figure 5). The number of oligodendrocytes ($Olig2^+$ cells) and mature oligodendrocytes ($NogoA^+$ cells) was not altered by DMF at this time point (Figure 5). As described above, the number of $NogoA^+$ cells decreases with ongoing cuprizone diet, a circumstance which could also be observed in this study (Kuhlmann et al., 2002). A possible explanation for the obtained results could be the strong toxic impact of cuprizone on oligodendrocytes which might override the DMF effect. Nevertheless, a slight reduction of apoptotic oligodendrocytes was still visible after 2 weeks. Conversely, it is also possible that DMF mainly affects only specific apoptotic mechanisms (e.g. caspase 3-dependent cell death) which may mainly occur during the early phase of cuprizone treatment and later changes to other cell death mechanism which are unaffected by DMF treatment (Kuhlmann et al., 2002).

Since it is assumed that the cytoprotective effects of DMF could be mainly mediated via the activation of Nrf2, a pilot experiment was performed to examine if the DMF effects observed after 7 days of cuprizone are also Nrf2-dependent. Therefore, DMF effects on the number of apoptotic cells were investigated in Nrf2 knock-out (Nrf2 k.o.) mice. In line with other studies, no protective DMF effects on oligodendrocytes could be seen in Nrf2 k.o. in these preliminary experiments,

suggesting that the observed effects after 7 days of cuprizone treatment may indeed be Nrf2-dependent (Figure 13) (Linker et al., 2011; Scannevin et al., 2012c). The obtained results further support the hypothesis that the neuroprotective effects of DMF could be mainly mediated by activation and stabilization of Nrf2.

4.1.2. DMF treatment increases differentiation and regeneration of oligodendrocytes after long-term cuprizone treatment

To analyze DMF effects on demyelination, mice were fed with cuprizone for 6 weeks which induces significant demyelination of the CC (Gudi et al., 2009; Matsushima and Morell, 2001b). DMF treatment of mice could only slightly decrease the demyelination occurring in the CC, whereas the number of mature oligodendrocytes ($NogoA^+$ cells) was significantly increased by DMF (Figure 6, Figure 9). Cuprizone-induced demyelination of the CC peaks at 5 weeks and remyelinated axons can already be observed between week 5 and 6 even with ongoing cuprizone treatment (Mason et al., 2001). DMF effects on demyelination were also investigated after 5 weeks of cuprizone exposure, and results were similar to data received after 6 weeks (data not shown). The received results are in line with the results of a previous study, where no significant effects of DMF on the demyelination of the CC could be observed (Moharregh-Khiabani et al., 2010). In addition to apoptosis of oligodendrocytes mediated by oxidative stress, cuprizone treatment also leads to disturbances of myelin protein synthesis and myelin lipid metabolism (Praet et al., 2014). Cuprizone intoxication reduces plasma levels of several amino acids leading to the activation of the amino acid response pathway (AAR) which in turn strongly reduces protein synthesis (Goldberg et al., 2013). A huge part of the myelin lipid layers consists of phospholipids, mainly plasmalogens (Farooqui and Horrocks, 2001). Cuprizone increases the activity of plasmalogenase and phospholipase A2 (PLA2), two enzymes which degrade membrane-bound plasmalogens and thereby contribute to myelin sheath destruction (Carey and Freeman, 1983). DMF treatment was shown to increase phospholipid synthesis by oligodendrocytes *in vitro*, but this effect might not be equally potent *in vivo*, which could explain the minor DMF effects on demyelination (Huang et al., 2015). Nevertheless, higher numbers of mature oligodendrocytes were observed under DMF after long-term cuprizone diet. These data suggest that long-term DMF treatment could be protective against cuprizone-induced oxidative stress while it may not majorly alter the cuprizone-induced metabolic disturbances contributing to myelin destruction. In a previous study, no significant DMF effect was found on the number of oligodendrocytes after long-

term cuprizone exposure but DMF effects after short-term cuprizone diet were not investigated at all (Moharregh-Khiabani et al., 2009). In our study, DMF treatment increased the number of mature oligodendrocytes after long term treatment. Most probably, the higher numbers of OPCs after short-term cuprizone exposure resulted in more OPCs that differentiated into mature oligodendrocytes. Thereby, it may be assumed that DMF promotes the regeneration and differentiation of oligodendrocytes. This DMF-mediated maintenance or increased differentiation of oligodendrocytes could potentially be important for MS treatment, since it was described that especially in chronic MS lesions OPCs largely fail to mature to oligodendrocytes (Kuhlmann et al., 2008b).

4.1.3. Therapeutic DMF treatment shows neuroprotective effects on axons

To investigate how DMF can influence remyelination, mice were fed with cuprizone for 5 weeks to induce profound demyelination of the CC. Then the cuprizone diet was stopped and mice were therapeutically treated with control or DMF for 3 days. No significant DMF effect on the extent of remyelinaton or the number of activated macrophages/microglia in the CC was found (Figure 10, Figure 11). Also, the overall number of oligodendrocytes and mature oligodendrocytes were not altered by DMF treatment (data not shown). As described above, remyelination already starts after 5 weeks, even with ongoing cuprizone exposure (Mason et al., 2001). After cuprizone withdrawal, almost complete remyelination can be observed after 4 weeks (Lindner et al., 2008b; Torkildsen et al., 2008). Remyelination is accompanied by migration and differentiation of OPCs as well as a reduction of activated microglia/macrophages in the CC (Matsushima and Morell, 2001b; Stangel and Hartung, 2002). Microglia/macrophage numbers peak in week 3-5 during cuprizone treatment (Mason et al., 2001). On the one hand, microglia and macrophages are considered as detrimental because of their pro-inflammatory cytokine production, contributing to an increased inflammation and damage within the CNS (Lampron et al., 2015). On the other hand, these phagocytic cells are important for the clearance of myelin debris. It could be demonstrated that decreased myelin removal by microglia/macrophages can prevent proper remyelination in the cuprizone model (Lampron et al., 2015; Skripuletz et al., 2013). DMF treatment could not alter the number of microglia/macrophages 3 days after cuprizone removal which could be a possible explanation why remyelination was not enhanced by DMF. Another fact which has to be taken into account is that the remyelination in mice is very effective and therapeutic effects may be

overridden by this fast process. Thus, the experimental setup used may not be suitable to show beneficial treatment effects on remyelination.

Importantly, DMF treatment significantly reduced the acute axonal damage 3 days after cuprizone withdrawal (Figure 11), suggesting a neuroprotective effect of therapeutic DMF application. Studies in the cuprizone model demonstrated that axonal damage could still be observed in the CC of mice long after remyelination was already completed (Manrique-Hoyos et al., 2012). Furthermore, persistent axonal loss despite sufficient remyelination was found after chronic cuprizone-mediated demyelination (Lindner et al., 2009). Therefore, therapeutic DMF treatment, although not influencing remyelination, could be an important tool to prevent axonal degeneration. Axonal loss occurs independent of the course of MS and majorly contributes to the development of brain atrophy (Chard et al., 2002; Kalkers et al., 2002). Hence, it is assumed that axonal loss leads to the development of permanent neurological deficits and long-term disability in MS patients (Ferguson et al., 1997; Grigoriadis et al., 2004; Haines et al., 2011). It was reported that axonal degeneration is already present at early stages of the disease highlighting the need of a neuroprotective therapy in MS at an early stage (Kalkers et al., 2002). Two recent studies demonstrated that especially an early DMF treatment mediates a beneficial effect on brain atrophy in MS patients (Dupuy et al., 2016; Kappos et al., 2016). Although, it is still unknown how DMF exerts its function on brain atrophy, beneficial effects on axonal damage may contribute to therapeutic effects observed in these studies. It is suggested that DMF facilitates mitochondrial function which was shown to be disturbed in axons of MS patients (Huang et al., 2015; Su et al., 2009). Since this mitochondrial dysfunction could contribute to axonal degeneration, a beneficial effect of DMF on mitochondria may subsequently reduce axonal damage.

In conclusion, the CNS intrinsic effects of DMF observed in this study may play an important role for the therapy of MS. After one week of cuprizone exposure, mice treated with DMF showed higher body weights compared to controls. After six weeks of cuprizone treatment body weights between control- and DMF-treated animals were comparable. These results indicate that the effects described above are not mediated by a reduced cuprizone intake of DMF mice, perhaps due to gastrointestinal side effects, but rather by DMF or its metabolite MMF itself. The latter was shown to reach the brain even when the BBB remains intact (Figure 12). In the present study, DMF decreased the cuprizone-mediated apoptosis of oligodendrocytes.

Initially, DMF treatment seems to mainly increase the number of OPCs and is potentially promoting their differentiation into mature oligodendrocytes, which were increased after long-term cuprizone treatment. Furthermore, DMF treatment concurrent to cuprizone intoxication as well as applied after cuprizone induced demyelination had occurred ("therapeutic DMF treatment") reduced the acute axonal damage significantly. These results suggest that DMF exerts neuroprotective and neuroregenerative effects independent of peripheral inflammation. Currently, therapy of MS mainly includes immunomodulatory and immunosuppressive drugs whereas neuroprotective or regenerative treatments are basically not available (Stangel, 2008). The sole application of immunomodulatory drugs cannot completely prevent CNS injury. Thus, the CNS intrinsic effects of DMF observed in this study could therefore be an important therapeutic tool for the treatment of MS.

4.2. DMF treatment shows opposing effects on lymphocytes in B cell-mediated EAE

After the investigation of DMF effects within the CNS, we further investigated the DMF effects on the peripheral immune system. EAE is a suitable animal model of MS in which immunomodulatory drugs, like DMF, can be initially tested for their potential therapeutic effectiveness in MS. The effects of DMF have been investigated in mainly T cell-mediated EAE models in which DMF could ameliorate the disease course and decreased the overall CNS damage (Linker et al., 2011; Reick et al., 2014; Schilling et al., 2006). Furthermore, several studies demonstrated that DMF induces the apoptosis of pro-inflammatory T cells, the development of anti-inflammatory dendritic cells and reduces the secretion of pro-inflammatory cytokines and chemokines (Ghoreschi et al., 2011; Gillard et al., 2015; Litjens et al., 2006; Treumer et al., 2003). The clinical efficacy of rituximab in MS patients elucidated that also B cells can majorly contribute to the pathogenesis of MS (Hauser et al., 2008b). Hence, a medication exerting immunomodulatory effects on B cells could be a promising medication for MS patients. So far, DMF effects on B cells have been poorly described and only two recent studies suggest that DMF also directly influences B cell activation and can change the distribution of subpopulations (Lundy et al., 2016; Schulze-Topphoff et al., 2016). We investigated the effect of DMF in an EAE model, in which B cells contribute in a more pathogenic manner. Clinical, histological and immunological analyses were performed to study the DMF effect on B cell and T cell activation, subpopulations and functions.

4.2.1. DMF treatment improves clinic and pathology of EAE mice

At first it was evaluated how DMF treatment affects clinical parameters like disease severity, serum antibody level as well as demyelination and inflammation of the spinal cord in EAE mice. In our EAE model, C57BL/6 mice were immunized with a recombinant mouse myelin oligodendrocyte glycoprotein ($rMOG_{1-117}$), which leads to the development of antigen-activated B cells and production of antibodies (Ab) directed against MOG (Weber et al., 2010). In this EAE model, B cells contribute majorly to the pathogenesis of the disease and support the development of pro-inflammatory IFNγ- and IL-17-producing T cells. Mice were treated preventively or therapeutically with 15 mg/kg bodyweight DMF or control twice a day for 60 or 50 days. Preventive and therapeutic DMF treatment could profoundly ameliorate the disease course of mice compared to control-treated animals (Figure 15). In the past, DMF was mainly investigated in MOG_{35-55} peptide induced EAE, which is a primarily T cell-mediated model. In contrast to these previous studies, in our EAE model therapeutic DMF treatment showed a pronounced effect on disease severity whereas previously only slight or no effects were seen in MOG_{35-55} peptide induced EAE (Kihara et al., 2015; Linker et al., 2011). These data suggest that this beneficial effect could be mediated by an immunomodulatory impact of DMF on B cells which, different from B cells in MOG_{35-55} peptide induced EAE, substantially promote the disease severity in $rMOG_{1-117}$ induced EAE. Moreover, these results also highlight the importance of appropriate medication dosage since therapeutically applied DMF showed no effect when administered twice a day at a concentration of 100 mg/kg bodyweight (Kihara et al., 2015). Nevertheless, the impact of preventive DMF treatment was still significantly more distinct when compared to therapeutic application of DMF. These results are comparable to findings in MOG_{35-55} peptide induced EAE where preventive DMF treatment also considerably improved the EAE course (Kihara et al., 2015; Linker et al., 2011; Reick et al., 2014; Schilling et al., 2006).

Activated B cells can differentiate into plasmablasts and plasma cells which secrete antigen-specific antibodies (Nutt et al., 2015). Immunization of mice with $rMOG_{1-117}$ leads to the development of anti-MOG antibodies which recently have been shown to play an important role in the initiation of CNS demyelinating disease (Kinzel et al., 2016). Therefore, it was interesting to analyze DMF effects on the production of antibodies. Serum anti-MOG Ab levels of mice preventively or therapeutically treated with control or DMF were determined weekly until day 42

p.i. (Figure 16). Neither preventive nor therapeutic DMF treatment significantly decreased the serum level of anti-MOG Ab levels. Preventive application of DMF even slightly increased anti-MOG Ab level when compared to controls. A recent study showed that the immunomodulatory agent IFNβ also enhanced serum anti-MOG IgG and IgM antibodies in EAE, but these increased antibodies did not correlate with EAE severity and occurred despite clinical benefit (Schubert et al., 2015). According to these data, preventive and therapeutic DMF treatment improved EAE severity, although auto-antibody levels were not majorly altered. These data suggest that injury of the CNS may not be primarily mediated by auto-antibodies in EAE (Schubert et al., 2015).

Hence, preventive and therapeutic DMF treatment decreased EAE severity, these effects were further examined by histology. Demyelination and overall inflammation of the spinal cord was profoundly reduced by therapeutic DMF treatment and slightly decreased under preventive DMF treatment (Figure 17). In line with previous findings, DMF treatment did not majorly alter T cell ($CD3^+$ cell) numbers in the spinal cord (Linker et al., 2011; Reick et al., 2014; Schilling et al., 2006). The DMF effects on the number of infiltrating B cells ($B220^+$ cells) were even less pronounced when compared to infiltrating T cell numbers. In contrast to preventive DMF treatment, therapeutic DMF application significantly decreased the number of infiltrating macrophages/microglia ($Mac3^+$ cells). Several studies demonstrated that preventive DMF treatment has no effect on the infiltration of microglia/macrophages and also in this study, no significant effect could be observed under preventive DMF administration (Linker et al., 2011; Reick et al., 2014). These results are comparable to results received in the cuprizone model, where DMF did also not influence the accumulation of microglia/macrophages. However, this study is the first demonstrating that therapeutic DMF treatment reduced demyelination and inflammation of the spinal cord as well as the number of accumulating microglia/macrophages. Thus, it can be assumed that the time point of treatment start influences the immunomodulatory effects mediated by DMF. In MS, microglia and macrophages are supposed to contribute to CNS injury by the production of high amounts of pro-inflammatory cytokines and chemokines as well as ROS (Jack et al., 2005). These recent findings lead to the suggestion that DMF treatment of MS patients might reduce the CNS inflammation mediated by infiltrating immune cells.

4.2.2. DMF treatment has immunomodulatory effects on peripheral B cells and T cells

The pathogenesis of MS is partly mediated by circulating B and T cells and it was shown that the composition and functions of B cell and T cell subsets are altered in MS patients (Jones et al., 2016). Studies of DMF effects on the adaptive immune system revealed that DMF might mediate a shift in T cell subsets towards more anti-inflammatory T cells and could induce the apoptosis of B cells and T cells (Ghoreschi et al., 2011; Mrowietz and Asadullah, 2005; Treumer et al., 2003). To analyze how DMF influences the adaptive immune system and thereby improves clinical course of EAE and CNS injury, DMF effects on B cells and T cells were investigated in the initial phase of EAE. C57BL/6 mice were treated 2 or 7 days prior to immunization until day 12 p.i. It was investigated how DMF treatment affects activation, composition of subpopulations and functional properties of B cells and T cells.

4.2.2.1. DMF has anti-inflammatory effects on peripheral T cells

Several studies in animal models and the observation of inflammatory cells and their effector functions in MS lesions led to the majorly accepted hypothesis that the disease is mediated by autoreactive T cells which cross the BBB and induce inflammation and damage inside the CNS (Fletcher et al., 2010). The EAE model mirrors clinical and pathological features of MS and was mainly used to achieve a better understanding of the pathogenesis of MS. Due to the important role of T cells in MS and EAE, it was investigated if the beneficial clinical effects of DMF could be mediated by an alteration of T cell activation and differentiation. It was reported that DMF induces apoptosis of human T cells and could lead to lymphopenia in MS patients (Gold et al., 2012; Treumer et al., 2003). In a first experiment it was therefore analyzed if these effects could be observed in EAE mice treated with DMF. The frequencies of $CD4^+$ T cells, $CD8^+$ T cells, $CD19^+$ cells (B cells) and $CD11b^+$ cells were examined in blood, lymph node and spleen of control- and DMF-treated mice. DMF treatment significantly reduced the frequency of $CD4^+$ T cells in the blood whereas the frequencies of $CD8^+$ T cells, $CD19^+$ cells (B cells) and $CD11b^+$ cells were only slightly reduced (Figure 18). These results are comparable to data reported for human peripheral blood lymphocyte subsets, where short term DMF treatment led to a decrease of $CD4^+$ T cells (Spencer et al., 2015). Conversely, only a slight reduction of $CD8^+$ T cells and $CD19^+$ cells could be observed in the blood of DMF-treated mice.

These result may reflect a discrepancy between EAE and MS, since $CD8^+$ T cells do not majorly contribute to the pathogenesis of EAE but are numerously found in lesions of MS patients (’t Hart et al., 2011). This might explain why circulating CD8+ T cells in EAE mice were not as strongly reduced by DMF as in humans. However, the most interesting result was that the frequency of $CD4^+$ T cells in lymph node and the frequencies of $CD4^+$ T cells and $CD8^+$ T cells in spleen were significantly increased under DMF treatment. These data would suggest that the decrease of T cells seen in the blood of MS patients and EAE mice could rather be mediated by reallocation of T cells than by DMF-mediated apoptosis. Initial studies of DMF, as a component of the anti-psoriatic drug Fumaderm®, demonstrated a reduction of T cells in the majority of patients (Altmeyer et al., 1996). A subsequent *in vitro* study of DMF seemed to confirm the ability of DMF to mediate apoptosis in human T cells (Treumer et al., 2003). An important fact which has to be taken into account is that only *in vitro* treatment with DMF, not its metabolite MMF, induced T cell apoptosis and this additionally was solely observed under very high concentrations (Gill and Kolson, 2013). No apoptotic effect of DMF was shown under physiologic concentrations which can be accomplished by its metabolite MMF *in vivo*. These data support the hypothesis that DMF and its metabolite MMF rather mediate an accumulation of T cells in secondary lymphoid organs and not primarily induce the apoptosis of T cells.

The DMF-mediated accumulation of T cells in lymph node and spleen raised the question of how these T cells are activated and which T cell subsets contribute to the high T cell frequencies. To address this question a flow cytometric analysis was performed and the activation markers CD69 and CD25 were measured on $CD4^+$ T cells and $CD8^+$ T cells of control or DMF-treated mice. The expression of CD69 and CD25 was profoundly decreased on $CD4^+$ T cells and $CD8^+$ T cells of DMF-treated mice (Figure 19). CD69 is one of the earliest activation markers and is upregulated on T cells after antigen-recognition (Groth et al., 2004). CD25 is the α-chain of the IL-2 receptor. Upon T cell activation, CD25 expression is upregulated leading to the creation of a high affinity IL-2 receptor (Gaffen, 2001). IL-2 is a cytokine which majorly drives T cell differentiation and proliferation. Effector T cells show the highest expression of CD69 and CD25 whereas naïve and memory T cells only show low or no expression of CD69 and CD25 (Hataye et al., 2006). Considering these data, DMF-mediated downregulation of CD69 and CD25 reflects a decreased activation of T cells and could thereby subsequently reduce the population of effector T cells.

The clinical benefit of DMF could thus be mediated by a suppressing effect on T cells, since especially autoreactive effector T cells exacerbate disease severity (Fletcher et al., 2010).

Additionally, it was studied if DMF alters the expression of the T cell activation marker CD44. $CD4^+$ T cells and $CD8^+$ T cells expressing high levels of CD44 ($CD44^{hi}$) were significantly decreased in spleens of DMF-treated mice (Figure 20, Figure 21). This effect was also slightly visible in the lymph node of DMF-treated mice. CD44 is an adhesion receptor and enhanced levels of CD44 are found on memory cells (Baaten et al., 2010b; Groth et al., 2004). Therefore, CD44 is widely used as a " memory marker" to differentiate naïve from activated and memory T cells (Budd et al., 1987). In this study, DMF treatment led to a decrease of $CD4^+$ and $CD8^+$ memory T cells whereas the population of naïve T cells remained unaltered. These results suggest that the increased population found in lymph node and spleen under DMF treatment is mainly composed of naïve T cells rather than of activated/memory T cells (Figure 18). Furthermore, these findings support the results concerning the activation status of T cells (CD69/CD25) (Figure 19). Naïve $CD4^+$ T cells show already an intermediate expression level of CD44, which explains why within the $CD4^+$ T cell population not only $CD44^{low}$ but also $CD44^{int}$ T cells are increased under DMF treatment (Figure 20) (Groth et al., 2004).

Activated $CD4^+$ T cells can differentiate into different subpopulations, such as IFNγ- (Th1), IL-17- (Th17) or IL-4/IL-10- (Th2) producing T cells. IFNγ- and IL-17-producing T cells (Th1, Th17 cells) are the commonly induced $CD4^+$ T cells in EAE (Fletcher et al., 2010; Kurschus, 2015; O'Connor et al., 2008). A recent study demonstrated that in MOG_{35-55} peptide induced EAE, DMF treatment led to decreased frequencies of Th1 and Th17 cells (Schulze-Topphoff et al., 2016). Furthermore, it was shown that lymphocytes of DMF-treated MS patients produce higher amounts of the cytokines IL-4 and IL-10, which are mainly produced by Th2 cells suggesting that DMF might mediate a "Th1 to Th2 shift" (Gill and Kolson, 2013). Thus, it was interesting to analyze if DMF also alters the differentiation of T cells in $rMOG_{1-117}$ induced EAE model. The frequency of splenic and lymphatic Th1 cells was significantly reduced by DMF treatment and Th17 cell frequencies were slightly decreased (Figure 22). Importantly, this effect was not due to reduced frequencies of viable $CD4^+$ T cells as shown in Figure 22. These results are comparable to previous studies in MOG_{35-55} peptide induced EAE where DMF treatment also decreased Th1 and Th17 cells (Schulze-Topphoff et al., 2016). A study of Baaten and colleagues could demonstrate that CD44 is crucial for the

development and survival of Th1 cells whereas Th2 and Th17 differentiation seems to be independent of CD44 (Baaten et al., 2010b). Consequently, the prominent decrease of Th1 cells under DMF treatment could partly be mediated by the DMF-induced downregulation of CD44 (Figure 20). Conclusively, this would also explain why the DMF effect was more prominent on the Th1 population compared to the Th17 population. Th1 and Th17 cells contribute in a large part to the pathogenesis of EAE. Thus, a DMF-mediated downregulation of these two cell populations could majorly improve the disease course, as it was seen in this study.

Regulatory T cells (Tregs) play an important role in downregulating or suppressing excessive inflammatory responses. In MS patients, the frequency of Tregs is reduced during relapses and increases again during remission (Fletcher et al., 2010). A medication enhancing the frequency of Tregs could therefore bear a therapeutic benefit. In our EAE model, DMF treatment did not majorly alter the frequency of regulatory T cells, although a slight increase could be observed in spleens from DMF-treated mice (Figure 23). These data suggest that the induction of Tregs is not profoundly altered by DMF treatment and that the clinical effects could be rather mediated by a downregulation of pro-inflammatory T cells.

4.2.2.2. DMF alters T cell proliferation

The previous *ex-vivo* experiments revealed that T cell activation and development of pro-inflammatory T cells (Th1 cells) is reduced in immunized EAE mice treated with DMF (Figures 19-22). Conferring to these results, a further experiment determined how DMF influences the proliferation of T cells when these are stimulated in an antigen-independent manner. Purified T cells from naïve C57BL/6 mice, treated with either control- or DMF for 19 days, were stimulated with anti-CD3/CD28 *in vitro* to induce T cell proliferation. Treating T cells with anti-CD3/CD28 simulates the activation by antigen-presenting cells (Trickett and Kwan, 2003). Ex vivo proliferation of $CD4^+$ T cells and $CD8^+$ T cells was significantly diminished when these were previously treated with DMF *in vivo* (Figure 24A-B). A detailed analysis of the proliferation revealed that T cells from DMF-treated animals showed lower proliferation rates compared to control-treated animals, illustrating that control-treated T cells divided themselves more often upon anti-CD3/CD28 stimulation. Considering these data, *in vivo* DMF treatment seems to have an anti-proliferative effect on naïve T cells when these are stimulated *in vitro*. These results are in line with the observations that DMF reduced the activation of T cells and decreases the frequency of

activated/memory T cells. Additionally, it was investigated how *in vivo* DMF treatment of T cells influences their differentiation *in vitro*. Supernatants of this T cell cultures were collected and the amount of secreted IFNγ and GM-CSF was measured by ELISA. Analysis revealed that DMF-treated T cells produced significantly less IFNγ and GM-CSF compared to control-treated T cells (Figure 24C). Taken together, it could be assumed that DMF treatment decreases the differentiation of pro-inflammatory Th1 cells by downregulating T cell activation and proliferation. In the recent years it could be frequently shown that also GM-CSF producing T cells majorly contribute to pathogenesis of EAE and also occur in higher frequencies in MS patients (Codarri et al., 2011; Grifka-Walk et al., 2015; Rasouli et al., 2015). Thus, the DMF-mediated downregulation of GM-CSF-producing T cells could be another effect leading to an improvement of EAE severity.

In summary, DMF treatment reduced the activation and proliferation of T cells as well as inhibited their differentiation into pro-inflammatory effector cells. Fewer frequencies of $CD4^+$ T cells and $CD8^+$ T cells were found in the blood of DMF-treated mice, but showed an increased accumulation in secondary lymphoid organs. Since DMF decreased the generation of Th1 and Th17 cells, but did not increase the frequency of Tregs, it could be assumed that DMF induced the development of Th2 cells which could account for the higher frequency of $CD4^+$ T cells. These results would be comparable to observations in DMF-treated patients where DMF mediates a “Th1 to Th2 cell shift” (Gill and Kolson, 2013). Furthermore, DMF treatment mediates a reduction of memory T cells and a relative expansion of naïve T cells, an effect which was also reported for MS patients treated with DMF (Gross et al., 2015; Longbrake et al., 2016). DMF treatment similarly decreased the activation of $CD8^+$ T cells which can contribute to MS pathogenesis and are numerously found in brain lesions of MS patients (Friese and Fugger, 2009; ’t Hart et al., 2011). This overall anti-inflammatory effect of DMF on T cells could have majorly contributed to the disease improvement in $rMOG_{1-117}$ induced EAE. In addition, the DMF effects observed in this study might be a hint on how DMF mediates the beneficial effects seen in MS therapy.

4.2.3. DMF-treated B cells are more potent antigen-presenting cells

Immunization with MOG_{35-55} peptide directly activates autoreactive $CD4^+$ T cells via an interaction with the MHC-II complex-bound peptide on APCs without the need to of internal processing (Slavin et al., 2001; Weber et al., 2010). In contrast, in $rMOG_{1-117}$ induced EAE the native MOG has to be internalized and processed by APCs to present the encephalitogenic peptide to autoreactive

$CD4^+$ T cells (Slavin et al., 2001). This leads to the generation of pathogenic B cells, which recognize the MOG-protein via their B cell receptor and subsequently activate MHC-II restricted $CD4^+$ T cells (Weber et al., 2010).

In this study, it was investigated how DMF treatment influences these pathogenic B cells and if the clinical benefits seen in this model could be mediated by an anti-inflammatory effect on pathogenic B cells. Similar to the analysis of T cells, first experiments examined DMF effects on the B cell activation at day 12 p.i. Data evaluation revealed that in contrast to T cells, DMF treatment rather increased the activation of B cells primarily by enhancing the MHC-II expression on lymphatic B cells (Figure 25). Although the co-stimulatory molecules CD80, CD86 and CD40 were not significantly altered their expression was slightly increased on lymphatic B cells of DMF-treated mice. The expression levels of the activation markers CD69, CD25 and Fas were not modified by DMF treatment (Figure 26). It could therefore be assumed that DMF primarily influences antigen-presenting and co-stimulatory functions of B cells and not so much the expression of activation markers. Additionally, no significant DMF-mediated enhanced expression of MHC-II could be observed at day 60 after immunization (data not shown). This would suggest that either MHC-II expression on B cells is not further inducible at this time point or that DMF influences MHC-II especially during the early and acute phase of EAE, where immune cells become mainly activated in the periphery. MHC-II is important for the cognate interaction between B cells and T cells (Scholl and Geha, 1994). The peptide/MHC-II-complex is recognized by the T cell receptor (TCR) of $CD4^+$ T cells and leads to the activation of antigen-specific T cells (Charles A Janeway et al., 2001). These activated T cells increase the expression of co-stimulatory molecules and secret cytokines and chemokines which subsequently stimulate the proliferation and differentiation of B cells. Taken together, it could be assumed that the DMF-mediated increase of MHC-II expression on B cells promotes the activation and proliferation of B cells and T cells and conclusively this data suggests that DMF has opposing effects on B cells and T cells. Nevertheless, there was no enhanced expression of activation markers on B cells under DMF treatment leading to the suggestion that DMF-mediated dampening effects on T cells did not result in increased B cell activation. Naïve B cells require pronounced stimulating signals from $CD4^+$ T cells or their respective antigen itself to proliferate and differentiate. Since DMF treatment decreased the frequency of activated T cells, it can be assumed that B cells admittedly provided a first strong

activation signal for T cells but that these T cells were not fully activated due to the immunomodulatory effects of DMF. Deductive, no effective T cell help was provided for antigen-presenting B cells which therefore did not become fully activated. Another hypothesis could be that DMF mediated a shift towards a more regulatory phenotype of B cells and following the initial activation of B cells, demonstrated by enhanced MHC-II expression, induced the development of anti-inflammatory B cells which can also be observed in individual DMF-treated MS patients (Li et al., 2017). This assumption would also explain why DMF treatment improved the course of EAE although it rather promotes activation of B cells by increasing their antigen-presenting properties.

The increased activation of B cells raised the question how DMF influences individual subpopulations of B cells. B cell subsets can be defined by their expression of CD21 and CD23, which differs on specific B cell subtypes (Shen and Fillatreau, 2015). Both markers are highly expressed on transitional B cells whereas for example follicular B cells show a lower expression of CD21 (Meyer-Bahlburg et al., 2008). In this study $CD21^{hi}$ $CD23^{+}$ B cells were referred to as transitional B cells and $CD21^{int}$ $CD23^{+}$ B cells were referred to as follicular B cells. *In vivo* DMF treatment induced a shift in B cell subsets towards fewer transitional and more follicular B cells in isolated splenic cells (Figure 27). The frequency of immature B cells ($CD21^{-}$ $CD23^{-}$) in the bone marrow was not altered suggesting that DMF-mediated changes only occur in the periphery (Figure 27). The observed results indicate that DMF treatment may promote the differentiation of B cells towards a population which exerts a potent antigen-presenting function, the follicular B cells. Inside secondary lymphoid organs like the spleen, naïve follicular B cells present antigens to $CD4^{+}$ T cells which results in an immune response to the presented antigen (Allman and Pillai, 2008).

Furthermore, DMF effects were analyzed on the frequency of immature naïve B cells, mature naïve B cells, memory B cells, regulatory B cells, germinal center B cells and antigen-activated B cells (Figure 28). Although DMF did not significantly alter any of these B cell phenotypes, higher frequencies of antigen-activated B cells and lower frequencies of immature naïve B cells could be observed in DMF-treated, $rMOG_{1-117}$ immunized animals. Antigen-activated B cells express CD69, CD80 and high levels of MHC-II, which supports the hypothesis that DMF contributes to the activation of B cells via an increased induction of MHC-II and co-stimulatory molecules such as CD80 (Figure 25). Furthermore, DMF seems to mediate a shift from immature naïve B cells to

mature naïve B cells in the spleen, indicating that DMF treatment could moderately facilitate B cell maturation. On one side, these findings lead to the assumption that the beneficial clinical effects of DMF may not be B cell-mediated since DMF rather promotes the generation of antigen-activated B cells which could contribute to the pathogenesis of the disease. On the other side, these activated B cells could also exert a more anti-inflammatory and/or regulatory function which could mediate an improvement of the disease (Ray and Basu, 2014). The latter hypothesis can be supported by the slightly increased frequency of regulatory B cells which were observed in DMF-treated animals (Figure 28).

As a first functional analysis, it was investigated if DMF can influence the antigen-recognition and antigen-binding of B cells. Therefore, *in vivo* control- and DMF-treated B cells were isolated and ex vivo incubated with a fluorescent-labeled $rMOG_{1-117}$ and the frequency B cells which were able to recognize and bind $rMOG_{1-117}$ could be analyzed via flow cytometry. DMF treatment did not alter the frequency of rMOG-binding B cells compared to controls (Figure 29). This suggest that DMF did not influence the antigen-recognition and antigen-binding abilities of B cells and that DMF therefore does not alter the antigen-affinity of the B cell receptor.

Another functional analysis focused more on the antigen-presenting function of B cells. Thus, B cells purified from control- or DMF-treated immunized mice were co-cultured with naïve CFSE-labeled 2D2 T cells, which have a transgenic T cell receptor specific for MOG, and were stimulated with $rMOG_{1-117}$ (Bettelli et al., 2003). Antigen-presenting function of these B cells was then analyzed via the extent of T cell proliferation. In this setting, T cell proliferation was significantly increased when these were co-cultured with DMF-treated B cells compared to control (Figure 30A-B). A more detailed quantification revealed that the frequencies of T cells with low, intermediate and high proliferation rate were increased by DMF-treated B cells when compared to controls. Additionally, cultured DMF-treated B cells also showed a slightly higher expression of MHC-II compared to control-treated B cells (Figure 30C). These data support the hypothesis that DMF treatment can lead to the development of more potent antigen-presenting B cells which caused the increased proliferation of T cells. These findings are also in line with the previous results illustrating an increased MHC-II expression and enhanced frequencies of follicular and antigen-activated B cells under DMF treatment. To receive a first hint if these DMF-treated B cells exert pro-inflammatory or anti-inflammatory functions, the frequency of IFNγ-producing T cells (Th1)

was measured in a similar co-culture. When compared to control-treated B cells, DMF-treated B cells did not alter the frequency of IFNγ-producing T cells (Figure 31). Thus, it could be assumed that the decrease of IFNγ-producing T cells found *ex vivo* under DMF treatment might not be a B cell-mediated effect. Furthermore, these data suggest that either DMF does not promote the development of a more anti-inflammatory and/or regulatory B cell phenotype or that this effect is not strong enough to exert a B cell-mediated immunomodulatory effect on T cell differentiation *in vitro*.

In conclusion, the present study could show that DMF treatment significantly ameliorated the clinical course of $rMOG_{1-117}$ induced EAE and that demyelination and inflammation in the spinal cord were profoundly decreased. Furthermore, DMF decreased T cell activation and the frequency of pro-inflammatory Th1 cells which majorly contribute to the disease pathogenesis. This anti-inflammatory effect did not seem to be profoundly mediated by B cells since DMF-treated B cells did not influence Th1 cell differentiation *in vitro*. It could therefore be assumed that DMF either directly affects T cell differentiation or that this effect is mediated by other immune cells. A study of Litjens et al. could demonstrate that the DMF-metabolite MMF alters the maturation and polarization of dendritic cells (DCs) resulting in a decreased generation of Th1 cells (Litjens et al., 2004b, 2006). This effect may have contributed to the amelioration of $rMOG_{1-117}$ induced EAE, since DCs are the most potent APCs which promote the antigen-specific activation of encephalitogenic T cells (Ganguly et al., 2013). Surprisingly, DMF treatment increased MHC-II expression on B cells and increased their ability to present antigen. In contrast to results in B cell-mediated EAE, DMF treatment decreased MHC-II expression on B cells in MOG_{35-55} peptide induced EAE suggesting that DMF may exerts opposing immunomodulatory effects on B cells with (rMOG EAE) or without (MOG-peptide EAE) major pathogenic functions (Schulze-Topphoff et al., 2016). The increased ability of these B cells to present antigen via MHC-II furthermore promoted the proliferation of T cells. It is still unclear if and how these potent antigen-presenting B cells could influence the T cell differentiation. Although, Th1 cell differentiation was not reduced by DMF-treated B cells, B cells may induce differentiation of Th2 cells, which can exert anti-inflammatory functions. This would explain the increased population of $CD4^+$ T cells found in lymph node and spleen of DMF-treated mice which was neither composed of Th1, Th17 cells nor of Tregs, leaving only Th2 cells. Although in this study no significant increase of regulatory B cells

could be found under DMF treatment, it could be shown that B cells with regulatory function are found in DMF-treated MS patients (Lundy et al., 2016). Conclusively, the B cell-activating functions mediated by DMF could thereby contribute to an improvement of the disease.

4.3. DMF altered B cell properties in MS patients

DMF treatment of $rMOG_{1-117}$ immunized mice ameliorated the disease course but seemed to simultaneously increase the activation of B cells, demonstrated by an increased expression of MHC-II and partly also co-stimulatory molecules. To analyze if this increased MHC-II expression could be found on human B cells, PBMCs from non-treated and DMF-treated MS patients (treatment duration ≥ 6 months) were analyzed by flow cytometry. Evaluation of data revealed that human B cells isolated from DMF-treated MS patients showed an increased MHC-II expression when compared to controls (Figure 32). These data support the results found in our EAE model (Figure 25). Furthermore, similar findings could be demonstrated in a study which showed that B cells isolated from DMF-treated MS patients showed an enhanced MHC-II expression (Staun-Ram et al., Poster 185 ISNI 2016). Recent studies reported that DMF treatment could induce an anti-inflammatory B cell phenotype which contributes to the regulation of the peripheral immune system (Li et al., 2017; Lundy et al., 2016). Although DMF treatment increases the MHC-II expression on B cells and increases their ability to present antigens, these B cells might still be able to possess anti-inflammatory and/or regulatory properties and thereby exert beneficial functions. Nevertheless, DMF seems to have an activating function on B cells which should be taken into account when choosing proper medication for individual MS patients. For example, it could recently be demonstrated in $rMOG_{1-117}$ induced EAE, B cells which reoccur after anti-CD20 treatment show enhanced pro-inflammatory properties (Linda Feldmann, group internal communication, data not published). It could therefore be assumed that DMF may not be the appropriate follow up treatment for B cell-depleting agents due to its “B cell-activating” effects.

5. Outlook

The present study provides evidence that DMF exerts axon- and cytoprotective effects and promotes regeneration of mature oligodendrocytes independent of the peripheral immune system. These DMF effects were potentially mediated by an increased activation of the transcription factor Nrf2 which leads to an enhanced protection of cells against oxidative stress. No significant effects were observed on demyelination and remyelination, but may also be due to limitations of this animal model. It could be interesting to analyze the DMF effects in a modified cuprizone model where the phase of extensive demyelination is prolonged and the process of remyelination is delayed (Bai et al., 2016).

In the second part of this study it could be show that DMF treatment improved clinical and pathological parameters of an EAE model with involvement of pathogenic B cells. Although DMF could profoundly decrease the activation and differentiation of pro-inflammatory T cells, it enhanced the antigen-presenting function of B cells. This study could not completely elucidate which B cell phenotype is promoted by DMF treatment and subsequently which T cell phenotype is induced by these B cells. Further analysis could focus on phenotyping these DMF-treated B cells and elucidate if they promote a pro- or anti-inflammatory milieu. One experimental approach to study the DMF-mediated B cell phenotype could be a B cell transfer experiment. Therefore, control- or DMF-treated CD20k.o. B cells could be transferred into immunized, B cell-depleted WT animals and clinical parameters such as EAE onset, severity and incidence could indicate if these B cells rather exert pro- or anti-inflammatory functions.

6. Bibliography

Acs, P., Selak, M.A., Komoly, S., and Kalman, B. (2013). Distribution of oligodendrocyte loss and mitochondrial toxicity in the cuprizone-induced experimental demyelination model. J. Neuroimmunol. *262*, 128–131.

Albrecht, P., Bouchachia, I., Goebels, N., Henke, N., Hofstetter, H.H., Issberner, A., Kovacs, Z., Lewerenz, J., Lisak, D., Maher, P., et al. (2012). Effects of dimethyl fumarate on neuroprotection and immunomodulation. J. Neuroinflammation *9*, 163.

Allman, D., and Pillai, S. (2008). Peripheral B cell subsets. Curr. Opin. Immunol. *20*, 149–157.

Altmeyer, P., Hartwig, R., and Matthes, U. (1996). [Efficacy and safety profile of fumaric acid esters in oral long-term therapy with severe treatment refractory psoriasis vulgaris. A study of 83 patients]. Hautarzt Z. Dermatol. Venerol. Verwandte Geb. *47*, 190–196.

Altmeyer, P.J., Mattlies, U., Pawlak, F., Hoffmann, K., Frosch, P.J., Ruppert, P., Wassilew, S.W., Horn, T., Kreysel, H.W., Lutz, G., et al. (1994). Antipsoriatic effect of fumaric acid derivatives. J. Am. Acad. Dermatol. *30*, 977–981.

Amor, S., Groome, N., Linington, C., Morris, M.M., Dornmair, K., Gardinier, M.V., Matthieu, J.M., and Baker, D. (1994). Identification of epitopes of myelin oligodendrocyte glycoprotein for the induction of experimental allergic encephalomyelitis in SJL and Biozzi AB/H mice. J. Immunol. Baltim. Md 1950 *153*, 4349–4356.

Ando, D.G., Clayton, J., Kono, D., Urban, J.L., and Sercarz, E.E. (1989). Encephalitogenic T cells in the B10.PL model of experimental allergic encephalomyelitis (EAE) are of the Th-1 lymphokine subtype. Cell. Immunol. *124*, 132–143.

Baaten, B.J., Li, C.-R., and Bradley, L.M. (2010a). Multifaceted regulation of T cells by CD44. Commun. Integr. Biol. *3*, 508–512.

Baaten, B.J.G., Li, C.-R., Deiro, M.F., Lin, M.M., Linton, P.J., and Bradley, L.M. (2010b). CD44 regulates survival and memory development in Th1 cells. Immunity *32*, 104–115.

Bai, C.B., Sun, S., Roholt, A., Benson, E., Edberg, D., Medicetty, S., Dutta, R., Kidd, G., Macklin, W.B., and Trapp, B. (2016). A mouse model for testing remyelinating therapies. Exp. Neurol. *283*, *Part A*, 330–340.

Bakker, D.A., and Ludwin, S.K. (1987). Blood-brain barrier permeability during Cuprizone-induced demyelination: Implications for the pathogenesis of immune-mediated demyelinating diseases. J. Neurol. Sci. *78*, 125–137.

Barkhof, F., Bruck, W., De Groot, C.J.A., Bergers, E., Hulshof, S., Geurts, J., Polman, C.H., and van der Valk, P. (2003). Remyelinated lesions in multiple sclerosis: magnetic resonance image appearance. Arch. Neurol. *60*, 1073–1081.

Barnett, M.H., and Prineas, J.W. (2004). Relapsing and remitting multiple sclerosis: pathology of the newly forming lesion. Ann. Neurol. *55*, 458–468.

Barnett, M.H., Parratt, J.D.E., Cho, E.-S., and Prineas, J.W. (2009). Immunoglobulins and complement in postmortem multiple sclerosis tissue. Ann. Neurol. *65*, 32–46.

Barr, T.A., Shen, P., Brown, S., Lampropoulou, V., Roch, T., Lawrie, S., Fan, B., O'Connor, R.A., Anderton, S.M., Bar-Or, A., et al. (2012). B cell depletion therapy ameliorates autoimmune disease through ablation of IL-6–producing B cells. J. Exp. Med. *209*, 1001–1010.

Bartholomäus, I., Kawakami, N., Odoardi, F., Schläger, C., Miljkovic, D., Ellwart, J.W., Klinkert, W.E.F., Flügel-Koch, C., Issekutz, T.B., Wekerle, H., et al. (2009). Effector T cell interactions with meningeal vascular structures in nascent autoimmune CNS lesions. Nature *462*, 94–98.

Bénardais, K., Kotsiari, A., Skuljec, J., Koutsoudaki, P.N., Gudi, V., Singh, V., Vulinović, F., Skripuletz, T., and Stangel, M. (2013). Cuprizone [bis(cyclohexylidenehydrazide)] is selectively toxic for mature oligodendrocytes. Neurotox. Res. *24*, 244–250.

Bettelli, E., Pagany, M., Weiner, H.L., Linington, C., Sobel, R.A., and Kuchroo, V.K. (2003). Myelin oligodendrocyte glycoprotein-specific T cell receptor transgenic mice develop spontaneous autoimmune optic neuritis. J. Exp. Med. *197*, 1073–1081.

Biancotti, J.C., Kumar, S., and Vellis, J. de (2008). Activation of Inflammatory Response by a Combination of Growth Factors in Cuprizone-Induced Demyelinated Brain Leads to Myelin Repair. Neurochem. Res. *33*, 2615–2628.

Bradl, M., and Lassmann, H. (2010). Oligodendrocytes: biology and pathology. Acta Neuropathol. (Berl.) *119*, 37–53.

Brück, W., and Stadelmann, C. (2003). Inflammation and degeneration in multiple sclerosis. Neurol. Sci. *24*, s265–s267.

Brück, W., Porada, P., Poser, S., Rieckmann, P., Hanefeld, F., Kretzschmarch, H.A., and Lassmann, H. (1995). Monocyte/macrophage differentiation in early multiple sclerosis lesions. Ann. Neurol. *38*, 788–796.

Budd, R.C., Cerottini, J.C., Horvath, C., Bron, C., Pedrazzini, T., Howe, R.C., and MacDonald, H.R. (1987). Distinction of virgin and memory T lymphocytes. Stable acquisition of the Pgp-1 glycoprotein concomitant with antigenic stimulation. J. Immunol. Baltim. Md 1950 *138*, 3120–3129.

Carey, E.M., and Freeman, N.M. (1983). Biochemical changes in cuprizone-induced spongiform encephalopathy. Neurochem. Res. *8*, 1029–1044.

Chan, K., Lu, R., Chang, J.C., and Kan, Y.W. (1996). NRF2, a member of the NFE2 family of transcription factors, is not essential for murine erythropoiesis, growth, and development. Proc. Natl. Acad. Sci. U. S. A. *93*, 13943–13948.

Chard, D.T., Griffin, C.M., Parker, G.J.M., Kapoor, R., Thompson, A.J., and Miller, D.H. (2002). Brain atrophy in clinically early relapsing-remitting multiple sclerosis. Brain J. Neurol. *125*, 327–337.

Charles A Janeway, J., Travers, P., Walport, M., and Shlomchik, M.J. (2001). B-cell activation by armed helper T cells.

Chen, L., and Flies, D.B. (2013). Molecular mechanisms of T cell co-stimulation and co-inhibition. Nat. Rev. Immunol. *13*, 227–242.

Chen, H., Assmann, J.C., Krenz, A., Rahman, M., Grimm, M., Karsten, C.M., Köhl, J., Offermanns, S., Wettschureck, N., and Schwaninger, M. (2014). Hydroxycarboxylic acid receptor 2 mediates dimethyl fumarate's protective effect in EAE. J. Clin. Invest. *124*, 2188–2192.

Claussen, M.C., and Korn, T. (2012). Immune mechanisms of new therapeutic strategies in MS: teriflunomide. Clin. Immunol. Orlando Fla *142*, 49–56.

Codarri, L., Gyülvészi, G., Tosevski, V., Hesske, L., Fontana, A., Magnenat, L., Suter, T., and Becher, B. (2011). ROR[gamma]t drives production of the cytokine GM-CSF in helper T cells, which is essential for the effector phase of autoimmune neuroinflammation. Nat. Immunol. *12*, 560–567.

Cohen, J.A., Barkhof, F., Comi, G., Hartung, H.-P., Khatri, B.O., Montalban, X., Pelletier, J., Capra, R., Gallo, P., Izquierdo, G., et al. (2010). Oral Fingolimod or Intramuscular Interferon for Relapsing Multiple Sclerosis. N. Engl. J. Med. *362*, 402–415.

Coles, A.J., Twyman, C.L., Arnold, D.L., Cohen, J.A., Confavreux, C., Fox, E.J., Hartung, H.-P., Havrdova, E., Selmaj, K.W., Weiner, H.L., et al. (2012). Alemtuzumab for patients with relapsing multiple sclerosis after disease-modifying therapy: a randomised controlled phase 3 trial. Lancet Lond. Engl. *380*, 1829–1839.

Constant, S., Sant'Angelo, D., Pasqualini, T., Taylor, T., Levin, D., Flavell, R., and Bottomly, K. (1995). Peptide and protein antigens require distinct antigen-presenting cell subsets for the priming of CD4+ T cells. J. Immunol. Baltim. Md 1950 *154*, 4915–4923.

Cross, S.A., Cook, D.R., Chi, A.W.S., Vance, P.J., Kolson, L.L., Wong, B.J., Jordan-Sciutto, K.L., and Kolson, D.L. (2011). Dimethyl fumarate, an immune modulator and inducer of the antioxidant response, suppresses HIV replication and macrophage-mediated neurotoxicity; a novel candidate for HIV-neuroprotection. J. Immunol. Baltim. Md 1950 *187*, 5015–5025.

Dowling, P., Shang, G., Raval, S., Menonna, J., Cook, S., and Husar, W. (1996). Involvement of the CD95 (APO-1/Fas) receptor/ligand system in multiple sclerosis brain. J. Exp. Med. *184*, 1513–1518.

Dupuy, S.L., Tauhid, S., Hurwitz, S., Chu, R., Yousuf, F., and Bakshi, R. (2016). The Effect of Dimethyl Fumarate on Cerebral Gray Matter Atrophy in Multiple Sclerosis. Neurol. Ther. *5*, 215–229.

Evangelou, N., Konz, D., Esiri, M.M., Smith, S., Palace, J., and Matthews, P.M. (2000). Regional axonal loss in the corpus callosum correlates with cerebral white matter lesion volume and distribution in multiple sclerosis. Brain J. Neurol. *123 (Pt 9)*, 1845–1849.

Farooqui, A.A., and Horrocks, L.A. (2001). Plasmalogens: workhorse lipids of membranes in normal and injured neurons and glia. Neurosci. Rev. J. Bringing Neurobiol. Neurol. Psychiatry *7*, 232–245.

Ferguson, B., Matyszak, M.K., Esiri, M.M., and Perry, V.H. (1997). Axonal damage in acute multiple sclerosis lesions. Brain J. Neurol. *120 (Pt 3)*, 393–399.

Filippi, M., Rocca, M.A., Ciccarelli, O., De Stefano, N., Evangelou, N., Kappos, L., Rovira, A., Sastre-Garriga, J., Tintorè, M., Frederiksen, J.L., et al. (2016). MRI criteria for the diagnosis of multiple sclerosis: MAGNIMS consensus guidelines. Lancet Neurol. *15*, 292–303.

Fillatreau, S., Sweenie, C.H., McGeachy, M.J., Gray, D., and Anderton, S.M. (2002). B cells regulate autoimmunity by provision of IL-10. Nat. Immunol. *3*, 944–950.

Fischer, M.T., Sharma, R., Lim, J.L., Haider, L., Frischer, J.M., Drexhage, J., Mahad, D., Bradl, M., van Horssen, J., and Lassmann, H. (2012). NADPH oxidase expression in active multiple sclerosis lesions in relation to oxidative tissue damage and mitochondrial injury. Brain *135*, 886–899.

Fletcher, J.M., Lalor, S.J., Sweeney, C.M., Tubridy, N., and Mills, K.H.G. (2010). T cells in multiple sclerosis and experimental autoimmune encephalomyelitis. Clin. Exp. Immunol. *162*, 1–11.

Fox, R.J., Miller, D.H., Phillips, J.T., Hutchinson, M., Havrdova, E., Kita, M., Yang, M., Raghupathi, K., Novas, M., Sweetser, M.T., et al. (2012). Placebo-controlled phase 3 study of oral BG-12 or glatiramer in multiple sclerosis. N. Engl. J. Med. *367*, 1087–1097.

Franciotta, D., Salvetti, M., Lolli, F., Serafini, B., and Aloisi, F. (2008). B cells and multiple sclerosis. Lancet Neurol. *7*, 852–858.

Fraussen, J., Claes, N., de Bock, L., and Somers, V. (2014). Targets of the humoral autoimmune response in multiple sclerosis. Autoimmun. Rev. *13*, 1126–1137.

Friese, M.A., and Fugger, L. (2009). Pathogenic CD8+ T cells in multiple sclerosis. Ann. Neurol. *66*, 132–141.

Frischer, J.M., Weigand, S.D., Guo, Y., Kale, N., Parisi, J.E., Pirko, I., Mandrekar, J., Bramow, S., Metz, I., Brück, W., et al. (2015). Clinical and Pathological Insights into the Dynamic Nature of the White Matter Multiple Sclerosis Plaque. Ann. Neurol. *78*, 710–721.

Furtado, G.C., Marcondes, M.C.G., Latkowski, J.-A., Tsai, J., Wensky, A., and Lafaille, J.J. (2008). Swift Entry of Myelin-Specific T Lymphocytes into the Central Nervous System in Spontaneous Autoimmune Encephalomyelitis. J. Immunol. Baltim. Md 1950 *181*, 4648–4655.

Gaffen, S.L. (2001). Signaling domains of the interleukin 2 receptor. Cytokine *14*, 63–77.

Ganguly, D., Haak, S., Sisirak, V., and Reizis, B. (2013). The role of dendritic cells in autoimmunity. Nat. Rev. Immunol. *13*, 566–577.

Ghoreschi, K., Brück, J., Kellerer, C., Deng, C., Peng, H., Rothfuss, O., Hussain, R.Z., Gocke, A.R., Respa, A., Glocova, I., et al. (2011). Fumarates improve psoriasis and multiple sclerosis by inducing type II dendritic cells. J. Exp. Med. *208*, 2291–2303.

Gill, A.J., and Kolson, D.L. (2013). Dimethyl fumarate modulation of immune and antioxidant responses: application to HIV therapy. Crit. Rev. Immunol. *33*, 307–359.

Gillard, G.O., Collette, B., Anderson, J., Chao, J., Scannevin, R.H., Huss, D.J., and Fontenot, J.D. (2015). DMF, but not other fumarates, inhibits NF-κB activity in vitro in an Nrf2-independent manner. J. Neuroimmunol. *283*, 74–85.

Gold, R., Linington, C., and Lassmann, H. (2006). Understanding pathogenesis and therapy of multiple sclerosis via animal models: 70 years of merits and culprits in experimental autoimmune encephalomyelitis research. Brain J. Neurol. *129*, 1953–1971.

Gold, R., Kappos, L., Arnold, D.L., Bar-Or, A., Giovannoni, G., Selmaj, K., Tornatore, C., Sweetser, M.T., Yang, M., Sheikh, S.I., et al. (2012). Placebo-controlled phase 3 study of oral BG-12 for relapsing multiple sclerosis. N. Engl. J. Med. *367*, 1098–1107.

Gold, R., Giovannoni, G., Selmaj, K., Havrdova, E., Montalban, X., Radue, E.-W., Stefoski, D., Robinson, R., Riester, K., Rana, J., et al. (2013). Daclizumab high-yield process in relapsing-remitting multiple sclerosis (SELECT): a randomised, double-blind, placebo-controlled trial. The Lancet *381*, 2167–2175.

Goldberg, J., Daniel, M., Heuvel, Y. van, Victor, M., Beyer, C., Clarner, T., and Kipp, M. (2013). Short-Term Cuprizone Feeding Induces Selective Amino Acid Deprivation with Concomitant Activation of an Integrated Stress Response in Oligodendrocytes. Cell. Mol. Neurobiol. *33*, 1087–1098.

Goldschmidt, T., Antel, J., König, F.B., Brück, W., and Kuhlmann, T. (2009). Remyelination capacity of the MS brain decreases with disease chronicity. Neurology *72*, 1914–1921.

Grifka-Walk, H.M., Giles, D.A., and Segal, B.M. (2015). IL-12-polarized Th1 cells produce GM-CSF and induce EAE independent of IL-23. Eur. J. Immunol. *45*, 2780–2786.

Grigoriadis, N., Ben-Hur, T., Karussis, D., and Milonas, I. (2004). Axonal damage in multiple sclerosis: a complex issue in a complex disease. Clin. Neurol. Neurosurg. *106*, 211–217.

Groebe, A., Clarner, T., Baumgartner, W., Dang, J., Beyer, C., and Kipp, M. (2009). Cuprizone treatment induces distinct demyelination, astrocytosis, and microglia cell invasion or proliferation in the mouse cerebellum. Cerebellum Lond. Engl. *8*, 163–174.

Gross, C.C., Schulte-Mecklenbeck, A., Klinsing, S., Posevitz-Fejfár, A., Wiendl, H., and Klotz, L. (2015). Dimethyl fumarate treatment alters circulating T helper cell subsets in multiple sclerosis. Neurol. Neuroimmunol. Neuroinflammation *3*.

Groth, B.F.D.S., Smith, A.L., and Higgins, C.A. (2004). T cell activation: in vivo veritas. Immunol. Cell Biol. *82*, 260–268.

Gudi, V., Moharregh-Khiabani, D., Skripuletz, T., Koutsoudaki, P.N., Kotsiari, A., Skuljec, J., Trebst, C., and Stangel, M. (2009). Regional differences between grey and white matter in cuprizone induced demyelination. Brain Res. *1283*, 127–138.

Haider, L., Fischer, M.T., Frischer, J.M., Bauer, J., Höftberger, R., Botond, G., Esterbauer, H., Binder, C.J., Witztum, J.L., and Lassmann, H. (2011). Oxidative damage in multiple sclerosis lesions. Brain *134*, 1914–1924.

Haines, J.D., Inglese, M., and Casaccia, P. (2011). Axonal Damage in Multiple Sclerosis. Mt. Sinai J. Med. N. Y. *78*, 231–243.

Harp, C.T., Ireland, S., Davis, L.S., Remington, G., Cassidy, B., Cravens, P.D., Stuve, O., Lovett-Racke, A.E., Eagar, T.N., Greenberg, B.M., et al. (2010). Memory B cells from a subset of treatment-naïve relapsing-remitting multiple sclerosis patients elicit CD4(+) T-cell proliferation and IFN-γ production in response to myelin basic protein and myelin oligodendrocyte glycoprotein. Eur. J. Immunol. *40*, 2942–2956.

't Hart, B.A., Gran, B., and Weissert, R. (2011). EAE: imperfect but useful models of multiple sclerosis. Trends Mol. Med. *17*, 119–125.

Hataye, J., Moon, J.J., Khoruts, A., Reilly, C., and Jenkins, M.K. (2006). Naive and memory CD4+ T cell survival controlled by clonal abundance. Science *312*, 114–116.

Hauser, S.L., Waubant, E., Arnold, D.L., Vollmer, T., Antel, J., Fox, R.J., Bar-Or, A., Panzara, M., Sarkar, N., Agarwal, S., et al. (2008a). B-cell depletion with rituximab in relapsing-remitting multiple sclerosis. N. Engl. J. Med. *358*, 676–688.

Hauser, S.L., Waubant, E., Arnold, D.L., Vollmer, T., Antel, J., Fox, R.J., Bar-Or, A., Panzara, M., Sarkar, N., Agarwal, S., et al. (2008b). B-Cell Depletion with Rituximab in Relapsing–Remitting Multiple Sclerosis. N. Engl. J. Med. *358*, 676–688.

Hauser, S.L., Bar-Or, A., Comi, G., Giovannoni, G., Hartung, H.-P., Hemmer, B., Lublin, F., Montalban, X., Rammohan, K.W., Selmaj, K., et al. (2017). Ocrelizumab versus Interferon Beta-1a in Relapsing Multiple Sclerosis. N. Engl. J. Med. *376*, 221–234.

healthline.com/health/multiple-sclerosis/facts-statistics-infographic Multiple Sclerosis by the Numbers: Facts, Statistics, and You.

Heigl, F., Hettich, R., Arendt, R., Durner, J., Koehler, J., and Mauch, E. (2013). Immunoadsorption in steroid-refractory multiple sclerosis: clinical experience in 60 patients. Atheroscler. Suppl. *14*, 167–173.

Hemmer, B., Kerschensteiner, M., and Korn, T. (2015). Role of the innate and adaptive immune responses in the course of multiple sclerosis. Lancet Neurol. *14*, 406–419.

Henderson, A.P.D., Barnett, M.H., Parratt, J.D.E., and Prineas, J.W. (2009). Multiple sclerosis: distribution of inflammatory cells in newly forming lesions. Ann. Neurol. *66*, 739–753.

Hesse, A., Wagner, M., Held, J., Brück, W., Salinas-Riester, G., Hao, Z., Waisman, A., and Kuhlmann, T. (2010a). In toxic demyelination oligodendroglial cell death occurs early and is FAS independent. Neurobiol. Dis. *37*, 362–369.

Hesse, A., Wagner, M., Held, J., Brück, W., Salinas-Riester, G., Hao, Z., Waisman, A., and Kuhlmann, T. (2010b). In toxic demyelination oligodendroglial cell death occurs early and is FAS independent. Neurobiol. Dis. *37*, 362–369.

Hibbits, N., Yoshino, J., Le, T.Q., and Armstrong, R.C. (2012). Astrogliosis During Acute and Chronic Cuprizone Demyelination and Implications for Remyelination. ASN Neuro *4*, AN20120062.

Hiremath, M.M., Saito, Y., Knapp, G.W., Ting, J.P.-Y., Suzuki, K., and Matsushima, G.K. (1998). Microglial/macrophage accumulation during cuprizone-induced demyelination in C57BL/6 mice. J. Neuroimmunol. *92*, 38–49.

Hoffmann, K., Lindner, M., Gröticke, I., Stangel, M., and Löscher, W. (2008). Epileptic seizures and hippocampal damage after cuprizone-induced demyelination in C57BL/6 mice. Exp. Neurol. *210*, 308–321.

Hori, S., Nomura, T., and Sakaguchi, S. (2003). Control of regulatory T cell development by the transcription factor Foxp3. Science *299*, 1057–1061.

Huang, H., Taraboletti, A., and Shriver, L.P. (2015). Dimethyl fumarate modulates antioxidant and lipid metabolism in oligodendrocytes. Redox Biol. *5*, 169–175.

Irvine, K.-A., and Blakemore, W.F. (2006). Age increases axon loss associated with primary demyelination in cuprizone-induced demyelination in C57BL/6 mice. J. Neuroimmunol. *175*, 69–76.

Jack, C., Ruffini, F., Bar-Or, A., and Antel, J.P. (2005). Microglia and multiple sclerosis. J. Neurosci. Res. *81*, 363–373.

Jones, A.P., Kermode, A.G., Lucas, R.M., Carroll, W.M., Nolan, D., and Hart, P.H. (2016). Circulating immune cells in multiple sclerosis. Clin. Exp. Immunol. n/a-n/a.

de Jong, R., Bezemer, A.C., Zomerdijk, T.P., van de Pouw-Kraan, T., Ottenhoff, T.H., and Nibbering, P.H. (1996). Selective stimulation of T helper 2 cytokine responses by the anti-psoriasis agent monomethylfumarate. Eur. J. Immunol. *26*, 2067–2074.

Juurlink, B.H.J., Thorburne, S.K., and Hertz, L. (1998). Peroxide-scavenging deficit underlies oligodendrocyte susceptibility to oxidative stress. Glia *22*, 371–378.

Kalkers, N.F., Ameziane, N., Bot, J.C.J., Minneboo, A., Polman, C.H., and Barkhof, F. (2002). Longitudinal brain volume measurement in multiple sclerosis: rate of brain atrophy is independent of the disease subtype. Arch. Neurol. *59*, 1572–1576.

Kappos, L., Freedman, M.S., Polman, C.H., Edan, G., Hartung, H.-P., Miller, D.H., Montalbán, X., Barkhof, F., Radü, E.-W., Bauer, L., et al. (2007). Effect of early versus delayed interferon beta-1b

treatment on disability after a first clinical event suggestive of multiple sclerosis: a 3-year follow-up analysis of the BENEFIT study. Lancet Lond. Engl. *370*, 389–397.

Kappos, L., Gold, R., Miller, D.H., Macmanus, D.G., Havrdova, E., Limmroth, V., Polman, C.H., Schmierer, K., Yousry, T.A., Yang, M., et al. (2008). Efficacy and safety of oral fumarate in patients with relapsing-remitting multiple sclerosis: a multicentre, randomised, double-blind, placebo-controlled phase IIb study. Lancet Lond. Engl. *372*, 1463–1472.

Kappos, L., Li, D., Calabresi, P.A., O'Connor, P., Bar-Or, A., Barkhof, F., Yin, M., Leppert, D., Glanzman, R., Tinbergen, J., et al. (2011). Ocrelizumab in relapsing-remitting multiple sclerosis: a phase 2, randomised, placebo-controlled, multicentre trial. The Lancet *378*, 1779–1787.

Kappos, L., Yousry, T., Fox, R., Gold, R., Arnold, D., Potts, J., and Marantz, J. (2016). Rate of Brain Volume Loss with Long-Term Delayed-Release Dimethyl Fumarate Treatment in Patients with Relapsing-Remitting Multiple Sclerosis: 6-Year Results from ENDORSE (P3.061). Neurology *86*, P3.061.

Karcher, D., Van Sande, M., and Lowenthal, A. (1959). Micro-electrophoresis in agar gel of proteins of the cerebrospinal fluid and central nervous system. J. Neurochem. *4*, 135–140.

Kihara, Y., Groves, A., Rivera, R.R., and Chun, J. (2015). Dimethyl fumarate inhibits integrin α4 expression in multiple sclerosis models. Ann. Clin. Transl. Neurol. *2*, 978–983.

Kinzel, S., Lehmann-Horn, K., Torke, S., Häusler, D., Winkler, A., Stadelmann, C., Payne, N., Feldmann, L., Saiz, A., Reindl, M., et al. (2016). Myelin-reactive antibodies initiate T cell-mediated CNS autoimmune disease by opsonization of endogenous antigen. Acta Neuropathol. (Berl.) *132*, 43–58.

Knippenberg, S., Peelen, E., Smolders, J., Thewissen, M., Menheere, P., Cohen Tervaert, J.W., Hupperts, R., and Damoiseaux, J. (2011). Reduction in IL-10 producing B cells (Breg) in multiple sclerosis is accompanied by a reduced naïve/memory Breg ratio during a relapse but not in remission. J. Neuroimmunol. *239*, 80–86.

Koo, E.H., Sisodia, S.S., Archer, D.R., Martin, L.J., Weidemann, A., Beyreuther, K., Fischer, P., Masters, C.L., and Price, D.L. (1990). Precursor of amyloid protein in Alzheimer disease undergoes fast anterograde axonal transport. Proc. Natl. Acad. Sci. U. S. A. *87*, 1561–1565.

Koutsoudaki, P.N., Skripuletz, T., Gudi, V., Moharregh-Khiabani, D., Hildebrandt, H., Trebst, C., and Stangel, M. (2009). Demyelination of the hippocampus is prominent in the cuprizone model. Neurosci. Lett. *451*, 83–88.

Krishnamoorthy, G., Lassmann, H., Wekerle, H., and Holz, A. (2006). Spontaneous opticospinal encephalomyelitis in a double-transgenic mouse model of autoimmune T cell/B cell cooperation. J. Clin. Invest. *116*, 2385–2392.

Krumbholz, M., and Meinl, E. (2014). B cells in MS and NMO: pathogenesis and therapy. Semin. Immunopathol. *36*, 339–350.

Krumbholz, M., Theil, D., Derfuss, T., Rosenwald, A., Schrader, F., Monoranu, C.-M., Kalled, S.L., Hess, D.M., Serafini, B., Aloisi, F., et al. (2005). BAFF is produced by astrocytes and up-regulated in multiple sclerosis lesions and primary central nervous system lymphoma. J. Exp. Med. *201*, 195–200.

Kuhlmann, T., Lingfeld, G., Bitsch, A., Schuchardt, J., and Brück, W. (2002). Acute axonal damage in multiple sclerosis is most extensive in early disease stages and decreases over time. Brain *125*, 2202–2212.

Kuhlmann, T., Lassmann, H., and Brück, W. (2008a). Diagnosis of inflammatory demyelination in biopsy specimens: a practical approach. Acta Neuropathol. (Berl.) *115*, 275–287.

Kuhlmann, T., Miron, V., Cuo, Q., Wegner, C., Antel, J., and Brück, W. (2008b). Differentiation block of oligodendroglial progenitor cells as a cause for remyelination failure in chronic multiple sclerosis. Brain *131*, 1749–1758.

Kurschus, F.C. (2015). T cell mediated pathogenesis in EAE: Molecular mechanisms. Biomed. J. *38*, 183–193.

Kutzelnigg, A., Lucchinetti, C.F., Stadelmann, C., Brück, W., Rauschka, H., Bergmann, M., Schmidbauer, M., Parisi, J.E., and Lassmann, H. (2005). Cortical demyelination and diffuse white matter injury in multiple sclerosis. Brain *128*, 2705–2712.

Lampron, A., Larochelle, A., Laflamme, N., Préfontaine, P., Plante, M.-M., Sánchez, M.G., Yong, V.W., Stys, P.K., Tremblay, M.-È., and Rivest, S. (2015). Inefficient clearance of myelin debris by microglia impairs remyelinating processes. J. Exp. Med. *212*, 481–495.

Langer-Gould, A., and Steinman, L. (2006). Progressive multifocal leukoencephalopathy and multiple sclerosis: lessons from natalizumab. Curr. Neurol. Neurosci. Rep. *6*, 253–258.

Larochelle, C., Alvarez, J.I., and Prat, A. (2011). How do immune cells overcome the blood-brain barrier in multiple sclerosis? FEBS Lett. *585*, 3770–3780.

Lassmann, H., Brück, W., and Lucchinetti, C.F. (2007). The Immunopathology of Multiple Sclerosis: An Overview. Brain Pathol. *17*, 210–218.

Lesley, R., Xu, Y., Kalled, S.L., Hess, D.M., Schwab, S.R., Shu, H.-B., and Cyster, J.G. (2004). Reduced competitiveness of autoantigen-engaged B cells due to increased dependence on BAFF. Immunity *20*, 441–453.

Li, R., Rezk, A., Ghadiri, M., Luessi, F., Zipp, F., Li, H., Giacomini, P.S., Antel, J., and Bar-Or, A. (2017). Dimethyl Fumarate Treatment Mediates an Anti-Inflammatory Shift in B Cell Subsets of Patients with Multiple Sclerosis. J. Immunol. *198*, 691–698.

Lindner, M., Heine, S., Haastert, K., Garde, N., Fokuhl, J., Linsmeier, F., Grothe, C., Baumgärtner, W., and Stangel, M. (2008a). Sequential myelin protein expression during remyelination reveals fast and efficient repair after central nervous system demyelination. Neuropathol. Appl. Neurobiol. *34*, 105–114.

Lindner, M., Heine, S., Haastert, K., Garde, N., Fokuhl, J., Linsmeier, F., Grothe, C., Baumgärtner, W., and Stangel, M. (2008b). Sequential myelin protein expression during remyelination reveals fast and efficient repair after central nervous system demyelination. Neuropathol. Appl. Neurobiol. *34*, 105–114.

Lindner, M., Fokuhl, J., Linsmeier, F., Trebst, C., and Stangel, M. (2009). Chronic toxic demyelination in the central nervous system leads to axonal damage despite remyelination. Neurosci. Lett. *453*, 120–125.

Linker, R.A., Lee, D.-H., Ryan, S., van Dam, A.M., Conrad, R., Bista, P., Zeng, W., Hronowsky, X., Buko, A., Chollate, S., et al. (2011). Fumaric acid esters exert neuroprotective effects in neuroinflammation via activation of the Nrf2 antioxidant pathway. Brain J. Neurol. *134*, 678–692.

Litjens, N.H.R., Rademaker, M., Ravensbergen, B., Rea, D., van der Plas, M.J.A., Thio, B., Walding, A., van Dissel, J.T., and Nibbering, P.H. (2004a). Monomethylfumarate affects polarization of monocyte-derived dendritic cells resulting in down-regulated Th1 lymphocyte responses. Eur. J. Immunol. *34*, 565–575.

Litjens, N.H.R., Rademaker, M., Ravensbergen, B., Rea, D., van der Plas, M.J.A., Thio, B., Walding, A., van Dissel, J.T., and Nibbering, P.H. (2004b). Monomethylfumarate affects polarization of monocyte-derived dendritic cells resulting in down-regulated Th1 lymphocyte responses. Eur. J. Immunol. *34*, 565–575.

Litjens, N.H.R., Rademaker, M., Ravensbergen, B., Thio, H.B., van Dissel, J.T., and Nibbering, P.H. (2006). Effects of monomethylfumarate on dendritic cell differentiation. Br. J. Dermatol. *154*, 211–217.

Litzenburger, T., Fässler, R., Bauer, J., Lassmann, H., Linington, C., Wekerle, H., and Iglesias, A. (1998). B Lymphocytes Producing Demyelinating Autoantibodies: Development and Function in Gene-targeted Transgenic Mice. J. Exp. Med. *188*, 169–180.

Loewe, R., Pillinger, M., de Martin, R., Mrowietz, U., Gröger, M., Holnthoner, W., Wolff, K., Wiegrebe, W., Jirovsky, D., and Petzelbauer, P. (2001). Dimethylfumarate inhibits tumor-necrosis-factor-induced CD62E expression in an NF-kappa B-dependent manner. J. Invest. Dermatol. *117*, 1363–1368.

Longbrake, E.E., Naismith, R.T., Parks, B.J., Wu, G.F., and Cross, A.H. (2015). Dimethyl fumarate-associated lymphopenia: Risk factors and clinical significance. Mult. Scler. J. - Exp. Transl. Clin. *1*.

Longbrake, E.E., Ramsbottom, M.J., Cantoni, C., Ghezzi, L., Cross, A.H., and Piccio, L. (2016). Dimethyl fumarate selectively reduces memory T cells in multiple sclerosis patients. Mult. Scler. Houndmills Basingstoke Engl. *22*, 1061–1070.

Lowenthal, A., Vansande, M., and Karcher, D. (1960). The differential diagnosis of neurological diseases by fractionating electrophoretically the CSF gamma-globulins. J. Neurochem. *6*, 51–56.

Lublin, F.D., and Reingold, S.C. (1996). Defining the clinical course of multiple sclerosis: results of an international survey. National Multiple Sclerosis Society (USA) Advisory Committee on Clinical Trials of New Agents in Multiple Sclerosis. Neurology *46*, 907–911.

Lublin, F.D., Reingold, S.C., Cohen, J.A., Cutter, G.R., Sørensen, P.S., Thompson, A.J., Wolinsky, J.S., Balcer, L.J., Banwell, B., Barkhof, F., et al. (2014). Defining the clinical course of multiple sclerosis. Neurology *83*, 278–286.

Lucchinetti, C., Brück, W., Parisi, J., Scheithauer, B., Rodriguez, M., and Lassmann, H. (2000). Heterogeneity of multiple sclerosis lesions: implications for the pathogenesis of demyelination. Ann. Neurol. *47*, 707–717.

Lukasova, M., Hanson, J., Tunaru, S., and Offermanns, S. (2011). Nicotinic acid (niacin): new lipid-independent mechanisms of action and therapeutic potentials. Trends Pharmacol. Sci. *32*, 700–707.

Lundy, S.K., Wu, Q., Wang, Q., Dowling, C.A., Taitano, S.H., Mao, G., and Mao-Draayer, Y. (2016). Dimethyl fumarate treatment of relapsing-remitting multiple sclerosis influences B-cell subsets. Neurol. Neuroimmunol. Neuroinflammation *3*.

Manrique-Hoyos, N., Jürgens, T., Grønborg, M., Kreutzfeldt, M., Schedensack, M., Kuhlmann, T., Schrick, C., Brück, W., Urlaub, H., Simons, M., et al. (2012). Late motor decline after accomplished remyelination: impact for progressive multiple sclerosis. Ann. Neurol. *71*, 227–244.

Marta, C.B., Oliver, A.R., Sweet, R.A., Pfeiffer, S.E., and Ruddle, N.H. (2005). Pathogenic myelin oligodendrocyte glycoprotein antibodies recognize glycosylated epitopes and perturb oligodendrocyte physiology. Proc. Natl. Acad. Sci. U. S. A. *102*, 13992–13997.

Mason, J.L., Langaman, C., Morell, P., Suzuki, K., and Matsushima, G.K. (2001). Episodic demyelination and subsequent remyelination within the murine central nervous system: changes in axonal calibre. Neuropathol. Appl. Neurobiol. *27*, 50–58.

Matsushima, G.K., and Morell, P. (2001a). The neurotoxicant, cuprizone, as a model to study demyelination and remyelination in the central nervous system. Brain Pathol. Zurich Switz. *11*, 107–116.

Matsushima, G.K., and Morell, P. (2001b). The Neurotoxicant, Cuprizone, as a Model to Study Demyelination and Remyelination in the Central Nervous System. Brain Pathol. *11*, 107–116.

McCormack, P.L., and Scott, L.J. (2004). Interferon-beta-1b: a review of its use in relapsing-remitting and secondary progressive multiple sclerosis. CNS Drugs *18*, 521–546.

McDonald, W.I., Compston, A., Edan, G., Goodkin, D., Hartung, H.-P., Lublin, F.D., McFarland, H.F., Paty, D.W., Polman, C.H., Reingold, S.C., et al. (2001). Recommended diagnostic criteria for multiple sclerosis: Guidelines from the international panel on the diagnosis of multiple sclerosis. Ann. Neurol. *50*, 121–127.

McMahon, E.J., Suzuki, K., and Matsushima, G.K. (2002). Peripheral macrophage recruitment in cuprizone-induced CNS demyelination despite an intact blood–brain barrier. J. Neuroimmunol. *130*, 32–45.

Meinl, E., Krumbholz, M., and Hohlfeld, R. (2006). B lineage cells in the inflammatory central nervous system environment: migration, maintenance, local antibody production, and therapeutic modulation. Ann. Neurol. *59*, 880–892.

Mendel, I., Kerlero de Rosbo, N., and Ben-Nun, A. (1995). A myelin oligodendrocyte glycoprotein peptide induces typical chronic experimental autoimmune encephalomyelitis in H-2b mice: fine specificity and T cell receptor V beta expression of encephalitogenic T cells. Eur. J. Immunol. *25*, 1951–1959.

Meyer-Bahlburg, A., Andrews, S.F., Yu, K.O.A., Porcelli, S.A., and Rawlings, D.J. (2008). Characterization of a late transitional B cell population highly sensitive to BAFF-mediated homeostatic proliferation. J. Exp. Med. *205*, 155–168.

Mikol, D.D., Barkhof, F., Chang, P., Coyle, P.K., Jeffery, D.R., Schwid, S.R., Stubinski, B., Uitdehaag, B.M.J., and REGARD study group (2008). Comparison of subcutaneous interferon beta-1a with glatiramer acetate in patients with relapsing multiple sclerosis (the REbif vs Glatiramer Acetate in Relapsing MS Disease [REGARD] study): a multicentre, randomised, parallel, open-label trial. Lancet Neurol. *7*, 903–914.

Miller, D.H., and Leary, S.M. (2007). Primary-progressive multiple sclerosis. Lancet Neurol. *6*, 903–912.

Moharregh-Khiabani, D., Linker, R.., Gold, R., and Stangel, M. (2009). Fumaric Acid and its Esters: An Emerging Treatment for Multiple Sclerosis. Curr. Neuropharmacol. *7*, 60–64.

Moharregh-Khiabani, D., Blank, A., Skripuletz, T., Miller, E., Kotsiari, A., Gudi, V., and Stangel, M. (2010). Effects of Fumaric Acids on Cuprizone Induced Central Nervous System De- and Remyelination in the Mouse. PLoS ONE *5*.

Mrowietz, U., and Asadullah, K. (2005). Dimethylfumarate for psoriasis: more than a dietary curiosity. Trends Mol. Med. *11*, 43–48.

Mrowietz, Christophers, Altmeyer, and The Participants in the German Multicentre Study (1998). Treatment of psoriasis with fumaric acid esters: results of a prospective multicentre study. Br. J. Dermatol. *138*, 456–460.

Nguyen, T., Sherratt, P.J., Nioi, P., Yang, C.S., and Pickett, C.B. (2005). Nrf2 controls constitutive and inducible expression of ARE-driven genes through a dynamic pathway involving nucleocytoplasmic shuttling by Keap1. J. Biol. Chem. *280*, 32485–32492.

Nguyen, T., Nioi, P., and Pickett, C.B. (2009). The Nrf2-Antioxidant Response Element Signaling Pathway and Its Activation by Oxidative Stress. J. Biol. Chem. *284*, 13291–13295.

Nibbering, P.H., Thio, B., Zomerdijk, T.P.L., Bezemer, A.C., Beijersbergen, R.L., and Furth, R. van (1993). Effects of monomethylfumarate on human granulocytes. J. Invest. Dermatol. *101*, 37–42.

Nieboer, C., de Hoop, D., Langendijk, P.N.J., van Loenen, A.C., and Gubbels, J. (1990). Fumaric Acid Therapy in Psoriasis: A Double-Blind Comparison between Fumaric Acid Compound Therapy and Monotherapy with Dimethylfumaric Acid Ester. Dermatology *181*, 33–37.

Norkute, A., Hieble, A., Braun, A., Johann, S., Clarner, T., Baumgartner, W., Beyer, C., and Kipp, M. (2009). Cuprizone treatment induces demyelination and astrocytosis in the mouse hippocampus. J. Neurosci. Res. *87*, 1343–1355.

Noseworthy, J.H., Lucchinetti, C., Rodriguez, M., and Weinshenker, B.G. (2000). Multiple sclerosis. N. Engl. J. Med. *343*, 938–952.

Nutt, S.L., Hodgkin, P.D., Tarlinton, D.M., and Corcoran, L.M. (2015). The generation of antibody-secreting plasma cells. Nat. Rev. Immunol. *15*, 160–171.

Obermeier, B., Lovato, L., Mentele, R., Brück, W., Forne, I., Imhof, A., Lottspeich, F., Turk, K.W., Willis, S.N., Wekerle, H., et al. (2011). Related B cell clones that populate the CSF and CNS of patients with multiple sclerosis produce CSF immunoglobulin. J. Neuroimmunol. *233*, 245–248.

Ockenfels, H.M., Schultewolter, T., Ockenfels, G., Funk, R., and Goos, M. (1998). The antipsoriatic agent dimethylfumarate immunomodulates T-cell cytokine secretion and inhibits cytokines of the psoriatic cytokine network. Br. J. Dermatol. *139*, 390–395.

O'Connor, R.A., Prendergast, C.T., Sabatos, C.A., Lau, C.W.Z., Leech, M.D., Wraith, D.C., and Anderton, S.M. (2008). Cutting Edge: Th1 Cells Facilitate the Entry of Th17 Cells to the Central Nervous System during Experimental Autoimmune Encephalomyelitis. J. Immunol. Baltim. Md 1950 *181*, 3750–3754.

Ontaneda, D., and Fox, R.J. (2015). Progressive multiple sclerosis. Curr. Opin. Neurol. *28*, 237–243.

Ontaneda, D., Thompson, A.J., Fox, R.J., and Cohen, J.A. (2016). Progressive multiple sclerosis: prospects for disease therapy, repair, and restoration of function. The Lancet.

Owens, G.P., Ritchie, A.M., Burgoon, M.P., Williamson, R.A., Corboy, J.R., and Gilden, D.H. (2003). Single-cell repertoire analysis demonstrates that clonal expansion is a prominent feature of the B cell response in multiple sclerosis cerebrospinal fluid. J. Immunol. Baltim. Md 1950 *171*, 2725–2733.

Parish, C.R. (1999). Fluorescent dyes for lymphocyte migration and proliferation studies. Immunol. Cell Biol. *77*, 499–508.

Patrikios, P., Stadelmann, C., Kutzelnigg, A., Rauschka, H., Schmidbauer, M., Laursen, H., Sorensen, P.S., Brück, W., Lucchinetti, C., and Lassmann, H. (2006). Remyelination is extensive in a subset of multiple sclerosis patients. Brain J. Neurol. *129*, 3165–3172.

Paty, D.W., and Li, D.K. (1993). Interferon beta-1b is effective in relapsing-remitting multiple sclerosis. II. MRI analysis results of a multicenter, randomized, double-blind, placebo-controlled trial. UBC MS/MRI Study Group and the IFNB Multiple Sclerosis Study Group. Neurology *43*, 662–667.

Pitarokoili, K., Ambrosius, B., Meyer, D., Schrewe, L., and Gold, R. (2015). Dimethyl Fumarate Ameliorates Lewis Rat Experimental Autoimmune Neuritis and Mediates Axonal Protection. PLoS ONE *10*.

Plavina, T., Subramanyam, M., Bloomgren, G., Richman, S., Pace, A., Lee, S., Schlain, B., Campagnolo, D., Belachew, S., and Ticho, B. (2014). Anti-JC virus antibody levels in serum or plasma further define risk of natalizumab-associated progressive multifocal leukoencephalopathy. Ann. Neurol. *76*, 802–812.

Pöllinger, B., Krishnamoorthy, G., Berer, K., Lassmann, H., Bösl, M.R., Dunn, R., Domingues, H.S., Holz, A., Kurschus, F.C., and Wekerle, H. (2009). Spontaneous relapsing-remitting EAE in the SJL/J mouse: MOG-reactive transgenic T cells recruit endogenous MOG-specific B cells. J. Exp. Med. *206*, 1303–1316.

Polman, C.H., Reingold, S.C., Edan, G., Filippi, M., Hartung, H.-P., Kappos, L., Lublin, F.D., Metz, L.M., McFarland, H.F., O'Connor, P.W., et al. (2005). Diagnostic criteria for multiple sclerosis: 2005 revisions to the "McDonald Criteria." Ann. Neurol. *58*, 840–846.

Polman, C.H., O'Connor, P.W., Havrdova, E., Hutchinson, M., Kappos, L., Miller, D.H., Phillips, J.T., Lublin, F.D., Giovannoni, G., Wajgt, A., et al. (2006). A Randomized, Placebo-Controlled Trial of Natalizumab for Relapsing Multiple Sclerosis. N. Engl. J. Med. *354*, 899–910.

Polman, C.H., Reingold, S.C., Banwell, B., Clanet, M., Cohen, J.A., Filippi, M., Fujihara, K., Havrdova, E., Hutchinson, M., Kappos, L., et al. (2011). Diagnostic criteria for multiple sclerosis: 2010 Revisions to the McDonald criteria. Ann. Neurol. *69*, 292–302.

Praet, J., Guglielmetti, C., Berneman, Z., Van der Linden, A., and Ponsaerts, P. (2014). Cellular and molecular neuropathology of the cuprizone mouse model: Clinical relevance for multiple sclerosis. Neurosci. Biobehav. Rev. *47*, 485–505.

Prineas, J.W. (1979). Multiple sclerosis: presence of lymphatic capillaries and lymphoid tissue in the brain and spinal cord. Science *203*, 1123–1125.

Ransohoff, R.M. (2012). Animal models of multiple sclerosis: the good, the bad and the bottom line. Nat. Neurosci. *15*, 1074–1077.

Rasouli, J., Ciric, B., Imitola, J., Gonnella, P., Hwang, D., Mahajan, K., Mari, E.R., Safavi, F., Leist, T.P., Zhang, G.-X., et al. (2015). Expression of GM-CSF in T Cells Is Increased in Multiple Sclerosis and Suppressed by IFN-β Therapy. J. Immunol. Baltim. Md 1950 *194*, 5085–5093.

Ray, A., and Basu, S. (2014). Regulatory B cells in experimental autoimmune encephalomyelitis (EAE). Methods Mol. Biol. Clifton NJ *1190*, 243–255.

Reick, C., Ellrichmann, G., Thöne, J., Scannevin, R.H., Saft, C., Linker, R.A., and Gold, R. (2014). Neuroprotective dimethyl fumarate synergizes with immunomodulatory interferon beta to provide enhanced axon protection in autoimmune neuroinflammation. Exp. Neurol. *257*, 50–56.

Rivers, T.M., Sprunt, D.H., and Berry, G.P. (1933). OBSERVATIONS ON ATTEMPTS TO PRODUCE ACUTE DISSEMINATED ENCEPHALOMYELITIS IN MONKEYS. J. Exp. Med. *58*, 39–53.

Rone, M.B., Cui, Q.-L., Fang, J., Wang, L.-C., Zhang, J., Khan, D., Bedard, M., Almazan, G., Ludwin, S.K., Jones, R., et al. (2016). Oligodendrogliopathy in Multiple Sclerosis: Low Glycolytic Metabolic Rate Promotes Oligodendrocyte Survival. J. Neurosci. *36*, 4698–4707.

Rosenkranz, T., Novas, M., and Terborg, C. (2015). PML in a patient with lymphocytopenia treated with dimethyl fumarate. N. Engl. J. Med. *372*, 1476–1478.

de Sa, J.C.C., Airas, L., Bartholome, E., Grigoriadis, N., Mattle, H., Oreja-Guevara, C., O'Riordan, J., Sellebjerg, F., Stankoff, B., Vass, K., et al. (2011). Symptomatic therapy in multiple sclerosis: a review for a multimodal approach in clinical practice. Ther. Adv. Neurol. Disord. *4*, 139–168.

Scannevin, R.H., Chollate, S., Jung, M., Shackett, M., Patel, H., Bista, P., Zeng, W., Ryan, S., Yamamoto, M., Lukashev, M., et al. (2012a). Fumarates promote cytoprotection of central nervous system cells against oxidative stress via the nuclear factor (erythroid-derived 2)-like 2 pathway. J. Pharmacol. Exp. Ther. *341*, 274–284.

Scannevin, R.H., Bai, B., Huang, R., Trapp, B., and Rhodes, K.J. (2012b). BG-12 (Dimethyl Fumarate) is Neuroprotective in the Murine Cuprizone/Rapamycin Model of Demyelination and Neurodegeneration.

Scannevin, R.H., Chollate, S., Jung, M., Shackett, M., Patel, H., Bista, P., Zeng, W., Ryan, S., Yamamoto, M., Lukashev, M., et al. (2012c). Fumarates promote cytoprotection of central nervous system cells against oxidative stress via the nuclear factor (erythroid-derived 2)-like 2 pathway. J. Pharmacol. Exp. Ther. *341*, 274–284.

Schilling, S., Goelz, S., Linker, R., Luehder, F., and Gold, R. (2006). Fumaric acid esters are effective in chronic experimental autoimmune encephalomyelitis and suppress macrophage infiltration. Clin. Exp. Immunol. *145*, 101–107.

Schimrigk, S., Brune, N., Hellwig, K., Lukas, C., Bellenberg, B., Rieks, M., Hoffmann, V., Pöhlau, D., and Przuntek, H. (2006). Oral fumaric acid esters for the treatment of active multiple sclerosis: an open-label, baseline-controlled pilot study. Eur. J. Neurol. *13*, 604–610.

Scholl, P.R., and Geha, R.S. (1994). MHC class II signaling in B-cell activation. Immunol. Today *15*, 418–422.

Schubert, R.D., Hu, Y., Kumar, G., Szeto, S., Abraham, P., Winderl, J., Guthridge, J.M., Pardo, G., Dunn, J., Steinman, L., et al. (2015). IFN-β treatment requires B cells for efficacy in neuroautoimmunity. J. Immunol. Baltim. Md 1950 *194*, 2110–2116.

Schulze-Topphoff, U., Varrin-Doyer, M., Pekarek, K., Spencer, C.M., Shetty, A., Sagan, S.A., Cree, B.A.C., Sobel, R.A., Wipke, B.T., Steinman, L., et al. (2016). Dimethyl fumarate treatment induces adaptive and innate immune modulation independent of Nrf2. Proc. Natl. Acad. Sci. U. S. A. *113*, 4777–4782.

Sellebjerg, F., Barnes, D., Filippini, G., Midgard, R., Montalban, X., Rieckmann, P., Selmaj, K., Visser, L.H., and Sørensen, P.S. (2005). EFNS guideline on treatment of multiple sclerosis relapses: report of an EFNS task force on treatment of multiple sclerosis relapses. Eur. J. Neurol. *12*, 939–946.

Shen, P., and Fillatreau, S. (2015). Antibody-independent functions of B cells: a focus on cytokines. Nat. Rev. Immunol. *15*, 441–451.

Shen, P., Roch, T., Lampropoulou, V., O'Connor, R.A., Stervbo, U., Hilgenberg, E., Ries, S., Dang, V.D., Jaimes, Y., Daridon, C., et al. (2014). IL-35-producing B cells are critical regulators of immunity during autoimmune and infectious diseases. Nature *507*, 366–370.

Skripuletz, T., Bussmann, J.-H., Gudi, V., Koutsoudaki, P.N., Pul, R., Moharregh-Khiabani, D., Lindner, M., and Stangel, M. (2010). Cerebellar cortical demyelination in the murine cuprizone model. Brain Pathol. Zurich Switz. *20*, 301–312.

Skripuletz, T., Hackstette, D., Bauer, K., Gudi, V., Pul, R., Voss, E., Berger, K., Kipp, M., Baumgärtner, W., and Stangel, M. (2013). Astrocytes regulate myelin clearance through recruitment of microglia during cuprizone-induced demyelination. Brain *136*, 147–167.

Slavin, A.J., Soos, J.M., Stuve, O., Patarroyo, J.C., Weiner, H.L., Fontana, A., Bikoff, E.K., and Zamvil, S.S. (2001). Requirement for endocytic antigen processing and influence of invariant chain and H-2M deficiencies in CNS autoimmunity. J. Clin. Invest. *108*, 1133–1139.

Smith, K.J., and McDonald, W.I. (1999). The pathophysiology of multiple sclerosis: the mechanisms underlying the production of symptoms and the natural history of the disease. Philos. Trans. R. Soc. Lond. B Biol. Sci. *354*, 1649–1673.

Spencer, C.M., Crabtree-Hartman, E.C., Lehmann-Horn, K., Cree, B.A.C., and Zamvil, S.S. (2015). Reduction of CD8+ T lymphocytes in multiple sclerosis patients treated with dimethyl fumarate. Neurol. Neuroimmunol. Neuroinflammation *2*.

Spencer, S.R., Wilczak, C.A., and Talalay, P. (1990). Induction of glutathione transferases and NAD(P)H:quinone reductase by fumaric acid derivatives in rodent cells and tissues. Cancer Res. *50*, 7871–7875.

Stadelmann, C., Wegner, C., and Brück, W. (2011). Inflammation, demyelination, and degeneration - recent insights from MS pathology. Biochim. Biophys. Acta *1812*, 275–282.

Stangel, M. (2008). Neuroprotection and neuroregeneration in multiple sclerosis. J. Neurol. *255 Suppl 6*, 77–81.

Stangel, M., and Hartung, H.-P. (2002). Remyelinating strategies for the treatment of multiple sclerosis. Prog. Neurobiol. *68*, 361–376.

Steinman, L., and Zamvil, S.S. (2005). Virtues and pitfalls of EAE for the development of therapies for multiple sclerosis. Trends Immunol. *26*, 565–571.

Stidworthy, M.F., Genoud, S., Suter, U., Mantei, N., and Franklin, R.J.M. (2003). Quantifying the Early Stages of Remyelination Following Cuprizone-induced Demyelination. Brain Pathol. *13*, 329–339.

Stoof, T.J., Flier, J., Sampat, S., Nieboer, C., Tensen, C.P., and Boorsma, D.M. (2001). The antipsoriatic drug dimethylfumarate strongly suppresses chemokine production in human keratinocytes and peripheral blood mononuclear cells. Br. J. Dermatol. *144*, 1114–1120.

Stromnes, I.M., and Goverman, J.M. (2006a). Active induction of experimental allergic encephalomyelitis. Nat. Protoc. *1*, 1810–1819.

Stromnes, I.M., and Goverman, J.M. (2006b). Passive induction of experimental allergic encephalomyelitis. Nat. Protoc. *1*, 1952–1960.

Stüve, O., Kita, M., Pelletier, D., Fox, R.J., Stone, J., Goodkin, D.E., and Zamvil, S.S. (2004). Mitoxantrone as a potential therapy for primary progressive multiple sclerosis. Mult. Scler. Houndmills Basingstoke Engl. *10 Suppl 1*, S58-61.

Su, K.G., Banker, G., Bourdette, D., and Forte, M. (2009). Axonal degeneration in multiple sclerosis: The mitochondrial hypothesis. Curr. Neurol. Neurosci. Rep. *9*, 411–417.

Tallantyre, E.C., Bø, L., Al-Rawashdeh, O., Owens, T., Polman, C.H., Lowe, J., and Evangelou, N. (2009). Greater loss of axons in primary progressive multiple sclerosis plaques compared to secondary progressive disease. Brain *132*, 1190–1199.

Thiessen, A., Schmidt, M.M., and Dringen, R. (2010). Fumaric acid dialkyl esters deprive cultured rat oligodendroglial cells of glutathione and upregulate the expression of heme oxygenase 1. Neurosci. Lett. *475*, 56–60.

Thompson, A.J., Polman, C.H., Miller, D.H., McDonald, W.I., Brochet, B., Filippi M Montalban, X., and De Sá, J. (1997). Primary progressive multiple sclerosis. Brain J. Neurol. *120 (Pt 6)*, 1085–1096.

Torkildsen, O., Brunborg, L.A., Myhr, K.-M., and Bø, L. (2008). The cuprizone model for demyelination. Acta Neurol. Scand. Suppl. *188*, 72–76.

Trapp, B.D., and Nave, K.-A. (2008). Multiple sclerosis: an immune or neurodegenerative disorder? Annu. Rev. Neurosci. *31*, 247–269.

Trebst, C., Reising, A., Kielstein, J.T., Hafer, C., and Stangel, M. (2009). Plasma exchange therapy in steroid-unresponsive relapses in patients with multiple sclerosis. Blood Purif. *28*, 108–115.

Treumer, F., Zhu, K., Gläser, R., and Mrowietz, U. (2003). Dimethylfumarate is a potent inducer of apoptosis in human T cells. J. Invest. Dermatol. *121*, 1383–1388.

Trickett, A., and Kwan, Y.L. (2003). T cell stimulation and expansion using anti-CD3/CD28 beads. J. Immunol. Methods *275*, 251–255.

Tuohy, V.K., Sobel, R.A., Lu, Z., Laursen, R.A., and Lees, M.B. (1992). Myelin proteolipid protein: minimum sequence requirements for active induction of autoimmune encephalomyelitis in SWR/J and SJL/J mice. J. Neuroimmunol. *39*, 67–74.

Venturini, G. (1973). Enzymic activities and sodium, potassium and copper concentrations in mouse brain and liver after cuprizone treatment in vivo. J. Neurochem. *21*, 1147–1151.

Vollmer, T., Stewart, T., and Baxter, N. (2010). Mitoxantrone and cytotoxic drugs' mechanisms of action. Neurology *74 Suppl 1*, S41-46.

Wakabayashi, T. (2002). Megamitochondria formation - physiology and pathology. J. Cell. Mol. Med. *6*, 497–538.

Wakabayashi, N., Slocum, S.L., Skoko, J.J., Shin, S., and Kensler, T.W. (2010). When NRF2 talks, who's listening? Antioxid. Redox Signal. *13*, 1649–1663.

Wallbrecht, K., Drick, N., Hund, A.-C., and Schön, M.P. (2011). Downregulation of endothelial adhesion molecules by dimethylfumarate, but not monomethylfumarate, and impairment of dynamic lymphocyte-endothelial cell interactions. Exp. Dermatol. *20*, 980–985.

Weber, M.S., Prod'homme, T., Patarroyo, J.C., Molnarfi, N., Karnezis, T., Lehmann-Horn, K., Danilenko, D.M., Eastham-Anderson, J., Slavin, A.J., Linington, C., et al. (2010). B cell activation influences T cell polarization and outcome of anti-CD20 B cell depletion in CNS autoimmunity. Ann. Neurol. *68*, 369–383.

Weinshenker, B.G. (1998). The natural history of multiple sclerosis: update 1998. Semin. Neurol. *18*, 301–307.

Williamson, E.M.L., and Berger, J.R. (2015). Central Nervous System Infections With Immunomodulatory Therapies. Contin. Minneap. Minn *21*, 1577–1598.

Wilms, H., Sievers, J., Rickert, U., Rostami-Yazdi, M., Mrowietz, U., and Lucius, R. (2010). Dimethylfumarate inhibits microglial and astrocytic inflammation by suppressing the synthesis of nitric oxide, IL-1β, TNF-α and IL-6 in an in-vitro model of brain inflammation. J. Neuroinflammation *7*, 30.

Witherick, J., Wilkins, A., Scolding, N., and Kemp, K. (2010). Mechanisms of oxidative damage in multiple sclerosis and a cell therapy approach to treatment. Autoimmune Dis. *2011*, 164608.

Zhu, K., and Mrowietz, U. (2001). Inhibition of Dendritic Cell Differentiation by Fumaric Acid Esters. J. Invest. Dermatol. *116*, 203–208.

CURRICULUM VITAE

Name:	**Sarah Traffehn**
Date of birth:	19.6.1988
Place of birth:	Hennigsdorf
Citizenship:	German
Address:	Hennebergstraße 8 37077 Göttingen
Education and professional experience	
10/2013 – 04/2017	University Medical Center Georg-August-University Göttingen **PhD thesis***: „Effects of dimethyl fumarate in two animal models of MS"*
10/2008 – 07/2013	Ernst-Moritz-Arndt-University Greifswald Diploma studies in Biochemistry (Grade: 1.9) **Diploma thesis:** *„Die T-Zellaktivierung bei einer murinen, polymikrobiellen Sepsis"*
07/2001 - 06/2008	Alexander S. Puschkin Gymnasium, Hennigsdorf Abitur (Grade: 1.9)